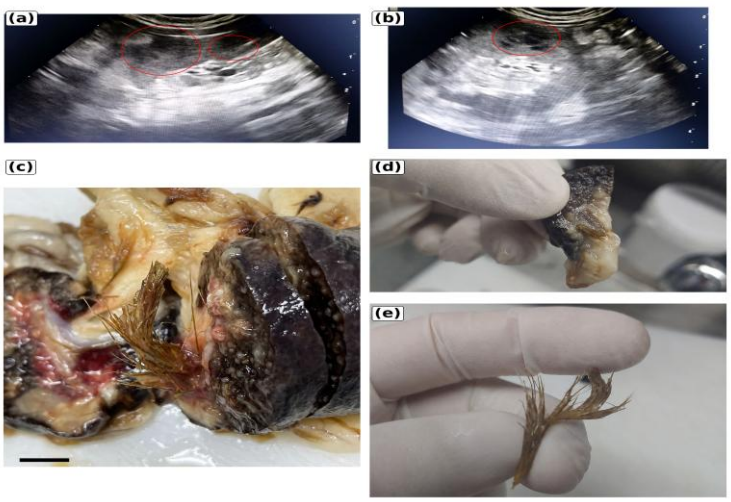
Societatea Romana Veterinara de Neurologie, Neurochirurgie si Medicina comportamentala
NEUROVET

ISSN 3153-3728 ISSN-L 2066-9399
CLUJ VET J 2026, VOL. 31, ISSUE 3
CLUJVETERINARYJOURNAL.RO
https://doi.org/10.52331/24xdfp29

CVJ | CLUJ VETERINARY JOURNAL

Table of contents

Research articles	PP
Comparative Evaluation of Injectable, Oral Gavage, and Sedative-Laden Feed Administration of Diazepam–Xylazine for Sedation in Guinea Fowl (*Numida meleagris*) *Ukwueze Celestine Okwdili, Uduak Joshua and Uwaegbulem Miracle Oluomachi*	1-9
Decoding the Glycan Signature of Hyalinized Pancreatic Carcinoma in Dogs: Histochemical and Lectin-Based Evidence of Ex-tracellular Matrix Heterogeneity *Ecaterina Semzenisi, Corina Toma, Haralambie Maria, Dragoș Hodor, Romelia Pop, Sorana Cătoi, Ibrahima Mamadou Sall, Alexia-Teodora-Hoța, and Alexandru Flaviu Tăbăran*	10-18
Histopathological Evaluation of Experimentally Induced Volumetric Muscle Loss in Rats Andreea-Alina Zăvoi, Alexandra Dreancă, Klara Magyari, Andrada Negoescu, Liviu Oana	19-27
Development of a Pilot Behaviour-Based Stress Screening Framework for Dogs and Cats During Veterinary Consultations *Andrei-Sebastian Csiplo, Silvana Popescu*	28-35
Case Reports	
Occurrence of *Ozobranchus margoi* (Hirudinea), an Important Sea Turtle Ectoparasite, on a *Caretta caretta* Individual at Kızılot Beach, Antalya *Fatih Polat, Selma Köle, Hikmet Buru, Deniz İnnal*	36-40
Splenic Abscessation Due to a Migrating Grass Awn in a Cat *Alexandr Morozov, Caren Dolgopolov and Ivan Manchev*	41-47
Review	
Early Cancer Screening in Companion Animals: Combining Traditional Diagnostics with Emerging Methods *Zhang Zhen, Guo Meiliang, Ma Baihe, Chen Xin, Liu Shuhua, Li Lianrui*	48-63



CVJ CLUJ VETERINARY JOURNAL

Article

Comparative Evaluation of Injectable, Oral Gavage, and Sedative-Laden Feed Administration of Diazepam–Xylazine for Sedation in Guinea Fowl (*Numida meleagris*)

Ukwueze Celestine Okwdili [1], Uduak Joshua [2,*] and Uwaegbulem Miracle Oluomachi [2]

[1] Department of Veterinary Surgery and Radiology, College of Veterinary Medicine, Michael Okpara University of Agriculture Umudike, 440109, Abia, Nigeria; ukwueze.okwudili@mouau.edu.ng
[2] Department of Veterinary Surgery and Radiology, College of Veterinary Medicine, Michael Okpara University of Agriculture Umudike, 440109, Abia, Nigeria; uwaegbulemp3030@gmail.com
[3] Department of Veterinary Surgery and Radiology, College of Veterinary Medicine, Michael Okpara University of Agriculture Umudike, 440109, Abia, Nigeria; joshua.uduak@mouau.edu.ng
* Correspondence: joshua.uduak@mouau.edu.ng; Tel.: +2348122462127

Abstract: This study evaluated the sedative effects of diazepam–xylazine administered via intramuscular injection, oral gavage, and sedative-laden feed in Guinea fowls (*Numida meleagris*). Eighteen clinically healthy Guinea fowls were randomly assigned to three groups (n = 6). Group A received diazepam–xylazine intramuscularly, Group B received the combination by oral gavage, and Group C received sedative-laden feed. Onset of sedation, duration of analgesia, sedation score, muscle relaxation score, heart rate, respiratory rate, and cloacal temperature were measured at predetermined intervals. Data were analyzed using one-way ANOVA, with significance set at $P < 0.05$. Route of administration significantly affected sedative efficacy. Oral gavage produced the shortest onset of sedation (1.33 ± 0.33 min) and the longest duration of analgesia (73.33 ± 3.84 min), whereas sedative-laden feed resulted in the longest onset (22.33 ± 5.36 min) and the shortest duration of analgesia (24.00 ± 3.06 min). Sedation and muscle relaxation scores were significantly higher in the oral gavage and intramuscular groups than in the feed-treated group during the early observation period ($P < 0.05$). Heart rate and respiratory rate decreased significantly after treatment in all groups, with the greatest reductions observed in birds receiving oral gavage ($P < 0.05$). Cloacal temperature decreased slightly after treatment but did not differ significantly among groups ($P > 0.05$). Diazepam–xylazine administered by oral gavage provided the most effective and consistent sedative profile in Guinea fowls, characterized by rapid onset, prolonged analgesia, superior sedation, and enhanced muscle relaxation. These findings indicate that oral gavage may be a practical alternative route for short-term chemical restraint in Guinea fowls.

Keywords: Guinea fowl; diazepam; xylazine; oral gavage; chemical restraint; sedation; avian anesthesia.

Received: 02.07.2026
Accepted: 27.07.2026
Published: 29.07.2026

*DOI:*10.52331/v31i3ej79

Copyright:© 2021by the authors. Submitted for possible open access publication under the terms and conditions of the Creative Commons Attribution (CC BY) license (http://creativecommons.org/licenses/by/4.0/).

1. Introduction

Guinea fowl (*Numida meleagris*) is one of the most important indigenous poultry species in Africa, contributing substantially to rural livelihoods, household income, food security, and genetic diversity [1]. Owing to its adaptability to harsh environmental conditions and relatively low production costs, interest in its commercial production, conservation, and research applications has increased considerably in recent years [2]. Routine veterinary procedures such as physical examination, blood collection, diagnostic imaging, wound management, and minor surgical interventions often require adequate restraint to ensure both animal welfare and personnel safety [3,4]. However, birds are highly susceptible to stress associated with capture and manual restraint. Excessive struggling may lead to hyperthermia, trauma, capture myopathy, physiological disturbances, and occasionally mortality. Consequently, procedural sedation has become an essential component of modern avian medicine because it minimizes stress, facilitates clinical procedures, and often serves as a practical alternative to general anesthesia for short-duration interventions [5].

Among the pharmacological agents used for avian sedation, benzodiazepines and α_2-adrenergic agonists remain some of the most widely employed because of their predictable sedative and muscle-relaxant effects [6]. Diazepam, a benzodiazepine, produces anxiolysis, sedation, and muscle relaxation primarily through enhancement of γ-aminobutyric acid (GABA)-mediated neurotransmission within the central nervous system. In contrast, xylazine exerts its effects through stimulation of central α_2-adrenergic receptors, producing sedation, muscle relaxation, and varying degrees of analgesia. The combination of these drug classes may provide synergistic effects, resulting in improved chemical restraint and greater patient compliance during clinical procedures [7]. Previous studies have demonstrated that benzodiazepine- and α_2-agonist-based protocols provide effective chemical restraint in several avian species, including parrots, pigeons, partridges, pheasants, and guinea fowl. For example, the addition of midazolam to a ketamine–xylazine protocol improved anesthetic quality and duration of analgesia in guinea fowl without significant adverse effects [8]. Similar findings in other avian species suggest that appropriate sedative combinations can enhance restraint quality while maintaining acceptable physiological stability [9].

Although numerous studies have evaluated sedative drugs and dose combinations in avian species, research has focused predominantly on pharmacological efficacy rather than drug delivery strategies. Intramuscular (IM) injection remains the conventional route because of its predictable absorption; however, it requires capture and restraint before sedation is achieved, potentially increasing stress responses [10]. Consequently, there is growing interest in alternative delivery methods that minimize handling while maintaining effective chemical restraint.

Recent advances in avian anesthesia and welfare emphasize refinement of restraint techniques, yet direct comparisons of injectable and non-invasive administration routes remain scarce [4]. Alternative drug delivery strategies may therefore improve animal welfare while maintaining adequate sedation [11]. Oral administration by gavage ensures accurate dose delivery while avoiding repeated injections, whereas incorporating sedative agents into feed offers an even less invasive strategy that could facilitate flock management, transportation, wildlife capture, and the handling of semi-domesticated or difficult-to-restrain birds.

Nevertheless, evidence regarding the effectiveness of sedative-laden feed remains limited, and direct comparisons between intramuscular administration, oral gavage (OG), and feed-mediated delivery are scarce. This represents an important knowledge gap in avian anesthesia and welfare-oriented restraint strategies.

Therefore, this study was designed to compare the sedative effects of a diazepam–xylazine combination administered through three different routes—IM injection, OG, and sedative-laden feed—in guinea fowl (*Numida meleagris*). Sedative indices, including onset of action, duration of analgesia, degree of sedation, degree of muscle relaxation, and selected physiological parameters, were evaluated to determine the relative effectiveness of each route of administration and to identify practical alternatives for clinical and flock management applications.

2. Materials and Methods

The study was conducted at the Department of Veterinary Surgery and Radiology, College of Veterinary Medicine, Michael Okpara University of Agriculture, Umudike, Abia State, Nigeria.

2.1. Ethical approval

The experimental protocol was reviewed and approved by the Animal Ethics Committee of the College of Veterinary Medicine, Michael Okpara University of Agriculture, Umudike (Approval No: MOUAU/CVM/REC/202620). All procedures involving animals were conducted in accordance with institutional guidelines for the care and use of animals in research.

2.2. Animals

Eighteen apparently healthy adult guinea fowls (*Numida meleagris*) of both sexes, weighing between 0.65 and 1.0 kg, were randomly allocated into three treatment groups (n = 6 per group) for the study. Birds were clinically examined and confirmed to be free of disease. They were acclimatized for two weeks under standard husbandry conditions, with free access to commercial feed and clean drinking water.

2.3. Sedative agents

- Xylazine hydrochloride injection (20 mg/mL; Xylased®, Bioveta Company, Czech Republic).
- Diazepam injection (10 mg/mL; Univall®, Swiss Pharma Nigeria Ltd., Nigeria).
- Diazepam tablets (5 mg; Univall®, Swiss Pharma Nigeria Ltd., Nigeria).

All drug doses were calculated individually according to body weight immediately before administration. Other materials used included disposable syringes, cotton wool, methylated spirit, hand gloves, digital thermometer, stethoscope, weighing balance, and permanent marker.

2.4. Preparation of Sedative-Laden Feed

Sedative-laden feed was prepared immediately before administration. Approximately 5 g of commercial feed pellets (Chikun®, Olam Agri. Nigeria) were weighed and crushed into a fine mash. Diazepam tablets were pulverized and thoroughly mixed with the calculated volume of xylazine solution needed to achieve the desired dose for each bird. The resulting mixture was homogenized and moulded into pellet-like forms using a sterile syringe plunger. The pellets were air-dried before administration and offered individually to birds assigned to the feed-treatment group.

2.5. Experimental Design

Following acclimatization, the birds were randomly allocated into three treatment groups (A, B, and C), each consisting of six birds:

- Group A (IM Administration): Birds received diazepam (2.5 mg/kg) and xylazine (1.5 mg/kg) administered intramuscularly into the thigh muscle using a sterile syringe.
- Group B (OG Administration): Birds received diazepam (5 mg/kg) and xylazine (3 mg/kg) orally via gavage. During administration, their necks were kept upright during tube insertion to completely clear the glottis. 2 mL of normal saline was consistently used to flush the tube to ensure no dry residue was left in the upper esophagus.
- Group C (Sedative-Laden Feed Administration): Birds in this group were separated into individual cages during the test to be able to control dosing. Each bird received diazepam (10 mg/kg) and xylazine (10 mg/kg) incorporated into sedative-laden feed.

The administration routes were selected to compare the effectiveness of conventional injectable sedation, controlled oral delivery through gavage, and voluntary consumption through sedative-laden feed as alternative approaches to chemical restraint in guinea fowl.

2.6. Evaluation of Sedative Indices

The birds were kept in sound-attenuated rooms because guinea fowl are highly sensitive to sudden noise, which can trigger an adrenaline surge and potentially override the sedative effects. The following were evaluated

2.6. 1. Onset of Sedation

The onset of sedation was defined as the interval between drug administration and the first observable signs of sedation, including reduced alertness, decreased responsiveness to external stimuli, postural relaxation, and associated behavioral changes. The onset time was recorded in minutes.

2.6.2. Duration of Analgesia

Analgesic duration was assessed using the toe-pinch reflex test. The time of disappearance of the withdrawal response following drug administration was recorded, as was the time of reappearance of the response. Duration of analgesia was calculated as the interval between loss and return of the toe-pinch reflex.

2.7. Evaluation of Sedation Scoring

Sedation and muscle relaxation were assessed using a previously described clinical scoring system. Birds were evaluated at predetermined intervals following drug administration by the same observer to minimize inter-observer variation (Table 1).

2.8. Physiological Measurements

Heart rate, respiratory rate, and cloacal temperature were recorded before drug administration (baseline) and at predetermined intervals after sedation, using a standardized procedure.

2.9. Statistical Analysis

Data are presented as mean ± standard error of the mean (SEM). Statistical analyses were performed using GraphPad Prism version 8.0 (GraphPad Software, San Diego, CA, USA).Differences among treatment groups were analyzed using two-way repeated-measures ANOVA, followed by Fisher's Least Significant Difference (LSD) test where appropriate. Statistical significance was accepted at $P < 0.05$.

Table 1. Clinical scoring system of level of sedation and muscle relaxation

Score	Sedation level	Muscle relaxation level
0	Standing and alert	Jaw tightly closed (full muscle tone)
1	Drooping of wings	Moderate resistance to jaw opening
2	Standing with reduced alertness	Mild resistance to jaw opening
3	Sternal recumbency	No resistance to jaw opening
4	Lateral recumbency with apparent sleep	Complete flaccid paralysis

3. Results

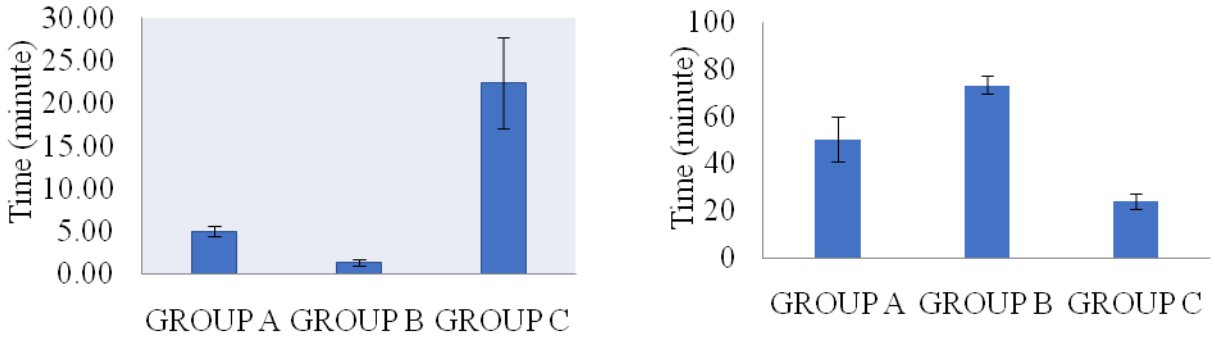
3.1. Indices of sedation

3.1.1. Onset of sedation

The route of administration did not significantly influence the onset of sedation ($P > 0.05$), although numerical differences were observed among treatment groups. However, the duration of analgesia differed significantly ($P < 0.05$), with OG producing the longest analgesic effect. Birds that received diazepam–xylazine by OG(Group B) exhibited the shortest onset of action (1.33 ± 0.33 min), whereas birds receiving sedative-laden feed (Group C) showed the longest onset time (22.33 ± 5.36 min). IM administration (Group A) produced an intermediate onset time of 5.00 ± 0.58 min. Although numerical differences were observed, no significant difference was detected among groups for onset of action ($P > 0.05$; Figure 1a).

3.1.2. Analgesic duration

Analgesic duration differed significantly among treatment groups ($P < 0.05$). OG resulted in the longest duration of analgesia (73.33 ± 3.84 min), followed by IM administration (50.33 ± 0.58 min), while sedative-laden feed produced the shortest duration (24.00 ± 3.06 min) (Figure 1b).



(**a**) (**b**)

Figure 1. Mean (±SEM) onset of sedation (min) (A) and analgesic duration (B) in Guinea fowls administered diazepam-xylazine through intramuscular injection (GROUP A), oral gavage (GROUP B) and sedative-laden feed (GROUP C).

3.2.Duration of analgesia

3.2.1. Degree of sedation

Sedation scores increased significantly following administration of diazepam–xylazine in all groups. At 10–30 min, Groups A and B maintained significantly higher sedation scores than Group C ($P < 0.05$). Maximum sedation scores of 4.00 ± 0.00 were observed in Groups A and B between 20 and 30 min, whereas Group C attained lower scores ranging from 3.00 ± 0.00 to 3.33 ± 0.33 during the same period. Sedation gradually declined after 40 min in all groups, approaching baseline values by 60 min (Figure 2a).

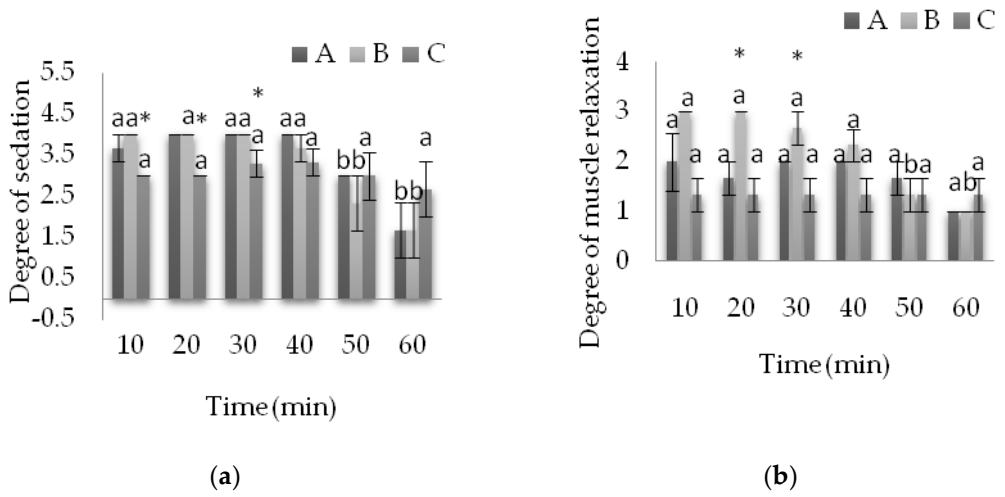


Figure 2. Mean (±SEM) Degree of sedation (a) and muscle relaxation (b) in Guinea fowls administered diazepam-xylazine via intramuscular injection (GROUP A), oral gavage (GROUP B) and sedative-laden feed (GROUP C). Different lowercase letters (a-b) indicate significant difference ($P < 0.05$) within the same group across time. An asterisk (*) indicate a significant difference ($P < 0.05$) (GROUP A), oral gavage (GROUP B) and sedative-laden feed (GROUP C) at the same time point

3.2.2. Degree of muscle relaxation

Muscle relaxation followed a similar trend. Group B exhibited the highest muscle relaxation scores, reaching 3.00 ± 0.00 at 20 min and remaining elevated at 30 min (2.67 ± 0.33). Group A showed moderate muscle relaxation with peak values of 2.00 ± 0.00 at 30–40 min, whereas Group C demonstrated minimal muscle relaxation throughout the observation period, with scores remaining between 1.00 ± 0.33 and 1.33 ± 0.33. Significant differences among groups were observed at selected time points ($P< 0.05$) (Figure 2b).

3.3. Physiological parameters

3.3.1. Heart rate

Heart rate decreased following administration of diazepam–xylazine in all treatment groups. Group B showed the greatest reduction, declining from a baseline value of 292.00 ± 18.90 beats/min to 174.67 ± 14.67 beats/min at 40 min. Group A decreased from 309.33 ± 10.73 beats/min at baseline to 236.67 ± 21.86 beats/min at 10 min, while Group C exhibited a less pronounced decline, decreasing from 299.00 ± 4.93 beats/min to 238.33 ± 19.70 beats/min at 40 min. Significant differences among treatment groups were observed at most observation periods following drug administration ($P< 0.05$). Heart rate progressively returned toward baseline values by 60 min (Table 2).

3.3.2. Respiratory rate

Respiratory rate decreased significantly following treatment in all groups ($P<0.05$). Group B showed the greatest reduction, declining from 43.67 ± 4.81 cycles/min at baseline to 13.33 ± 2.67 cycles/min at 50 min. Group A decreased from 23.33 ± 2.67 cycles/min to 12.00 ± 3.00 cycles/min, while Group C showed a comparatively smaller reduction, declining from 30.00 ± 4.73 cycles/min to 20.00 ± 5.00 cycles/min at 40 min. Respiratory rates gradually increased during the recovery period but remained below baseline values at 60 min (Table 2).

3.3.3 Cloacal temperature

Cloacal temperature decreased slightly following administration of diazepam–xylazine in all groups. The greatest reduction was observed in Group B, where temperature decreased from 42.17 ± 0.30°Cat baseline to 40.43 ± 0.33°C at 60 min. Group A showed a decline from 42.37 ± 0.23°C to 40.73 ± 0.64°C, whereas Group C exhibited minimal changes throughout the observation periods, remaining above 41°C. However, no significant differences among treatment groups were detected at any observation time ($P> 0.05$) (Table 2).

Table 2. Mean ± SEM physiological parameters of the sedative effect of diazepam-xylazine administered intramuscularly (A), by oral gavage (B), and through sedative-laden feed(C) in Guinea fowl (*Numida meleagris*)

Mean values with different superscript letters within the same column for the same parameter differ significantly at $P< 0.05$. Means with different numerals within the same row differ significantly ($P< 0.05$)

Physiological parameters	Time (minutes)	0	10	20	30	40	50	60
Heart rate (beats/minutes)	A	309.33±10.73^{c1}	236.67±21.86^{a2}	243.33±12.02^{b3}	271.67±26.19^{c4}	243.33±20.282^{c3}	274.00±13.122^{c4}	274.33±23.14^{b4}
	B	292.00±18.90^{a1}	236.00±18.90^{a5}	210.67±23.70^{a4}	186.67±24.69^{a3}	174.67±14.67 ^{a2}	242.00±21.07^{a6}	260.67±10.48^{a7}
	C	299.00±4.93^{b1}	274.33±7.22^{b5}	245.00±13.23^{b3}	248.67±30.69^{b3}	238.33±19.70^{b2}	264.67±13.92^{b4}	265.00±13.23^{a4}
Respiratory rate (cycle/minutes)	A	23.33±2.67^{a1}	15.33±2.60^{a2}	13.33±1.45^{a2}	12.00±3.06^{a2}	12.00±3.61^{a2}	12.00±3.00^{a2}	14.67±3.84^{a2}
	B	43.67±4.81^{c1}	18.00±3.06^{a2}	15.33±2.91^{a2}	15.00±3.26^{a2}	14.67±3.53^{a2}	13.33±2.67^{a2}	16.67±1.76^{a2}
	C	30.00±4.73^{b1}	24.67±6.17^{b2}	23.00±5.51^{b2}	20.33±6.01^{b2}	20.00±5.00^{b2}	21.67±4.91^{b2}	21.00±5.29^{b2}
Cloacal temperature (ºC)	A	42.37±0.23^{a1}	41.77±0.35^{a1}	41.73±0.41^{a1}	41.20±0.49^{a1}	41.07±0.38^{a1}	41.23±0.62^{a1}	40.73±0.64^{a1}
	B	42.17±0.30^{a1}	40.27±1.63^{a1}	41.07±0.38^{a1}	40.87±0.15^{a1}	40.70±0.31^{a1}	40.57±0.47^{a1}	40.43±0.33^{a1}
	C	41.77±0.23^{a1}	41.43±0.30^{a1}	41.57±0.29^{a1}	41.40±0.45^{a1}	41.40±0.40^{a1}	41.47±0.44^{a1}	41.57±0.44^{a1}

4. Discussion

The present study demonstrated that the route of administration significantly influenced the clinical response to diazepam–xylazine sedation in Guinea fowls. Although all treatment protocols produced observable sedation, OG was associated with the most favorable overall sedative profile, characterized by the shortest onset of action, the longest duration of analgesia, higher sedation scores, greater muscle relaxation, and more pronounced reductions in heart and respiratory rates. These findings suggest that the method of drug delivery plays an important role in determining the efficacy and predictability of chemical restraint in avian species.

Although the onset of sedation did not differ significantly among treatment groups ($P > 0.05$), OG had the numerically shortest mean onset time. This trend may reflect more rapid gastrointestinal absorption of the diazepam–xylazine combination under the experimental conditions, although further studies with larger sample sizes are needed to determine whether this numerical difference is biologically meaningful. In contrast, birds receiving sedative-laden feed showed a markedly delayed onset of sedation, likely due to variations in feed consumption and gastrointestinal absorption. Similar observations have been reported in avian and poultry medicine, where oral administration under controlled conditions produced more consistent pharmacological responses than voluntary drug intake through feed [12, 11]. Although IM administration is widely regarded as a reliable route for rapid systemic drug absorption, the present findings suggest that OG resulted in a numerically earlier onset of sedation. However, because this difference was not statistically significant, the observation should be interpreted with caution.

A major finding of this study was a significantly longer analgesic duration in the OG group compared with the intramuscular and feed-treated groups. Xylazine produces analgesia by stimulating central α_2-adrenergic receptors, thereby inhibiting nociceptive transmission and reducing sympathetic activity, while diazepam contributes anxiolytic and muscle-relaxant effects [7]. The prolonged analgesia observed following OG may therefore reflect more effective systemic drug availability and sustained pharmacological activity [11]. In clinical practice, prolonged analgesia is desirable because it provides a wider time window for examination and minor procedures without the need for repeated drug administration.

Sedation and muscle relaxation scores followed a similar pattern, with OG and IM administration producing significantly greater effects than sedative-laden feed during the early observation period. These findings are consistent with the known pharmacological actions of diazepam and xylazine. Diazepam enhances γ-aminobutyric acid (GABA)-mediated inhibitory neurotransmission within the central nervous system, resulting in anxiolysis and skeletal muscle relaxation, whereas xylazine produces sedation through central α_2-adrenoceptor activation. The greater muscle relaxation observed in the OG group is particularly relevant because adequate muscle relaxation facilitates handling, positioning, and clinical procedures while minimizing stress and the risk of injury [12]. The progressive decline in sedation scores after 40 min indicates gradual recovery from the drug's effects and suggests that the protocol provides temporary, reversible chemical restraint suitable for short clinical procedures.

The reductions in heart rate observed in all treatment groups are consistent with the well-documented cardiovascular effects of α_2-adrenergic agonists. Xylazine decreases sympathetic outflow and increases vagal tone, resulting in bradycardia and reduced cardiac output [13]. The greater decline observed in the oral gavage group may reflect both deeper sedation and reduced stress-associated sympathetic stimulation. Similar decreases in heart rate following xylazine-containing protocols have been reported in domestic birds and other veterinary species [14]. Importantly, heart rates gradually increased toward baseline values during recovery, indicating that the cardiovascular effects were transient and reversible.

Respiratory rate also decreased significantly following administration of diazepam–xylazine, with the most pronounced reduction occurring in birds receiving OG [15]. Sedative-induced reductions in respiratory frequency have been widely reported and are generally attributed to central nervous system depression, decreased muscular activity, and reduced metabolic demand [15, 9]. Although respiratory depression is a recognized effect of α_2-adrenergic agonists, the gradual return toward baseline values observed in the present study suggests that respiratory function remained adequately maintained throughout the observation period. Nevertheless, respiratory monitoring remains essential during avian sedation because birds possess a unique respiratory system that may be particularly sensitive to depressant drugs.

Cloacal temperature decreased slightly in all groups, although no significant differences were observed among treatments. Mild reductions in body temperature during sedation are expected because decreased muscular activity and metabolic heat production impair normal thermoregulatory processes. Similar findings have been reported in avian anesthesia studies, where sedative administration frequently re-

sults in transient decreases in body temperature [15]. Although the reductions observed in the present study were relatively small, maintenance of appropriate environmental temperature remains important during sedation to minimize the risk of hypothermia. No mortality or clinically significant morbidity was observed in any treatment group throughout the study. All guinea fowls recovered uneventfully following sedation without apparent adverse effects.

5. Conclusions

Overall, the present findings demonstrate that the route of administration influences the quality and duration of diazepam–xylazine-induced sedation in guinea fowl. While OG produced a numerically shorter onset of sedation, it significantly prolonged analgesia and provided satisfactory muscle relaxation, highlighting its potential as a practical alternative to intramuscular administration when repeated handling or injections are undesirable. Nevertheless, the absence of statistically significant differences in onset of sedation indicates that further investigations using larger sample sizes are warranted to confirm these observations and optimize sedation protocols for guinea fowl and other avian species. Although birds receiving sedative-laden feed were individually housed during feeding to minimize competition and facilitate observation, complete ingestion of the administered medicated feed could not be objectively verified. Consequently, slight variations in the amount of drug consumed may have contributed to variability in the sedative response.

Author Contributions: Conceptualization, U.C.O. and U.M.O.; Methodology, U.C.O.; Validation, U.C.O., U.M.O. and U.J.; Data analysis, U.C.O., U.M.O. and U.J.; Investigation, U.C.O. and U.M.O.; Resources, U.M.O.; Writing – Original Draft Preparation, U.J.; Writing – Review & Editing, U.J. and U.C.O.; Visualization, U.C.O. and U.M.O.; Supervision, U.C.O.; Project Administration, U.C.O.; Funding Acquisition, none.

Funding: This research received no external funding.

Institutional Review Board Statement: The study protocol was approved by the Animal Ethics Committee of the College of Veterinary Medicine, Michael Okpara University of Agriculture, Umudike (Approval No MOUAU/CVM/REC/202620).

Data Availability Statement: Research data is made available by authors upon reasonable request.

Conflicts of Interest: The authors declare no conflicts of interest.

References

1. Oluwaseun, O.; Nasir, A. Guinea fowl production in Africa: Economic importance and constraints. *Egypt. J. Vet. Sci*. **2024,** https://doi.org/10.21608/EJVS.2024.332205.2458.
2. Rahman, S.F.; Baccouri, W.; Wanjala, G. A systematic review of guinea fowl diversity and its economic, socio-cultural and ecological significance in Africa. *Trop. Anim. Health Prod*. **2025**, https://doi.org/10.1007/s11250-025-04723-x.
3. Brando, S.; Norman, M. Handling and training of wild animals: Evidence- and ethics-based approaches and best practices in the modern zoo. *Animals* **2023,** *13*, 2247–2249.
4. Kumar, R.; Kumar, S.; Gupta, R.K.; Yadav, I. Avian models for biomedical research. In Animal Models in Research: Principles and Practice; Sreelatha, H.V.; Patel, S.; Nagarajan, P., Eds.; Springer Nature Singapore: Singapore, **2024;** pp. 169–190.
5. Hettmannsperger, M.A.; Ruhnke, I. Manual catching and transportation of poultry with a focus on chickens and European practices. *Poultry* **2026,** *5*, 30–33.
6. Heard, D. Pigeons and doves (Columbiformes). In Zoo Animal and Wildlife Immobilization and Anesthesia, 3rd ed.; West, G.; Heard, D.; Caulkett, N., Eds.; John Wiley & Sons: Hoboken, NJ, USA, **2025;** pp. 513–520.
7. Mahmood, M.B. A comparison between ketamine-xylazine and ketamine-midazolam or all of them to induce balanced anesthesia in rabbits. *Iraqi J. Vet. Sci.* **2022,** *36*, 499–506.
8. Escobar, A.; Dzikiti, B.T.; Roman, K.; Rogers, A.; Maney, J.K. Effects of ketamine on the minimum anesthetic concentration of isoflurane in chickens (Gallus gallus domesticus). *Vet. Anaesth. Analg* **2025,** *52*, 786–793.
9. Baldrey, V.; Stanford, M.; Bacon, H. A comparison of the pharmacodynamic effects of intravenous ketamine-xylazine with alfaxalone in mute swans (Cygnus olor) presenting at a wildlife veterinary hospital. *Vet. Anaesth. Analg*. **2021**, *48*, 716–724.
10. Joat, N.N.; Khan, S.; Chousalkar, K. Understanding the effects of intramuscular injection and feed withdrawal on Salmonella Typhimurium shedding and gut microbiota in pullets. *J. Anim. Sci. Biotechnol.* **2021,** *12*, 78–81.
11. Coutant, T.; Vergneau-Grosset, C.; Langlois, I. Overview of drug delivery methods in exotics, including their anatomic and physiologic considerations. *Vet. Clin. Exot. Anim. Pract.* **2018,** *21*, 215–259.
12. Ogbuagu, N.E.; Ayo, J.O.; Aluwong, T.; et al. Orally administrated L-serine modulates physiological and oxidative responses in broiler chickens exposed to feed restriction and heat stress. *Discover Animals* **2025,** https://doi.org/10.1007/s44338-025-00143-1.
13. Puzovic, G.; Wolan, M.J.; Shi, Y.; Collins, G.T. Interactions between cardiorespiratory effects of fentanyl and xylazine and their reversal in male and female Sprague-Dawley rats. *J. Pharmacol. Exp. Ther.* **2025**, https://doi.org/10.1016/j.jpet.2025.103711.

14. Bigham-Sadegh, A.; Shadkhast, M.; Shafiei, Z.; Ziaei, B. Sedation with xylazine-diazepam and epidural administration of lidocaine and xylazine for castration and ovariohysterectomy in cats. *Vet. Res. Forum* **2010**, *1*, 21–25.
15. Romano, J.; Hasse, K.; Johnston, M. Sedative, cardiorespiratory, and thermoregulatory effects of alfaxalone on budgerigars (Melopsittacus undulatus). *J. Zoo Wildl. Med*. **2020,** *51*, 96–101.

CVJ CLUJ VETERINARY JOURNAL

Research article

Decoding the Glycan Signature of Hyalinized Pancreatic Carcinoma in Dogs: Histochemical and Lectin-Based Evidence of Extracellular Matrix Heterogeneity

Ecaterina Semzenisi [1*], Corina Toma [1], Haralambie Mara [1], Dragoș Hodor [1], Romelia Pop [1], Sorana Cătoi [1], Ibrahima Mamadou Sall [1], Alexia-Teodora-Hoța [1], and Alexandru Flaviu Tăbăran [1]

1 Department of Veterinary Pathology, Faculty of Veterinary Medicine, University of Agricultural Sciences and Veterinary Medicine, Cluj-Napoca, Romania
* Correspondence: ecaterina.semzenisi@student.usamvcluj.ro

Abstract: Hyalinizing pancreatic carcinoma in dogs is a rare tumors characterized by abundant eosinophilic extracellular material of uncertain composition. The aim of this study was to characterize the nature of hyaline deposits using histochemical and lectin-based methods. Pancreatic tissues from three dogs (two Boxers and one American Staffordshire Terrier) were examined following necropsy. Sections were stained with hematoxylin and eosin, Masson's Trichrome, and Congo Red, and analyzed using lectin histochemistry (SNA, PHA-L, ECL). All cases showed similar architecture, with neoplastic epithelial cells embedded in abundant hyaline stroma. Masson's Trichrome demonstrated collagen-rich deposits in all cases. Congo Red staining revealed heterogeneity, with negative staining in two cases and weak to transitional positivity in one case, interpreted as equivocal and not sufficient to confirm amyloid deposition. Lectin histochemistry showed variable glycosylation patterns among tumors. These findings indicate that hyaline in canine pancreatic carcinoma is not a uniform entity, but a heterogeneous extracellular material composed predominantly of collagen-rich stroma and glycoprotein-associated matrix, with inter-case biochemical variability. Combined histochemical and lectin-based approaches provide additional insight into the molecular complexity of these lesions.

Keywords: hyalinizing pancreatic carcinoma, dog, lectin histochemistry, SNA, PHA-L, ECL, extracellular matrix, pancreas.

1. Introduction

The term *hyaline* was first used simply to describe extracellular material of uncertain nature that appeared glassy and eosinophilic on routine hematoxylin and eosin (H&E) sections. In the early decades of pathology, when special stains such as Congo Red were not yet widely available, this label served as a practical placeholder for deposits that looked similar but might have very different biological origins. As histopathology advanced, the concept of hyaline expanded to include a wide variety of smooth, homogeneous, pink-staining materials encountered in both neoplastic and non-neoplastic tissues. Early pancreatic studies had already noted hyaline in islet cell tumors [1], and mid-century investigations further complicated the picture by showing that some of these depos-its behaved like amyloid in diabetic pancreases [2,3]. More recent work has shown that pancreatic hyaline is far from a uniform entity. In experimental rodent models, hyaline may accumulate within ductal epithelial cells [4], while in canine hyalinizing pancreatic adenocarcinoma, the deposits have been clearly demonstrated to be non-amyloid, lacking Congo Red positivity and immunoreactivity for amyloid A or islet amyloid polypeptide [5]. Together, these findings reveal that hyaline can represent a spectrum of extracellular products ranging from collagen-rich fibrotic stroma to glycoprotein-laden matrix material often arising from chronic inflammation, degeneration, or tumor-associated remodeling. Because many of these substances appear deceptively similar on H&E, distinguishing between them requires targeted histochemical and immuno-histochemical techniques.

Hyaline material has also been reported in a number of human pancreatic tumors, including solid pseudopapillary neoplasms (SPNs), intraductal papillary mucinous

Received: 21.03.2026
Accepted: 03.06.2026
Published: 09.06.2026

DOI:10.52331/v31i3xh43

Copyright: © 2021 by the authors. Submitted for possible open access publication under the terms and conditions of the Creative Commons Attribution (CC BY) license (http://creativecommons.org/licenses/by/4.0/).

neoplasms (IPMNs), and ductal adenocarci-nomas. In these contexts, it often appears as intracytoplasmic or stromal globules that are PAS-positive and diastase-resistant [6,7]. Hyalinizing changes may also accompany exocrine neoplastic or metaplastic pro-cesses [8] and can occasionally be seen in endocrine tumors or syndromic conditions such as MEN.

Given that many forms of hyaline contain glycoproteins or other carbohydrate-rich molecules, lectin histochemistry offers an attractive strategy for deeper biochemical characterization. Lectins bind selectively to defined glycan motifs and have been widely used to characterize glycosylation patterns in pancreatic tissues, including acinar cells and neoplastic lesions [9–11]. In pancreatic cancer models, lectin binding studies have demonstrated tumor-specific glycosylation patterns associated with malignant transformation [12–14]. Lectins such as Sambucus nigra agglutinin (SNA), Phaseolus vulgaris leucoagglutinin (PHA-L), and Erythrina cristagalli lectin (ECL) are particularly informative because they map specific glycan signatures respectively, α2,6-linked sialic acids, complex branched N-glycans, and galactose-containing residues [15,16]

Although hyalinizing pancreatic carcinoma has been reported in dogs [5], the biochemical nature of the hyaline material in these tumors remains poorly defined. To date, no study has applied lectin histochemistry to investigate the glycan composition of hyalinized stroma in canine pancreatic neoplasms.

The aim of this study was to characterize the glycosylation profile and biochemical nature of hyaline material in three canine pancreatic carcinomas using lectin histochemistry and histochemical stains, and to determine whether these deposits represent collagenous or glycoprotein-rich extracellular components and to assess whether any cases show Congo Red reactivity suggestive of proteinaceous extracellular component.

2. Materials and Methods

2.1. Case Selection

Pancreatic tissue samples were obtained from three dogs: a 10-year-old male Boxer (Case 1), a 12-year-old American Staffordshire Terrier (Case 2), and a 12-year-old female Boxer (Case 3). All animals were diagnosed with pancreatic neoplasia during routine diagnostic necropsy performed at the Department of Pathology, University of Agricultural Sciences and Veterinary Medicine (USAMV), Cluj-Napoca, Romania.

2.2. Ethical Approval

The study was conducted in accordance with national and European regulations on animal research and was approved by the Bioethics Committee of the University of Agricultural Sciences and Veterinary Medicine (USAMV) Cluj-Napoca, Romania, under Ethical Approval Decision corresponding to Application Form No. 513/29.09.2025

2.3.Necropsy, Sample Collection, and Tissue Preparation

Necropsies were carried out following standard anatomical and pathological dissection protocols. Pancreatic lesions were identified macroscopically, excised together with adjacent parenchyma, and immediately immersed in 10% neutral-buffered formalin for fixation. Given the minute size and complex cellular architecture of neuroendocrine structures examined in related cases, meticulous handling was required to preserve tissue integrity. Fixed samples were processed routinely, dehydrated through graded ethanol (80%, 95%, 100%), cleared in xylene, and embedded in paraffin. Serial sections of 2–3 μm thickness were obtained using a rotary microtome and mounted on charged slides.

2.4.Histology and Special Stains

Routine histological examination was performed on hematoxylin and eosin (H&E) stained sections. To further characterize the extracellular matrix and the hyaline stromal component Masson's Trichrome staining was performed to evaluate collagen deposition and stromal fibrosis using a standard protocol with hematoxylin, Biebrich scarlet–acid fuchsin, and aniline blue [17].

Congo Red staining was performed to evaluate the affinity of extracellular material for Congo Red and to differentiate Congo Red-reactive deposits from other eosinophilic extracellular materials. Sections were stained following a Highman-based protocol with alkaline differentiation and evaluated under bright-field microscopy [18,19].

2.5.Lectin Histochemistry

Lectin histochemistry was employed to investigate the glycosylation patterns of tumor cells and hyalinized stroma, based on the established utility of lectins in mapping carbohydrate structures and identifying glycoprotein-rich secretory zones in endocrine and neuroendocrine tissues (Shimomura, 2018; Syed, 2016). Paraffin sections were deparaffinized in xylene, rehydrated through descending alcohols, and rinsed in distilled water. Slides were then incubated for 60 minutes at room temperature with a panel of fluorescein-labeled lectins, each targeting specific glycan motifs:

Sambucus nigra agglutinin (SNA): α2,6-linked sialic acid

Phaseolus vulgaris leucoagglutinin (PHA-L): β1,6-branched complex N-glycans

Erythrina cristagalli lectin (ECL): Galβ1-4GlcNAc residues

Following lectin incubation, slides were washed twice in distilled water and counterstained with Draq5 (5 minutes) to highlight nuclei. All staining procedures were performed exactly according to the manufacturer's recommendations and previously validated protocols [20].

2.6. Confocal Microscopy and Image Acquisition

Fluorescent lectin binding was evaluated using a Zeiss LSM 710 laser-scanning confocal microscope mounted on an Axio Observer Z1 inverted platform. Image acquisition parameters were as follows: Excitation: 543 nm for Rhodamine-labeled lectins (emission BP 548–629 nm) and 633 nm for Draq5 (emission BP 661–759 nm) Objective: Plan-Apochromat 63×/1.4 NA oil immersion (DIC 27). Beam splitter: MBS 488/543/633. Images were captured, processed, and analyzed using ZEN software (Zeiss). Fluorescence intensity values were expressed as arbitrary units (AU), following established quantification protocols for lectin-based confocal analysis [13].

2.7. Lectin Binding Evaluation

Lectin reactivity was assessed semi-quantitatively by two independent observers, using the following scoring system: 0: no labeling +: weak labeling ++: moderate labeling +++: strong labeling Discrepancies were resolved by consensus assessment during joint slide review sessions.

Table 1. Lectins used in the study and their binding specificities

Lectin	Binding specificity	Application	Reference
Sambucus nigra agglutinin (SNA)	α2,6-linked sialic acid residues	Detection of increased sialylation in pancreatic neoplasia	Wagatsuma et al., 2020; Holst et al., 2017
Phaseolus vulgaris leucoagglutinin (PHA-L)	β1,6-branched complex N-glycans	Identification of altered N-glycan branching in tumors and fibrotic tissue	Wagatsuma et al., 2020; McDowell et al., 2021
Erythrina cristagalli lectin (ECL)	Galβ1-4GlcNAc residues	Detection of galactose-containing glycans in inflammation and neoplasia	Wagatsuma et al., 2020;

3. Results

3.1. Histopathology

Three cases of hyalinizing pancreatic carcinoma were examined, and the main findings are presented below, including histopathological features, special stains, and lectin-binding profiles.

Histologically, the neoplasms were unencapsulated and infiltrative, consisting of neoplastic epithelial cells arranged predominantly in irregular tubular, acinar, and tubulocystic structures supported by a fibrovascular stroma. Neoplastic cells were cuboidal to columnar, with moderate to abundant eosinophilic cytoplasm containing fine apical granules and round to oval basally located nuclei with coarsely stippled chromatin and prominent nucleoli. Mild to moderate anisocytosis and anisokaryosis were observed.

A prominent hyalinized collagenous stroma surrounded and separated the neoplastic glands, forming broad eosinophilic extracellular deposits. Multifocally, the hyalinized material expanded the

interstitialstroma and accumulated within glandular lumina. The neoplastic proliferation exhibited an infiltrative growth pattern, extending into the adjacent pancreatic parenchyma and surrounding connective tissues.

Mitotic activity was low, with 3 mitotic figures per 2.37 mm² in Cases 1 and 2 and 5 mitotic figures per 2.37 mm² in Case 3. Occasional intraluminal accumulations of cellular debris and rare inflammatory cells were observed. Tumor necrosis was absent in all cases. The stromal inflammatory response was minimal and consisted of scattered lymphocytes and macrophages.

Vascular invasion was identified in Case 3, characterized by aggregates of neoplastic epithelial cells within endothelial-lined vascular spaces. Omental metastases were also present in Case 3. No vascular invasion or metastatic lesions were identified in Cases 1 and 2. Overall, the tumors were well differentiated and exhibited features consistent with hyalinizing pancreatic adenocarcinoma (Fig. 1A-I).

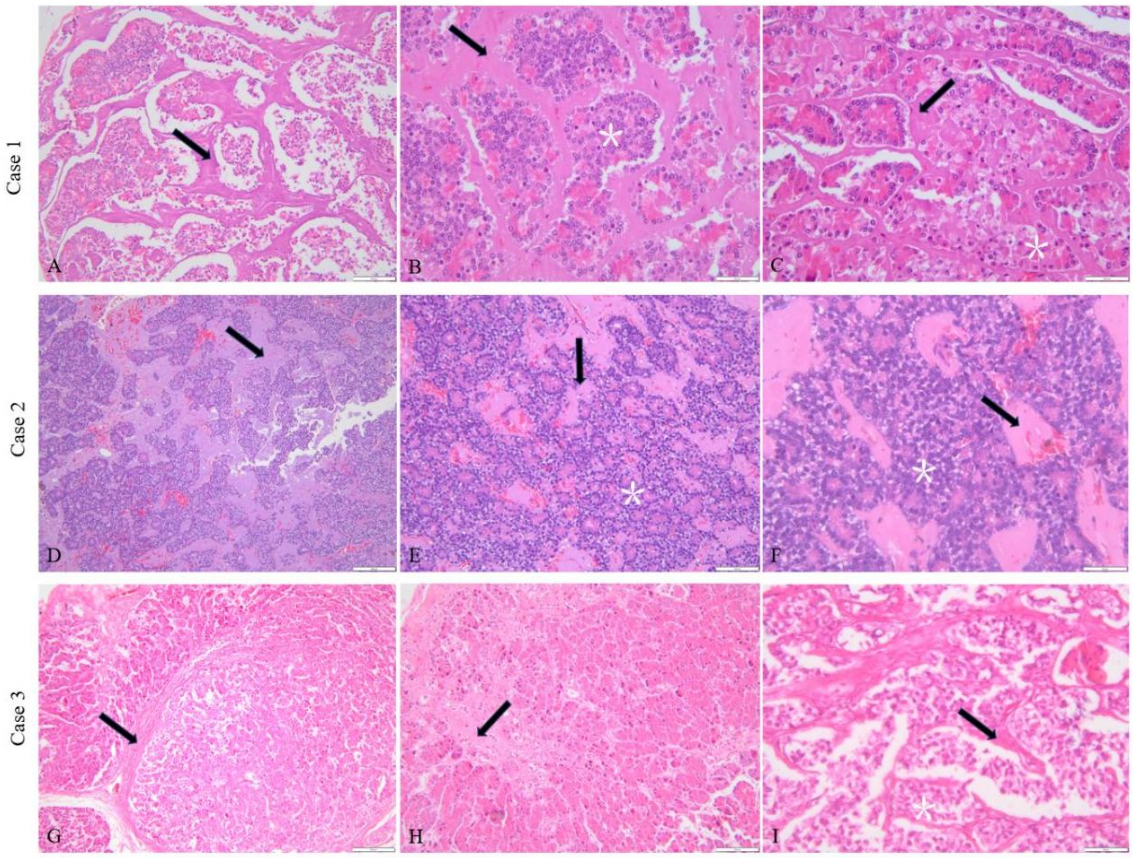


Figure 1. Pancreatic adenocarcinoma. (A–C) Neoplastic cells predominantly arranged in acinar structures (*asterisks*), separated by abundant eosinophilic, homogeneous hyaline stroma (arrows). (A) 20×, scale bar = 200 μm. (B) 10×, scale bar = 50 μm. (C) 20×, scale bar = 50 μm.

3.2. Histochemical characterization of hyaline material

3.2.1. Masson's Trichrome staining

In all three cases, Masson's Trichrome strongly highlighted the hyaline material as collagen-rich pale blue stromal deposits separating nests of tumor cells. Fine collagen septa extended between tumor islands, confirming the collagenous nature of the stroma (Fig. 2A–C).

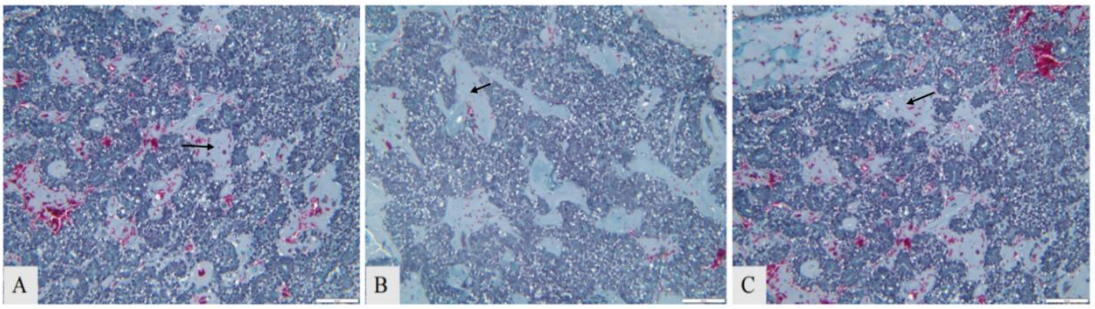


Figure 2. Histological appearance of hyalinizing pancreatic carcinoma using Masson's Trichrome staining. Cases 1–3 (A–C). The hyaline stroma is highlighted as broad pale blue collagen-rich de-posits (arrow) separating nests of tumor cells. Fine collagen septa extend between tumor islands, confirming the collagenous nature of the stroma. Scale bar: 50 μm.

3.2.2. Congo Red staining

Congo Red staining revealed heterogeneity among cases. Two cases were negative, whereas one case showed weak to transitional Congo Red reactivity within the hyaline material (Fig. 3A–C). Because polarized light examination and additional confirmatory analyses were not performed, the findings were considered equivocal and insufficient to confirm amyloid deposition.

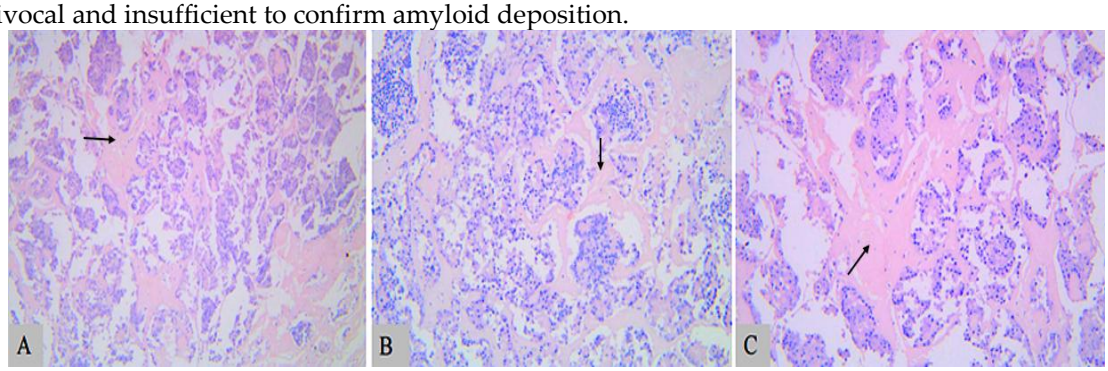


Figure 3. Histological appearance of hyalinizing pancreatic carcinoma using Congo Red staining. Case 2 (A–C). Arrows indicate areas of weak to transitional Congo Red reactivity within homogeneous eosinophilic hyaline deposits located in the tumor stroma. Because polarized light examination and confirmatory analyses were not per-formed, the findings were considered equivocal and not diagnostic of amyloid deposi-tion. Cases 1 and 3 were negative (not shown). Scale bar: 50 μm.

3.3. Lectin histochemistry

In Cases 1 and 2, SNA and ECL labeling was observed predominantly within the extracellular hyalinized stromal matrix (indicated by white asterisks), whereas only limited staining was present in neoplastic epithelial cells. In contrast, Case 3 exhibited predominantly cytoplasmic and membranous SNA labeling of neoplastic cells. PHA-L reactivity was localized mainly within the cytoplasm of neoplastic epithelial cells, being strongest in Cases 1 (Fig. 5) and 3 and weak in Case 2. No specific nuclear lectin labeling was observed; blue fluorescence corresponds to DRAQ5 nuclear counterstaining (Fig. 4A–C).

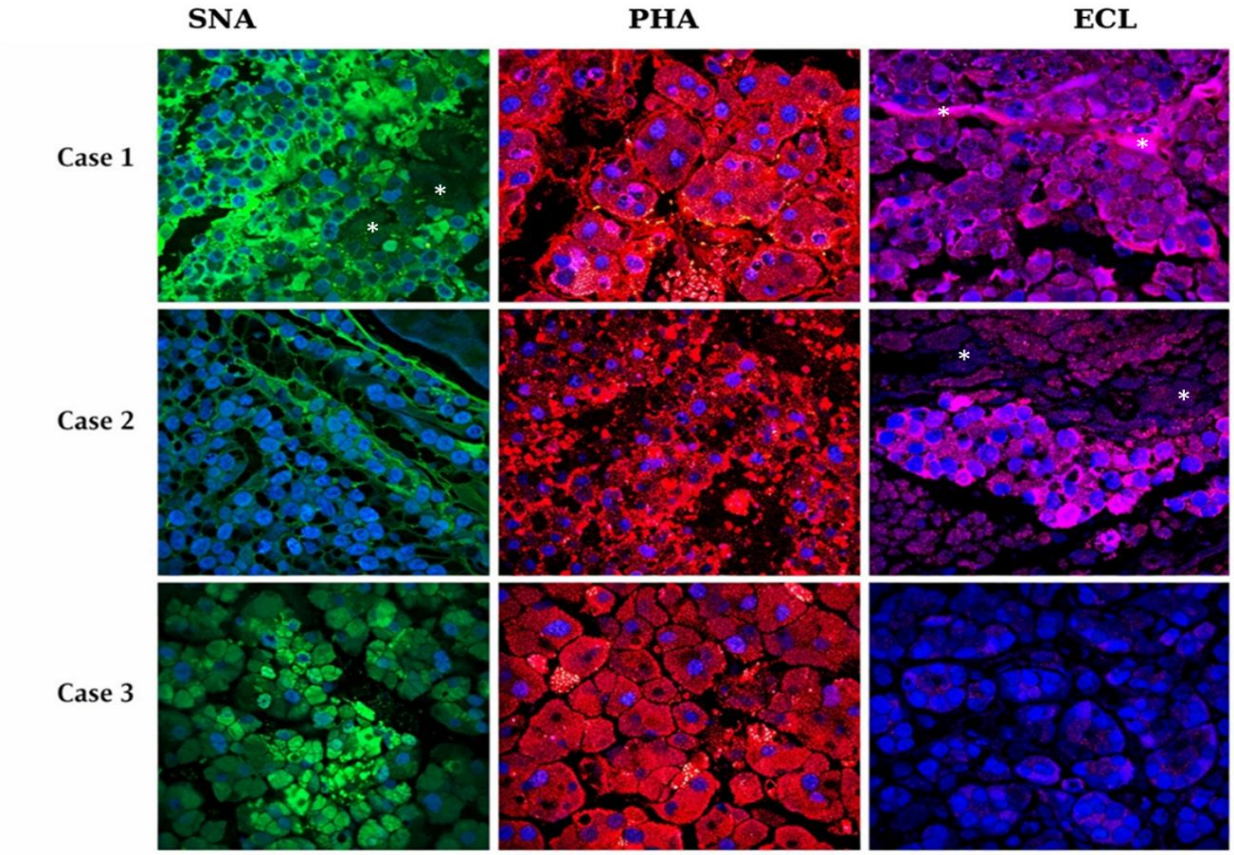


Figure 4. Lectin histochemical staining patterns in hyalinizing pancreatic carcinoma. Cases 1–3 (A–C). White asterisks indicate the hyalinized stromal matrix. Blue fluorescence corresponds to DRAQ5 nuclear counterstaining. In Case 1, strong SNA (+++) reactivity was observed predominantly within the hyalinized stromal matrix, while PHA-L showed moderate to strong cytoplasmic labeling of neoplastic epithelial cells and ECL demonstrated weak reactivity. Case 2 exhibited weak SNA labeling and weak cytoplasmic PHA-L (+) reactivity in neoplastic epithelial cells. In Case 3, moderate SNA (++) labeling was observed, accompanied by strong cytoplasmic and membranous PHA-L re-activity, whereas ECL labeling was absent or minimal. No consistent lectin labeling was observed within vascular structures or necrotic areas. These findings indicate variability in lectin-binding pat-terns and extracellular matrix heterogeneity among cases.

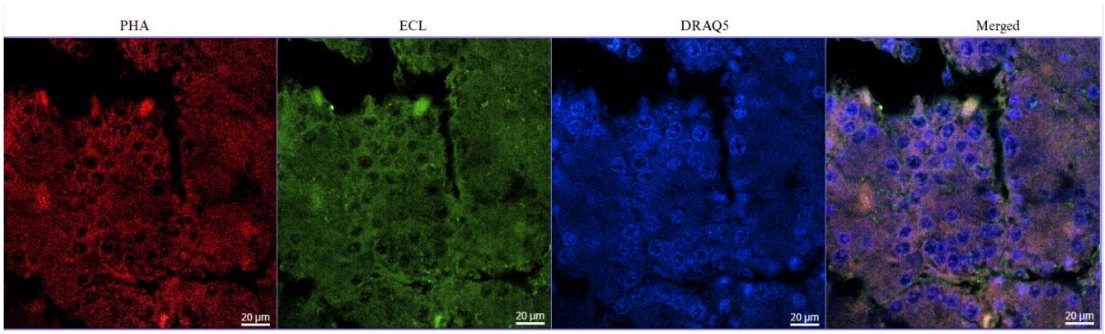


Figure 5. Representative confocal image of hyalinizing pancreatic carcinoma (Case 1) stained with *Phaseolus vulgaris leucoagglutinin* (PHA-L; red) and *Erythrina cristagalli* lectin (ECL; green). DRAQ5 (blue) was used as a nuclear counterstain. PHA-L showed strong diffuse cytoplasmic and membra-nous labeling of neoplastic epithelial cells, while ECL exhibited weaker diffuse cytoplasmic staining. The merged image highlights the distribution of lectin-reactive glycoconjugates within the tumor cell population. Scale bar = 20 µm.

4. Discussion

The findings of this study indicate that hyaline material in canine pancreatic carcinoma should not be viewed as a single, uniform structure. Although it appears similar under routine histological examination, its composition varies between cases. In all tumors examined, Masson's Trichrome staining demonstrated a strong collagen component, supporting the idea that hyalinization is largely driven by extracellular matrix remodeling and collagen deposition within the tumor microenvironment.

At the same time, Congo Red staining revealed a different layer of complexity. Two cases showed no reactivity, whereas one case displayed weak to transitional positivity within the hyaline areas. This result suggests that, in some instances, the stromal material may include an additional proteinaceous component with affinity for Congo Red. However, the staining intensity and distribution were limited, and therefore insufficient to support a definitive diagnosis of amyloid. In this context, the observed reactivity should be interpreted cautiously and considered suggestive rather than conclusive. These observations are generally in agreement with previous reports describing hyaline stroma in canine pancreatic tumors as predominantly non-amyloid [5]. The presence of weak Congo Red reactivity in one case, however, raises the possibility that the biochemical composition of this material may be more variable than previously assumed. Such variability could be related to differences in tumor biology, local microenvironmental conditions, or the dynamic nature of extracellular matrix production and modification. It may also reflect technical and interpretative factors inherent to histochemical staining. The mechanisms underlying hyaline formation in these tumors are likely multifactorial [21]. The consistent presence of collagen supports the role of stromal activation and fibroblast-driven matrix production. In contrast, the case showing partial Congo Red reactivity may represent either a distinct form of extracellular protein accumulation or a modification of existing matrix components. It is also possible that the staining reflects structural or chemical alterations in the matrix rather than true amyloid deposition. Without confirmatory methods such as polarized light examination or immunohistochemical characterization, this distinction cannot be definitively made [22].

Additional insight was provided by lectin histochemistry, which revealed differences in glycosylation patterns among the cases. Variations in SNA, PHA-L, and ECL binding indicate that the carbohydrate composition of the extracellular matrix is not consistent across tumors. These differences suggest that even when hyaline material appears morphologically similar, these differences may reflect variation in lectin binding patterns and extracellular matrix composition among cases. Interestingly, the case with weak Congo Red reactivity also showed a distinct lectin-binding profile, further supporting the idea of biochemical heterogeneity [12].

Taken together, these findings highlight the importance of using multiple complementary techniques when evaluating extracellular material in neoplastic tissues. While standard histochemical stains provide valuable structural information, lectin histochemistry offers additional insight into molecular composition. The combined approach used in this study underscores that hyaline material in canine pancreatic carcinoma represents a spectrum of extracellular matrix alterations rather than a single defined entity.

This study is not without limitations. The relatively small number of cases limits the extent to which these findings can be generalized. In addition, the nature of the Congo Red-reactive material in one case remains uncertain, as no confirmatory analyses were performed. Future investigations involving larger case series and additional diagnostic methods will be necessary to better define the composition and biological significance of hyaline material in these tumors. Additional limitations include the absence of polarized light evaluation and the lack of normal or adjacent non-neoplastic pancreatic tissue for comparative lectin analysis. Therefore, Congo Red reactivity and lectin binding patterns should be interpreted descriptively and cannot be considered diagnostic of amyloid deposition or tumor-specific glycosylation.

5. Conclusions

In summary, the results of this study show that hyaline material in canine pancreatic carcinoma is heterogeneous in nature and cannot be considered a single, uniform structure. Collagen deposition, as demonstrated by Masson's Trichrome staining, was a consistent feature in all cases and appears to play a central role in the formation of this material.

Congo Red staining further highlighted variability between tumors, with two cases showing no reactivity and one case exhibiting weak to transitional positivity. Although this finding may suggest the presence of an additional protein component with Congo Red affinity, it does not provide sufficient evidence to confirm amyloid deposition.

Lectin histochemistry demonstrated variation in lectin binding among cases, supporting extracellular matrix heterogeneity.

Overall, this study emphasizes the value of combining histochemical and lectin-based methods to achieve a more nuanced understanding of extracellular matrix changes in canine pancreatic carcinoma. Further research, including confirmatory techniques, will be essential to clarify the nature of Congo Red-reactive material and to better understand the mechanisms underlying hyaline formation in these tumors.

Author Contributions: Conceptualization, E.S. and A.F.T.; methodology, E.S., C.T. and H.M.; software, E.S.; validation, E.S., C.T. and S.C.; formal analysis, E.S. and A.F.T.; investigation, E.S., C.T., H.M. and H.D.; resources, A.F.T., R.P. and S.C.; data curation, E.S.; writing—original draft preparation, E.S.; writing—review and editing, A.F.T., C.T. and S.C.; visualization, E.S. and A.-T.H.; supervision, A.F.T.; project administration, A.F.T.; funding acquisition, A.F.T. All authors have read and agreed to the published version of the manuscript.

Funding: This study was supported by the University of Agricultural Sciences and Veterinary Medicine, Cluj-Napoca.

Institutional Review Board Statement: Not Applicable

Acknowledgments: The authors gratefully acknowledge the technical staff of the Department of Veterinary Pathology, University of Agricultural Sciences and Veterinary Medicine, Cluj-Napoca, for their valuable assistance with tissue processing, histological staining, and laboratory procedures. The authors also thank the personnel involved in confocal microscopy and imaging support.

Conflicts of Interest: The authors declare no conflict of interest.

References

1. Laidlaw, G.F. Nesidioblastoma, the islet tumor of the pancreas. *Am J Pathol* **1938**, *14*, 125–134.
2. Ahronheim, J. The nature of the hyaline material in the pancreatic islands in diabetes mellitus. *Am J Pathol* **1943**, 19, 873–880.
3. Warren, S.; LeCompte; P.M. *The pathology of diabetes mellitus*. 3rd ed: Lea & Febiger, Philadelphia, 1952.
4. Nolte, T.; Brander-Weber, P.; Dangler, C.; Deschl, U.; Elwell, M.R.; Greaves, P.; et al. Nonproliferative and proliferative lesions of the gastrointestinal tract, pancreas and salivary glands of the rat and mouse. *J Toxicol Pathol* **2016**, *29*(Suppl), 1S–125S.
5. Dennis, M.M.; O'Brien, T.D.; Wayne, T.; Kiupel, M.; Williams, M.; Powers, B.E. Hyalinizing pancreatic adenocarcinoma in six dogs. *Vet Pathol* **2008**, *45*, 475–483.
6. Samad, A.; Shah, A.A.; Stelow, E.B.; Alsharif, M.; Cameron, S.E.H.; Pambuccian, S.E. Cercariform cells: another cytologic feature distinguishing solid pseudopapillary neoplasms from pancreatic endocrine neoplasms and acinar cell carcinomas in endoscopic ultrasound-guided fine-needle aspirates. *Cancer Cytopathol* **2013**, *121*, 298–310.
7. Bhatnagar, R.; Olson, M.T.; Fishman, E.K.; Hruban, R.H.; Lennon, A.M.; Ali, S.Z. Solid-pseudopapillary neoplasm of the pancreas: cytomorphologic findings and literature review. *Acta Cytol* **2014**, *58*, 347–355.
8. Stanger, B.Z.; Stiles, B.; Lauwers, G.Y.; Bardeesy, N.; Mendoza, M.; Wang, Y.; et al. Pten constrains centroacinar cell expansion and malignant transformation in the pancreas. *Cancer Cell* **2000**, *8*, 185–195.
9. Shimomura, O.; Oda, T.; Tateno, H.; Ozawa, Y.; Kimura, S.; Sakashita, S.; et al. A novel therapeutic strategy for pancreatic cancer: targeting cell surface glycan using rBC2LC-N lectin-drug conjugate (LDC). *Mol Cancer Ther* **2018**, *17*, 183–195.
10. Syed, P.; Gidwani, K.; Kekki, H.; Leivo, J.; Pettersson, K.; Lamminmäki, U. Role of lectin microarrays in cancer diagnosis. *Prote-omics*. **2016**, *16*, 1257–1265.
11. Jonas, L.; Fulda, G.; Walzel, H.; Schulz, U. Lectin binding studies with FITC-marked WGA and UEA I and flow-cytometric measurements on isolated rat pancreatic acinar cells. *Acta Histochem* **1993**, *95*, 45–52.
12. Wagatsuma, T.; Nagai-Okatani, C.; Matsuda, A.; Masugi, Y.; Imaoka, M.; Yamazaki, K.; et al. Discovery of pancreatic ductal adenocarcinoma-related aberrant glycosylations: a multilateral approach of lectin microarray-based tissue glycomic profiling with public transcriptomic datasets. *Front Oncol* **2020**, *10*, 338.
13. McDowell, C.T.; Klamer, Z.; Hall. J.; West, C.A.; Wisniewski, L.; Powers, T.W.; Angel, P.M.; Mehta, A.S.; Lewin D.N.; Haab, B.B.; Drake, R.R. Imaging mass spectrometry and lectin analysis of N-linked glycans in carbohydrate antigen-defined pancreatic cancer tissues. *Mol Cell Proteomics* **2021**, *20*, 100012.
14. Nishimura, N.; Saito, S.; Kubota, Y.; Moto-o, N.; Taguchi, K.; Yamazaki, K.; et al. Newly established human pancreatic carcinoma cell lines and their lectin binding properties. *Int J Pancreatol* **1993**, *13*, 31–41.
15. Xiao, X.; Fischbach, S.; Fusco, J.; Zimmerman, R.; Song, Z.; Nebres, P.; et al. PNA lectin for purifying mouse acinar cells from the inflamed pancreas. *Sci Rep* **2016**, *6*, 21127.
16. Holst. S.; Belo, A.I.; Giovannetti, E.; Van Die, I.; Wuhrer, M. Profiling of different pancreatic cancer cells used as models for metastatic behaviour shows large variation in their N-glycosylation. *Sci Rep* **2017,** *7*, 16623.
17. Bancroft, J.D.; Gamble, M. *Theory and practice of histological techniques*. 6th ed.; Churchill Livingstone Elsevier; Philadelphia, 2008.

18. Highman, B. Improved methods for demonstrating amyloid in paraffin sections. *Arch Pathol* **1946**, *41*, 559–562.
19. Yakupova, E.I.; Bobyleva, L.G.; Vikhlyantsev, I.M.; Bobylev, A.G. Congo Red and amyloids: history and relationship. *Biosci Rep* **2019**, *39*, BSR20181415.
20. Rebelo, A.L.; Contessotto, P.; Joyce, K.; Kilcoyne, M.; Pandit, A. An optimized protocol for combined fluorescent lectin/immuno-histochemistry to characterize tissue-specific glycan distribution in human or rodent tissues. STAR Protoc **2021**, *2*, 100237.
21. Shiratori, S.; Sugiura, R.; Kuwatani, M.; Oda, S.; Nozawa, S.; Yonemura, H.; et al. Rare pancreatic neuroendocrine tumor with hyalinization exhibiting atypical imaging features: a case report. *Pancreas* **2025**, *54*, e499–e501.
22. Shashi, A.; Sharma, N.; Bhardwaj, M. Pathological evaluation of pancreatic exocrine glands in experimental fluorosis. *Asian Pac J Trop Med* **2010**, *3*, 36–40.

CVJ CLUJ VETERINARY JOURNAL

Article

Histopathological Evaluation of Experimentally Induced Volumetric Muscle Loss in Rats

Andreea-Alina Zăvoi [1], Alexandra Dreancă [1,2,*], Klara Magyari [2], Andrada Negoescu [1], Liviu Oana [1]

[1] University of Agricultural Sciences and Veterinary Medicine, Calea Mănăștur no 3-5, 400372, Cluj-Napoca, România; andreea-alina.zavoi@usamvcluj.ro; alexandra.dreanca@usamvcluj.ro; andrada.negoescu@usamvcluj.ro; liviu.oana@usamvcluj.ro;
[2] Nanostructured Materials and Bio-Nano-Interfaces Center, Interdisciplinary Research Institute on Bio-Nano-Sciences, Babes-Bolyai University, T. Laurian 42, 400271 Cluj-Napoca, Romania; klara.magyari@ubbcluj.ro;
* Correspondence: alexandra.dreanca@usamvcluj.ro

Abstract: Unlike minor muscle injuries, which can heal through the activation of resident satellite cells, VML injuries involve the removal of large tissue volumes and disruption of the extracellular matrix architecture required for effective regeneration. Consequently, the healing process is often dominated by fibrosis, chronic inflammation, and incomplete muscle regeneration. To overcome these limitations, considerable attention has been directed toward the development of biomimetic scaffolds and regenerative therapies designed to restore both the structural organization and functional properties of skeletal muscle. Understanding the histopathological lesions associated with VML is therefore crucial for assessing tissue repair and for developing effective treatment strategies capable of improving muscle recovery and functional outcomes.

Keywords: volumetric muscle loss; immunohistochemistry; rats.

Received: 16.06.2026
Accepted: 24.06.2026
Published: 25.06.2026

DOI:10.52331/v31i3dw89

Copyright: © 2021 by the authors. Submitted for possible open access publication under the terms and conditions of the Creative Commons Attribution (CC BY) license (http://creativecommons.org/licenses/by/4.0/).

1. Introduction

Severe skeletal muscle loss can occur in a variety of clinical contexts, including traumatic injuries, congenital conditions, surgical resections, and degenerative myopathies. Volumetric muscle loss (VML) is defined as the loss of skeletal muscle tissue that exceeds the endogenous regenerative capacity of the tissue, leading to incomplete structural and functional recovery [1,2]. Although skeletal muscle has a strong intrinsic ability to regenerate following minor injuries through satellite cell activation and coordinated repair mechanisms [3,4], extensive defects such as VML often result in persistent deficits in muscle architecture and function.

Current therapeutic approaches for VML primarily involve surgical reconstruction techniques, such as muscle flap transfers or autologous grafting procedures. However, these strategies are limited by donor-site morbidity, restricted availability of suitable tissue, and incomplete restoration of full muscle function. As a result, there has been increasing interest in the development of regenerative and tissue-engineering-based alternatives aimed at improving functional recovery [5-7].

Recent advances have focused on the design of biomimetic and tissue-engineered constructs, including scaffold-free, multi-phasic skeletal muscle units intended to restore both structural organization and contractile capacity. These engineered constructs often integrate muscle tissue with supportive anchoring structures to better replicate native musculoskeletal architecture. Preclinical evaluation of such therapies is commonly performed using rat models of VML, particularly involving injuries to the tibialis anterior (TA) muscle [8,9].

Despite widespread use of animal models, there remains significant variability in experimental design, including differences in species, injury geometry, and percentage of muscle removed. Common approaches include longitudinal excisions, transverse resections, and biopsy punch injuries, all of which typically exceed the regenerative threshold of skeletal muscle [10]. However, the degree of long-term functional impairment varies across studies, and recent findings suggest that some injury sizes previously considered representative of VML may still allow substantial recovery over extended time periods [11,12].

Consequently, there is a need to refine and standardize VML models to better reflect clinically relevant, long-lasting functional deficits. This includes systematic evaluation of different defect sizes and their long-term outcomes in order to identify injury thresholds that result in irreversible loss of muscle function. Such standardized models are essential for improving the comparability of studies and for the reliable assessment of emerging regenerative therapies [13].

The aim of this study was to evaluate the histological response of volumetric muscle loss defects treated with two bioactive glass-based biomaterials, bioactive glass-alginate-agarose (BG-Alg-Agar) and bioactive glass-agarose (BG-Agar), in a rat tibialis anterior model. A standardized full-thickness muscle defect corresponding to approximately 20% of muscle mass was surgically induced and subsequently treated with the biomaterials or left untreated as a control. Animals were euthanized at 4-, 6-, 8-, and 12-weeks post-implantation for histological and immunohistochemical evaluation.

Histological examination revealed progressive muscle regeneration in the treated groups, characterized by the appearance of centrally nucleated regenerating fibers, neovascularization, and active mesenchymal proliferation. Immunohistochemical analysis demonstrated sustained myogenic activity, particularly in the BG-Alg-Agar group, where muscle maturation and tissue organization improved over time. In contrast, BG-Agar-treated defects showed a less favorable regenerative outcome, with gradual replacement of the defect area by fibrous connective tissue and limited muscle fiber formation at later time points. Peri-implant calcifications were observed at 8 weeks in both biomaterial groups but regressed by 12 weeks, suggesting a temporary tissue response associated with remodeling rather than progressive pathological mineralization. Untreated defects exhibited persistent fibro-adipose tissue deposition and minimal evidence of muscle regeneration throughout the study period.

2. Materials and Methods

Twenty medium weighted males, Wistar rats, weighing 360 ± 50 g, were used for this experiment. Following the clinical examination, animals underwent a brief assessment of their general condition, including hydration status, appetite, and skin integrity. Both hindlimb surgical sites were aseptically prepared by shaving and disinfection, applied in concentric circular motions from the center outward. The limbs were draped under sterile conditions, with the right limb serving as an internal control. A longitudinal incision was made distal to the knee to expose the tibialis anterior (TA). Volumetric muscle loss was induced using a 6 mm biopsy punch, generating a full-thickness defect (~20% muscle mass) (Figure 1). Defects were filled with biomaterials (BG-Alg-Agar, n=10; BG-Agar, n=10) or left untreated as controls. Fascia and skin were continuously closed. This work was conducted in compliance with the European guidelines and rules 337, as established by the EU Directive 2010/63/EU and the Romanian law 43/2014. . As a biomaterial it was used sol-gel derived bioactive glass (BG; $60SiO_2{\cdot}32CaO{\cdot}8P_2O_5$ mol%) [14]. The BG was added in agarose (BG-Agar), and in alginate-agarose (BG-Alg-Agar) polymeric solutions in a ratio of 12 wt%. The weight ratio of alginate–agarose composite was 3:1 (Alg-Agar). All procedures were approved by the Research Ethics Committee of the University of Agricultural Sciences and Veterinary Medicine (USAMV) Cluj-Napoca, Romania, and they were authorised by the State Veterinary Authority (ethical approval number 369 /13.06.2023).

For microscopic analysis, tibialis anterior (TA) muscle samples were collected from both control and treated groups (BG-Alg-Agar and BG-Agar) at 4-, 6-, 8-, and 12- post-intervention. Specimens were fixed in 10% formalin for 24 h and processed using standard histological procedures. Paraffin-embedded tissues were sectioned at 3 μm using a Thermo Scientific™ Citadel 2000 rotary microtome and stained with hematoxylin and eosin (H&E).

For immunohistochemical analysis, heat-induced epitope retrieval was performed at pH = 9.0. using Novocastra™ Epitope Retrieval solution (1:10 dilution) for 30 minutes. Immunostaining was carried out using the Dako EnVision Flex+ (Mouse, high pH) system according to the manufacturer's instructions. Primary antibodies included anti-MyoD1 (ab203383, Abcam; 1:1000 dilution) and anti-α-smooth muscle actin (α-SMA, ab5694, Abcam; 1:100 dilution).

Slides were evaluated by two anatomical pathologists, and images were acquired using an Olympus SP-350 digital camera with Stream Basic imaging software (v1.5.1, Olympus Corporation, Tokyo, Japan).

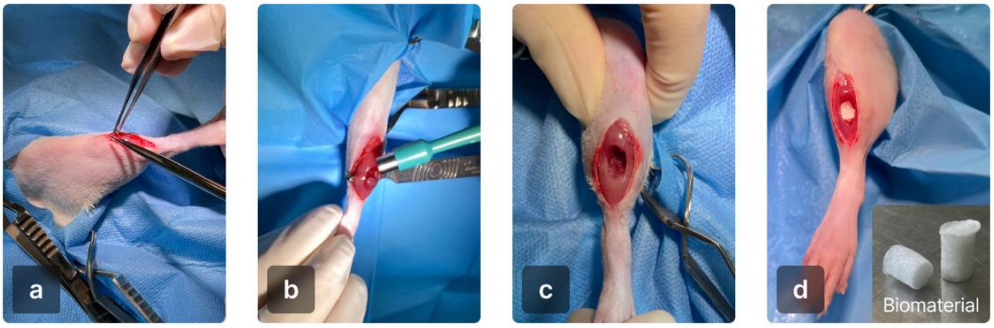


Figure 1. Schematic overview of VML surgery with BG-Alg-Agar and BG-Agar: (**a**) After shaving, skin and fascia were incised to expose the tibialis anterior muscle; (**b, c**) A 6 mm biopsy punch created a VML defect; (**d**) followed by hydrogel implantation or left untreated.

3. Results

Animals were euthanized by prolonged isoflurane anesthesia followed by cervical dislocation, and tibialis anterior (TA) muscles were harvested for analysis at 4-, 6-, 8-, and 12-weeks post-intervention.

3.1. Histologic features of fibrosis following VML injury

- BG-Alg-Agar group

At 4 weeks post-implantation, centrally nucleated muscle fibers indicate active regeneration. The tissue shows ongoing repair characterized by mesenchymal proliferation and inflammatory infiltration, predominantly macrophages involved in phagocytosis, without evidence of necrosis. However, tissue organization remains immature, with incomplete structural restoration and persistent but expected inflammatory activity (Figure 2a, b).

At 6 weeks, muscle fibers display staining patterns consistent with myoblastic activity, indicating continued but more advanced regeneration. The process is in an intermediate stage, with overlap between proliferation and differentiation. Inflammation is still present but shows signs of regression. The biomaterial is integrating into the tissue; however, focal dystrophic mineralization suggests a low-grade chronic inflammatory response. Mesenchymal activity persists, contributing to tissue remodeling, but regeneration remains incomplete and not fully physiological (Figure 2c, d).

At 8 weeks postoperatively, the defect region shows muscle fibers at an advanced stage of maturation, with increased diameter, peripheral nuclei, and improved cytoplasmic organization. These fibers are separated by thin connective tissue septa. Muscle regeneration is accompanied by ongoing but reduced neovascularization and partial integration of the biomaterial within the host tissue, which supports cellular migration and mesenchymal activity. However, remodeling remains incomplete, as evidenced by focal peri-implant calcifications and residual connective tissue deposition. These calcifications appear as dense basophilic deposits located between muscle fibers and within interstitial spaces, likely reflecting ongoing tissue remodeling and low-grade inflammatory activity (Figure 3a, b).

At 12 weeks, regenerated muscle fibers are uniformly aligned with peripheral nuclei and well-developed perimysial and endomysial organization. Tissue architecture shows marked improvement compared with earlier time points, although complete restoration of native skeletal muscle structure is not achieved. Low-grade inflammatory infiltrates and sparse calcifications persist, along with thin connective tissue septa between fibers, indicating residual remodeling activity. Mesenchymal proliferation is markedly reduced, reflecting transition toward tissue stabilization and maturation. The previously observed calcifications are now only sporadically present, suggesting a transient process. The biomaterial shows progressive resorption, contributing to consolidation of the regenerated tissue architecture (Figure 3c, d).

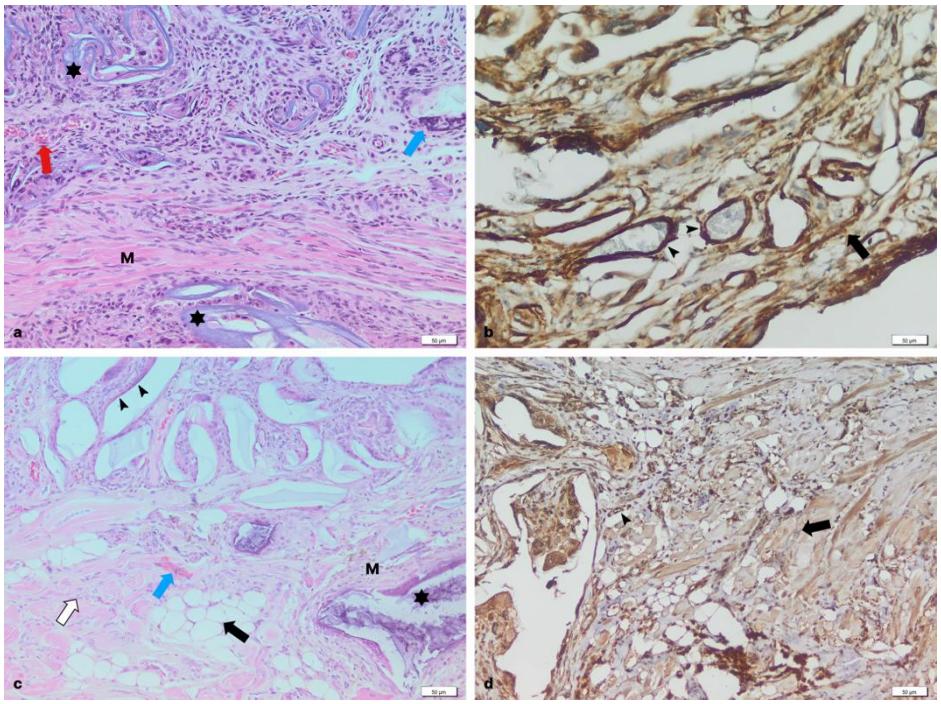


Figure 2. Histological evaluation of the tissue response in muscle defects at (**a, b**) 4 and (**c, d**) 6 weeks postoperatively in rats from the treated group. The defect is occupied by fragments of implanted material (black asterisk), surrounded by mesenchymal cells, blood vessels (blue arrow), collagen fibers, and mononuclear inflammatory cells; (**c**; arrowheads) Multinucleated myotubes are present at the periphery of the implant (red and white arrows), indicating ongoing myogenic activity; (**a, b**) Heterotopic bone formation with osteoblast rimming is also observed, H&E staining; (**b, d**; arrowheads) Immunohistochemistry shows vascular structures consistent with active angiogenesis and (**b, d**; black arrow) identifies positively stained myofibroblasts. Scale bars: (a,c) 100 μm and (b,d) 50 μm.

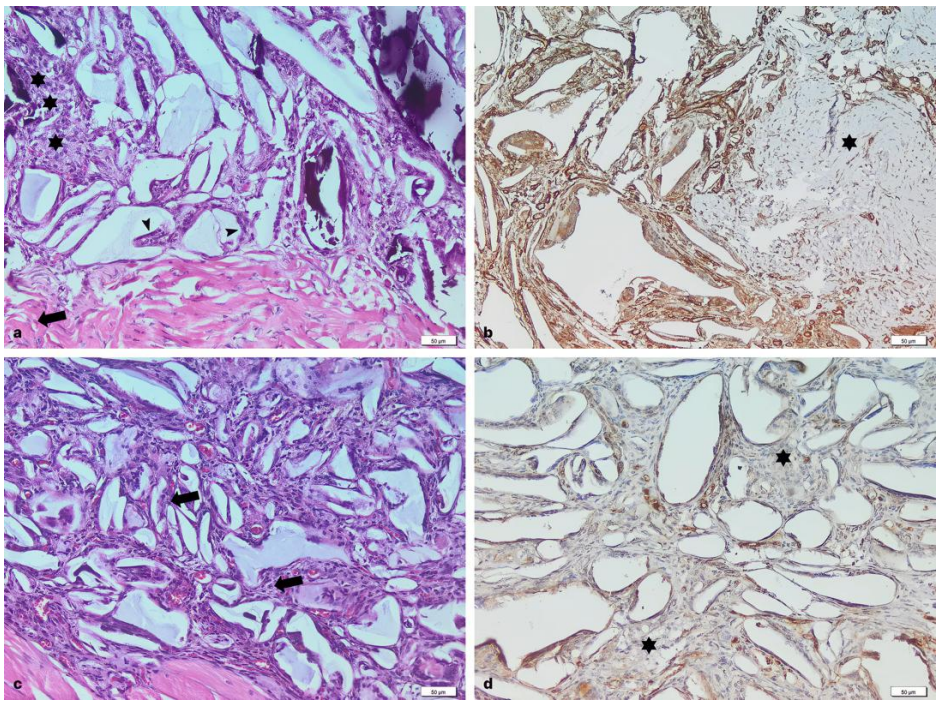


Figure 3. Histological evaluation of the tissue response in muscle defects at (**a, b**) 8 and (**c, d**) 12 weeks postoperatively in rats from the treated group. The defect area shows progressive tissue maturation characterized by reduced cellularity and predominance of remodeled connective tissue. Adipose infiltration and stabilized blood vessels are present, indicating ongoing tissue remodeling; (**a,**

c; black arrows) The inflammatory response is reduced compared with earlier stages; (**a**; arrowheads) Focal peri-implant hypertrophic calcifications are observed; (**a, c**) H&E staining. Immunohistochemistry shows organized extracellular matrix with reduced vascular density, consistent with late-stage tissue remodeling (asterisk). (a-d) Scale bar: 50 μm.

- BG-Agar group

At 4 weeks post-implantation, the muscle tissue consists of small fibers with centrally located nuclei, consistent with immature myotubes and early-stage regeneration. The defect area shows active and well-regulated repair, characterized by a predominant macrophage population involved in phagocytic clearance of cellular debris. Mesenchymal proliferation is evident, contributing to initial tissue restoration. The biomaterial remains present and may influence local diffusion and cellular activity. Overall, the histological pattern indicates an immature repair process without evidence of robust muscle reconstruction (Figure 4a, b).

At 6 weeks, muscle fibers show increased organization, although focal disruption and interstitial collagen deposition indicate early fibrotic remodeling. This suggests a transition toward a fibrotic repair trajectory that may limit further muscle regeneration despite ongoing mesenchymal activity. No active myofibroblasts are observed, and tissue remodeling appears limited, consistent with a transitional stabilization phase. Macrophages remain the dominant inflammatory cell population, reflecting low-grade chronic inflammation. The biomaterial demonstrates progressive integration into the host tissue, potentially accompanied by mild dystrophic mineralization, while mesenchymal proliferation persists at a reduced level, supporting residual reparative activity (Figure 4c, d).

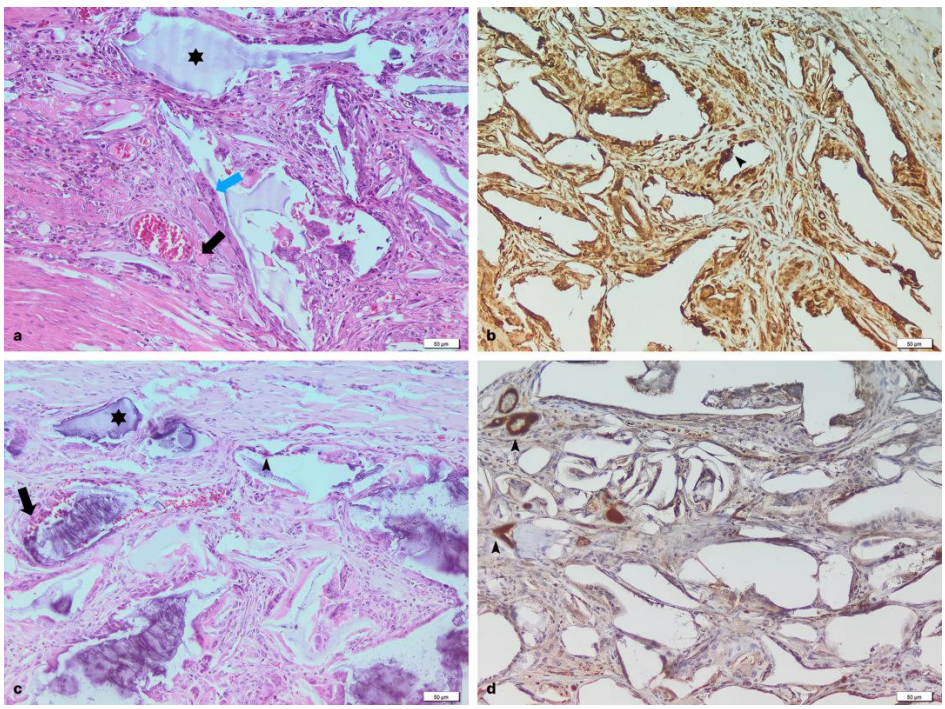


Figure 4. Histological evaluation of tissue response in muscle defects at (**a, b**) 4 and (**c, d**) 6 weeks postoperatively in the treated group. The muscle defect is occupied by fragments of the implanted material (black asterisk); (**a**, blue arrow) Immature myotubes are present; (**a, c**; black arrow) Presence of macrophages; (**c**; arrowhead) Mineralization; (**a, c**) H&E staining; (**b, d**; arrowheads) Immunohistochemical staining highlights vascular structures and confirms active angiogenesis in the tissue. (a, b, c, and d) Scale bar: 50 μm.

At 8 weeks, histological examination demonstrated incomplete muscle regeneration characterized by disorganized fibers, irregular alignment, increased connective tissue deposition, and expanded interstitial spaces. These features suggest a progressive shift toward fibrotic remodeling rather than functional muscle restoration. Immunohistochemical analysis (Figure 5a, b) revealed marker expression within the regenerated

tissue; however, staining was heterogeneous, with variable intensity and areas of reduced immunoreactivity, indicating uneven tissue maturation.

At 12 weeks, muscle fibers exhibited improved organization and a more compact architecture compared with earlier time points. Nevertheless, focal connective tissue persistence and irregular fiber arrangement remained, indicating incomplete remodeling. Immunohistochemical staining (Figure 5c, d) showed continued marker expression within regenerated tissue, but with non-uniform intensity across regions. These findings indicate progressive regeneration without full structural or functional maturation. Despite partial improvement in tissue organization, residual fibrotic areas and heterogeneous immunoreactivity suggest that skeletal muscle regeneration remained incomplete, with fibrotic remodeling still contributing to the overall tissue architecture.

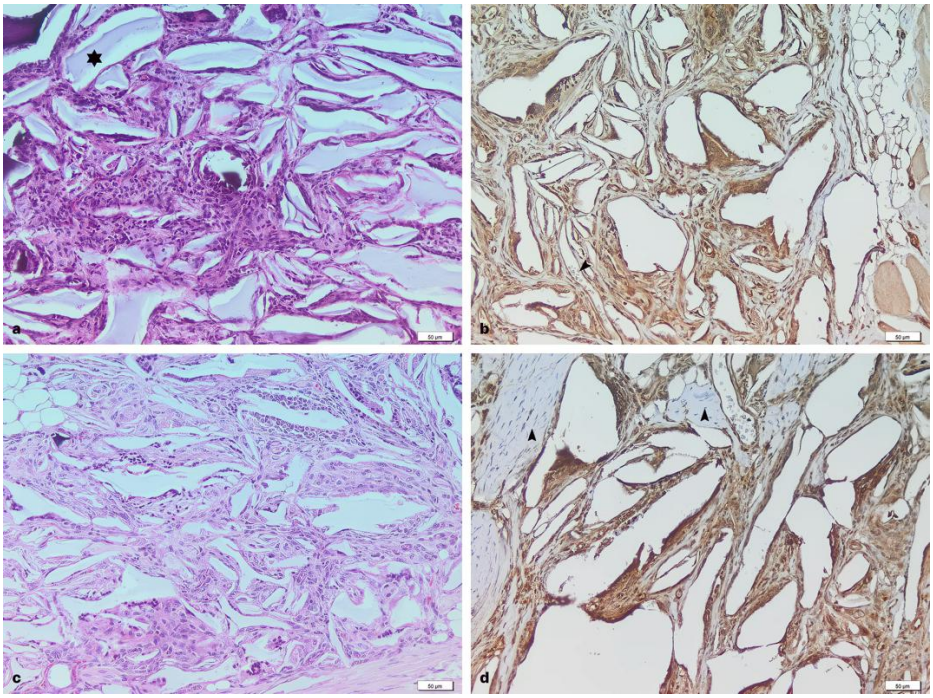


Figure 5. Histological evaluation of tissue response in muscle defects at (**a, b**) 8 and (**c, d**) 12 weeks postoperatively in the treated group. At 8 weeks, reduced and localized muscle fibers with occasional MyoD-positive cells are observed, indicating ongoing but limited regeneration. Inflammation is reduced, and partial biomaterial resorption is evident (black asterisk). At 12 weeks, muscle fibers are scarce and the defect is largely replaced by fibrous tissue, with complete biomaterial resorption and absence of active regeneration; (**a, c**) H&E staining; (**b, d**) Immunohistochemistry shows heterogeneous positive staining with variable intensity across regions (arrowheads). Scale bar: 50 μm.

- Control group

At 4 weeks postoperatively, the defect area showed neovascularization and active mesenchymal proliferation, indicating an early reparative response. The muscle defect was partially filled with fibro-adipose tissue composed of sparse fibroblasts, thick collagen fibers, and differentiated adipocytes, with limited neovascularization. At the interface with residual skeletal muscle, occasional myotubes were observed, indicating minimal regenerative activity (Figure 6a). *From 6 to 12 weeks*, the histological appearance of the defect remained largely unchanged. The lesion was consistently occupied by fibro-adipose tissue with vascular structures, without evidence of meaningful skeletal muscle regeneration. Occasional inflammatory lesions persisted, while new muscle fiber formation was absent or minimal throughout the observation period (Figure 6b).

Overall, untreated defects failed to regenerate functional skeletal muscle, with fibro-adipose tissue replacement representing the predominant healing response throughout the study period.

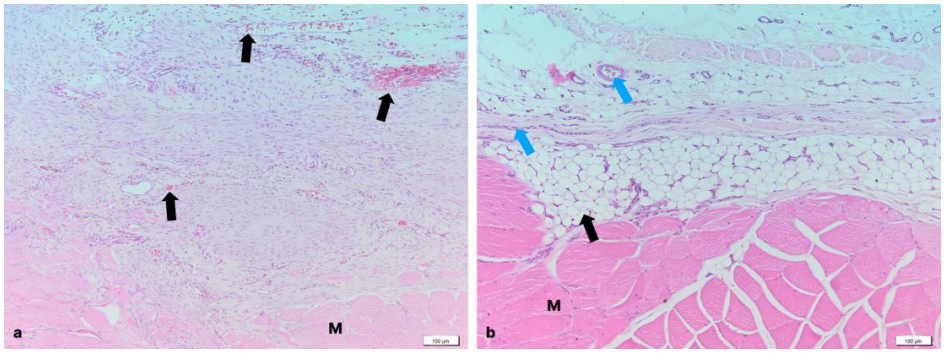


Figure 6. Histological evaluation of the tissue response in muscle defects at (a) 4 weeks and (b) 6, 8, and 12 weeks postoperatively in rats from the control group. *M* indicates skeletal muscle. (a, black arrows). Blood vessel formation can be observed. (b, black arrow) The presence of adipose tissue and blood vessels (blue arrows - b) is also noted. (a,b) H&E staining. The scale bar represents 100 μm.

3.2 Comparative histological outcomes of the investigated biomaterials

The histopathological evaluation demonstrated that both biomaterials were capable of supporting an initial regenerative response following volumetric muscle loss. However, neither scaffold achieved complete restoration of normal skeletal muscle architecture during the experimental period. The regenerative process remained heterogeneous and was accompanied by varying degrees of connective tissue deposition, indicating that the biological response was only partially successful.

Among the two investigated biomaterials, BG-Alg-Agar exhibited the most favorable regenerative profile. Histological examination revealed active myogenesis, angiogenesis, and mesenchymal cell proliferation during the early stages of healing, followed by progressive tissue organization and biomaterial integration. Nevertheless, complete muscle regeneration was not achieved, as residual connective tissue, persistent low-grade inflammation, and transient peri-implant calcifications were still evident at later time points. These findings suggest that although BG-Alg-Agar provided a supportive microenvironment for muscle repair, additional optimization of its composition or biological activity may be necessary to obtain complete structural recovery.

In contrast, the BG-Agar biomaterial demonstrated a less favorable histological outcome. While early regenerative activity was observed after implantation, the repair process progressively shifted toward fibrotic tissue formation, with irregular muscle fiber organization and persistent connective tissue deposition. The heterogeneous immunohistochemical staining pattern and incomplete maturation of regenerating fibers indicated limited myogenic potential, suggesting that this biomaterial alone was insufficient to sustain effective long-term skeletal muscle regeneration.

Despite these limitations, both biomaterials promoted a more organized reparative response than the untreated defects, in which fibro-adipose tissue predominated and muscle regeneration remained minimal throughout the observation period. The overall histological findings indicate that the regenerative capacity of the investigated scaffolds remains incomplete, emphasizing the need for further improvements in biomaterial design, degradation kinetics, and biological functionalization to enhance muscle regeneration and reduce fibrosis.

4. Discussion

Pathological fibrosis negatively affects skeletal muscle function by increasing tissue stiffness and reducing contractile capacity. In the context of volumetric muscle loss, early post-injury healing is characterized by transient extracellular matrix remodeling, including elevated collagen type III deposition and a loosely organized matrix within the defect area, reflecting an initial reparative phase [15].

A key finding of this study is the occurrence of transient heterotopic calcification within the implant region. Although ectopic mineralization is generally considered an undesirable outcome in regenerative therapies, the temporal pattern observed (presence at 8 weeks followed by regression at 12 weeks) suggests that these deposits are associated with active tissue remodeling rather than progressive pathological ossification [17-19]. Similar transient mineralization phenomena have been reported in biomaterial implantation studies and are frequently linked to local ionic fluctuations, macrophage-mediated inflammatory responses,

and extracellular matrix remodeling [20]. However, the mechanisms underlying this phenomenon in the present model were not investigated in detail and require further analysis using dedicated imaging modalities and mineral-specific histological techniques.

Immunohistochemical analysis using MyoD and α-SMA provided additional insight into the regenerative process. Sustained MyoD expression and the presence of regenerating fibers indicate prolonged myogenic activity, particularly in the BG-Alg-Agar group. MyoD is a key regulator of satellite cell activation and myogenic differentiation, and its expression is generally associated with active muscle repair [21]. The persistence of MyoD-positive cells at intermediate stages suggests that the regenerative process remains active beyond the acute injury phase, consistent with previous studies reporting prolonged myogenic responses in successfully regenerating VML defects treated with biomaterials [22].

Despite these regenerative signals, the histopathological assessment was primarily qualitative and lacked extensive histomorphometric quantification of fibrosis, vascularization, and muscle regeneration. In addition, a broader panel of molecular markers was not employed to fully characterize inflammatory and fibrotic pathways, limiting mechanistic interpretation.

Future studies should focus on a multifaceted optimization strategy. From a biomaterials perspective, tuning composition, degradation kinetics, surface chemistry, porosity, and ion exchange properties may reduce local conditions favoring ectopic mineralization and excessive inflammatory signaling. From a biological standpoint, modulation of macrophage polarization and inhibition of osteogenic signaling pathways may further improve regenerative outcomes and limit calcification [24,25].

More clinically relevant preclinical models, such as rabbits, pigs, or sheep, may provide improved translational relevance due to their closer approximation of human muscle architecture, vascularization, and mechanical loading conditions [23]. These models may better capture tissue remodeling dynamics and susceptibility to heterotopic ossification.

Clinically, heterotopic ossification remains a relevant complication in muscle injuries, particularly those adjacent to bone. It has been reported in up to 20% of patients following muscle contusion injuries and in up to 65% of cases of traumatic volumetric muscle loss [27-29].

5. Conclusions

Overall, the findings indicate that BG-Alg-Agar provides a more favorable regenerative microenvironment than BG-Agar, supporting early myogenic activity, angiogenesis, and biomaterial integration, while partially limiting fibrotic progression. However, neither scaffold achieved complete restoration of native skeletal muscle architecture within the 12-week period. Persistent connective tissue deposition and transient peri-implant calcifications indicate that tissue remodeling remained incomplete at the study endpoint. Although bioactive glass-based composite scaffolds show promise for volumetric muscle loss repair, further optimization of their physicochemical and biological properties is required to enhance functional muscle regeneration and reduce fibrotic healing outcomes. Future studies should incorporate quantitative histomorphometric and functional assessments, as well as larger animal models, to improve translational relevance. Local anatomical conditions may also influence regenerative outcomes, particularly in muscle defects adjacent to bone, where altered mechanical and biochemical microenvironments may shift the balance between muscle regeneration, fibrosis, and ectopic mineralization.

Author Contributions: Conceptualization, A.M, A.D. and K.M.; methodology, A.D and K.M.; validation, A.D.; methodology and investigation, A.N and K.M.; writing - original draft preparation, A.M. and A.D.; writing - review and editing, K.M. and A.D.; validation and supervision, L.O.; project administration, L.O. All authors have read and agreed to the published version of the manuscript.

Funding: This research received no external funding

Institutional Review Board Statement: This work was conducted in compliance with the European guidelines and rules 337, as established by the EU Directive 2010/63/EU and the Romanian law 43/2004. All procedures were approved by the Research Ethics Committee of the University of Agricultural Sciences and Veterinary Medicine (USAMV) Cluj-Napoca, Romania, and they were authorized by the State Veterinary Authority (number 369/13.06.2023)

Conflicts of Interest: The authors declare no conflict of interest.

References

1. Garg, K., Brockhouse, J., McAndrew, C.M., Reiter, A.J., Owens, J.G., Mueller, R.J., Pena, G., Ridolfo, A. and Johnson, D.L., Regenerative rehabilitation: Navigating the gap between preclinical promises and clinical realities for treating trauma-induced volumetric muscle loss. *J Physiol* **2025**, *603*, 7421-7439.
2. Corona, B. T., Wenke, J. C., Ward, C. L. Pathophysiology of volumetric muscle loss injury. *Cells Tissues Organs* **2016**, *202(3-4)*, 180-188.
3. Tang, X., Daneshmandi, L., Awale, G., Nair, L.S., Laurencin, C.T. Skeletal Muscle Regenerative Engineering. *Regen Eng Transl Med* **2019**, *5*(*3*), 233-251.
4. Garg, K., Ward, C. L., Hurtgen, B. J., Wilken, J. M., Stinner, D. J., Wenke, J. C., Owens J.G., Corona, B. T. Volumetric muscle loss: persistent functional deficits beyond frank loss of tissue. *J Orthop Res* **2015**, *33(1*), 40-46.
5. Shayan, M., Huang, N.F. Pre-Clinical Cell Therapeutic Approaches for Repair of Volumetric Muscle Loss. *Bioeng* **2020**, *7*, 97.
6. Eugenis, I., Wu, D., Rando, T.A. Cells, scaffolds, and bioactive factors: Engineering strategies for improving regeneration following volumetric muscle loss. *Biomaterials* **2021**, *278*, 121173.
7. Shayan, M., Huang, N.F. Pre-Clinical Cell Therapeutic Approaches for Repair of Volumetric Muscle Loss. *Bioengineering (Basel)* **2020**, 20, *7(3)*, 97.
8. Cittadella Vigodarzere, G., Mantero, S. Skeletal muscle tissue engineering: strategies for volumetric constructs. *Front Physiol* **2014**, *22(5),* 362.
9. Rodriguez, B. L., Florida, S. E., VanDusen, K. W., Syverud, B. C., Larkin, L. M. The maturation of tissue-engineered skeletal muscle units following 28-day ectopic implantation in a rat. *Regen Eng Transl Med* **2019**, *5(1)*, 86-94.
10. Sicherer, S.T., Venkatarama, R.S., Grasman, J.M. Recent Trends in Injury Models to Study Skeletal Muscle Regeneration and Repair. *Bioengineering* (Basel) **2020**, 20, *7(3)*, 76.
11. Greising, S.M., Dearth, C.L., Corona, B.T. Regenerative and Rehabilitative Medicine: A Necessary Synergy for Functional Recovery from Volumetric Muscle Loss Injury. *Cells Tissues Organs* **2016**, *202(3-4)*, 237-249.
12. Testa, S., Fornetti, E., Fuoco, C., Sanchez-Riera, C., Rizzo, F.; Ciccotti, M., Cannata, S., Sciarra, T., Gargioli, C. The War after War: Volumetric Muscle Loss Incidence, Implication, Current Therapies and Emerging Reconstructive Strategies, a Comprehensive Review. *Biomedicines* **2021**, *9*, 564.
13. Wu, X., Corona, B.T., Chen, X., Walters, T.J. A standardized rat model of volumetric muscle loss injury for the development of tissue engineering therapies. *Biores Open Access* **2012**, *1(6)*, 280-90.
14. Magyari, K., Baia, L., Vulpoi, A., Simon, S., Popescu, O., Simon, V. Bioactivity evolution of the surface functionalized bioactive glasses. *J Biomed Mater Res B Appl Biomater* **2015**, *103(2)*, 261-72.
15. Dolan, C.P., Motherwell, J.M., Franco, S.R., Janakiram, N.B., Valerio, M.S., Goldman, S.M., Dearth. C.L. Evaluating the potential use of functional fibrosis to facilitate improved outcomes following volumetric muscle loss injury. *Acta Biomater* **2022**, *140*, 379-388.
16. Meyers, C., Lisiecki, J., Miller, S., Levin, A., Fayad, L., Ding, C., Sono, T., McCarthy, E., Levi, B., James, A.W. Heterotopic Ossification: A Comprehensive Review. *JBMR Plus* **2019**, 27, *3(4)*:e10172.
17. Li, Q., Jiang, Q., Uitto, J. Ectopic mineralization disorders of the extracellular matrix of connective tissue: molecular genetics and pathomechanisms of aberrant calcification. *Matrix Biol.* **2014**, *33*, 23-8.
18. Song, J.H., Liu, M.Y., Ma, Y.X., Wan, Q.Q., Li, J., Diao, X.O., Niu, L.N. Inflammation-associated ectopic mineralization. *Fundam Res* **2022**, *3(6)*, 1025-1038.
19. Giachelli, C.M. Ectopic calcification: gathering hard facts about soft tissue mineralization. *Am J Pathol.* **1999**, *154(3)*, 671-5.
20. Frumento, D.; Ţălu, Ş. Advanced Coating Strategies for Immunomodulatory Biomaterials for Reconstructive Osteogenesis: Mitigating Foreign Body Reaction and Promoting Tissue Regeneration. *Coat* **2025**, *15*, 1026.
21. Careccia, G., Mangiavini, L., Cirillo, F. Regulation of Satellite Cells Functions during Skeletal Muscle Regeneration: A Critical Step in Physiological and Pathological Conditions. *Int J Mol Sci* **2023**, *25(1)*, 512.
22. Tanner, G.I., Schiltz, L., Narra, N., Figueiredo, M.L., Qazi, T.H. Granular Hydrogels Improve Myogenic Invasion and Repair after Volumetric Muscle Loss. *Adv Healthc Mater* **2024**, *13(25)*, e2303576.
23. Rao, Y., Saiz-Gonzalo, G., Prateeksha, P., Wang, A., Shi, H., Wang, W., Li, C. Selection of experimental animals and modeling methods in developmental dysplasia of the hip research. *EFORT Open Rev* **2025**, *10(7)*, 496-509.
24. Ten Brink, T., Damanik, F., Rotmans, J.I., Moroni, L. Unraveling and Harnessing the Immune Response at the Cell-Biomaterial Interface for Tissue Engineering Purposes. *Adv Healthc Mater* **2024**, *13(17)*, e2301939.
25. Li, J., Xie, J., Wang, Y., Li, X., Yang, L., Zhao, M., Chen, C. Development of Biomaterials to Modulate the Function of Macrophages in Wound Healing. *Bioeng* **2024**, *11*, 1017.
26. Järvinen, T.A. Neovascularisation in tendinopathy: from eradication to stabilisation? *Br J Sports Med* **2020**, *54(1)*, 1-2.
27. Beiner, J.M., Jokl, P. Muscle contusion injury and myositis ossificans traumatica. *Clin Orthop Relat Res* **2002**, *403* Suppl: S110-9.
28. King, J.B. Post-traumatic ectopic calcification in the muscles of athletes: a review. *Br J Sports Med* **1998**, *32(4)*, 287-90.
29. Forsberg, J.A., Pepek, J.M., Wagner, S., Wilson, K., Flint, J., Andersen, R.C., Tadaki, D., Gage, F.A., Stojadinovic, A., Elster, E.A. Heterotopic ossification in high-energy wartime extremity injuries: prevalence and risk factors. *J Bone Joint Surg Am* **2009**, *91*(5), 1084-91.

CVJ CLUJ VETERINARY JOURNAL

Research article

Development of a Pilot Behaviour-Based Stress Screening Framework for Dogs and Cats During Veterinary Consultations

Andrei-Sebastian Csiplo [1, 2, *], Silvana Popescu [1, *]

[1] Department of Animal Hygiene and Welfare, Faculty of Veterinary Medicine, University of Agricultural Sciences and Veterinary Medicine Cluj-Napoca, 3-5 Calea Mănăștur, 400372, Cluj-Napoca, Romania
[2] Centre for Animal Welfare, University of Veterinary Medicine Budapest, István u. 2, H-1078, Budapest, Hungary
* Correspondence: andrei-sebastian.csiplo@usamvcluj.ro

Abstract: Veterinary consultations are commonly associated with acute stress in companion animals due to transportation, unfamiliar environments, handling procedures, and previous negative experiences. Although behavioural observations are widely used to recognise stress, practical behaviour-based screening frameworks suitable for routine veterinary practice remain limited. The aim of this pilot study was to identify owner-reported behavioural observations in dogs and cats during veterinary consultations and to develop a preliminary behaviour-based stress screening framework for clinical use. Behavioural data were collected from 50 companion animal owners using a structured questionnaire completed immediately after routine veterinary consultations. Owners reported behavioural responses observed before entering the veterinary practice, immediately after entering, and approximately 10 minutes after entering the waiting area. Behavioural observations were analysed using descriptive statistics according to their frequency and apparent intensity to support the development of a preliminary clinical framework. Attempting escape, fear, trembling, vocalization, and agitation were the most frequently reported stress-related behavioural indicators, while multiple concurrent behaviours were commonly observed, suggesting that behavioural profiles provide more meaningful information than isolated responses. Based on these findings, a preliminary behaviour-based stress screening framework was developed to facilitate rapid clinical interpretation of behavioural observations during routine veterinary consultations. Although further validation using standardized behavioural assessments, independent observers, and larger study populations is required, this pilot study suggests the feasibility of integrating structured behavioural observations into routine veterinary practice and may serve as a starting point for the future development of standardized behaviour-based stress screening methods.

Keywords: companion animals; behaviour; animal welfare; stress; veterinary consultation

Received: 05.07.2026
Accepted: 13.08.2026
Published: 25.08.2026

DOI:10.52331/v31i3rj25

Copyright: © 2021 by the authors. Submitted for possible open access publication under the terms and conditions of the Creative Commons Attribution (CC BY) license (http://creativecommons.org/licenses/by/4.0/).

1. Introduction

Incompatibility between the behaviour of companion animals and the behavioural expectations of their owners remains an important factor contributing to relinquishment, rehoming, and, in some cases, euthanasia of dogs and cats [1]. Consequently, veterinarians play an essential role not only in maintaining animal health but also in promoting positive behavioural development and recognising behavioural problems at an early stage [1]. Veterinary consultations are frequently perceived by companion animals as stressful events due to transportation, unfamiliar environments, novel sensory stimuli, restraint, handling procedures, and previous negative experience [2-6].

Behavioural and physiological responses to these stressors may begin before the animal enters the consultation room, as exposure to multiple consecutive stressors can result in cumulative activation of the stress response, commonly referred to as *stress stacking* [2,3,6]. Acute stress during veterinary visits may compromise clinical examination, reduce the reliability of behavioural assessment, increase the risk of defensive reactions, and negatively influence both animal welfare and owner experience [6-8].

Several approaches have been proposed to minimise stress during veterinary visits, including low-stress handling techniques, environmental modifications, Fear Free®

principles, and clinical audit procedures designed to improve patient care and practice management [6–9]. Although these strategies have significantly improved veterinary practice, practical behaviour-based screening methods that can be rapidly incorporated into routine consultations remain limited. Behavioural observations represent one of the most accessible and clinically applicable approaches for recognising acute stress in companion animals. Behaviours such as attempting escape, fear, trembling, vocalization, agitation, avoidance, and defensive aggression are widely recognised indicators of negative emotional states and may provide valuable information regarding an animal's affective experiences [2-6,10]. Within the Five Domains Model, behavioural responses contribute primarily to the assessment of the mental state domain, reflecting the animal's emotional experiences generated by nutrition, physical environment, health, and behavioural interactions [11,12]. However, behavioural observations alone cannot provide a comprehensive assessment of animal welfare and should therefore be interpreted within the broader context of welfare evaluation.

Therefore, the aim of this pilot study was to identify owner-reported stress-related behavioural indicators in dogs and cats during veterinary consultations and to develop a preliminary behaviour-based stress screening framework suitable for routine veterinary practice. Rather than proposing a validated diagnostic or welfare assessment tool, this study represents an initial step towards the future development and validation of standardized clinical screening methods for recognising acute stress in companion animals.

2. Materials and Methods

2.1. Study Design and Dataset

This pilot observational study was conducted to identify stress-related behavioural indicators in companion animals during routine veterinary consultations and to develop a preliminary behaviour-based stress screening framework suitable for clinical practice. The study was exploratory and descriptive in nature, focusing on the feasibility of behavioural screening rather than on the validation of a diagnostic or welfare assessment instrument.

Behavioural information was collected using a structured questionnaire completed by pet owners immediately after routine veterinary consultations. The study was designed to characterize behavioural responses at different stages of the veterinary visit and to identify behavioural profiles that could support rapid clinical recognition of acute stress.

2.2. Study Population

The study included 50 companion animals (27 dogs and 23 cats) presented for routine veterinary consultations. Only clinically healthy animals, as determined by the attending veterinary team during the consultation, were included in the analysis. Participation was voluntary. Before enrolment, owners received information regarding the objectives of the study and provided informed consent for the anonymous use of the collected data.

Collected data were anonymized in accordance with Regulation (EU) 2016/679 on the protection of personal data [13].

2.3. Questionnaire Design

A structured questionnaire comprising 47 questions was developed to collect information regarding the veterinary visit, the home environment, and owner-reported behavioural observations.

The first section included general information regarding owner consent, the reason for the veterinary visit, and basic characteristics of the animal. The second section addressed aspects of the animal's home environment, including outdoor access, the presence of conspecifics or other animal species, and owner–animal interactions.

The third section focused on behavioural observations recorded at three predefined stages of the veterinary consultation:

- immediately before entering the veterinary practice;
- immediately after entering the practice;
- approximately 10 minutes after entering the waiting area.

Owners selected behavioural descriptors from a predefined list of 19 behaviours commonly associated with stress. Behavioural indicators were selected based on a list provided in a previous research study on pet owners' perceptions of key factors affecting animal welfare during routine veterinary consultations [14]. They were also given the opportunity to describe additional behaviours using free-text responses.

The questionnaire was available in both paper-based and electronic formats according to owner preference.

2.4. Selection of Behavioural Indicators

Behavioural indicators included in the screening framework were selected according to their clinical relevance, reproducibility, and documented association with acute stress responses in companion animals reported in the scientific literature [2-6,10,15].

The evaluated behaviours included escape attempts, fear-related responses, trembling, vocalization, agitation, anxiety, hyperexcitability, insecurity, tail tucking, refusal to enter the veterinary practice, aggression, shyness, and other owner-reported behaviours. These indicators were considered practical behavioural markers that can be readily observed during routine veterinary consultations without specialised equipment or prolonged behavioural assessment.

2.5. Development of the Preliminary Behaviour-Based Stress Screening Framework

Following descriptive evaluation of owner-reported behavioural observations, behavioural indicators were organized according to their apparent association with low, moderate, and high levels of acute stress. Classification of behavioural indicators into low, moderate or high levels of acute stress was based on the relative frequency of owner-reported behavioural traits in their pets during the routine veterinary consultation. The proposed classification was developed exclusively as a preliminary clinical framework intended to facilitate rapid behavioural screening during routine veterinary consultations. It should not be interpreted as a validated welfare assessment or diagnostic instrument. The conceptual basis of the framework was informed by the Five Domains Model, particularly the Mental State domain, while recognising that behavioural observations alone cannot provide a comprehensive assessment of animal welfare [11].

2.6. Methodological Considerations

The proposed framework was based exclusively on owner-reported behavioural observations obtained during routine veterinary consultations. Consequently, behavioural interpretation may have been influenced by owners' experience, perception, and ability to recognise behavioural expressions.

Furthermore, behavioural observations represented only one component of animal welfare assessment and were not validated using physiological measurements, independent behavioural observers, or standardized behavioural assessment protocols.

Accordingly, the present study should be regarded as a pilot exploratory investigation intended to support future development and validation of standardized behaviour-based stress screening methods.

2.7. Statistical Analysis

Data were analysed using descriptive statistics. Behavioural indicators observed at each stage of the veterinary consultation were summarized as frequencies and percentages.

Because the primary objective of this pilot study was exploratory and focused on the development of a preliminary behaviour-based stress screening framework rather than hypothesis testing, no inferential statistical analyses were performed.

3. Results

3.1. Distribution of Stress-Related Behavioural Indicators

A total of 50 questionnaires completed by companion animal owners were included in the analysis. The behavioural indicators used are presented in Table 1.

3.2. Frequency of Stress-Related Behavioural Indicators

The frequency of all owner-reported stress-related behavioural indicators observed at the three stages of the veterinary consultation is presented in Table 1, while the temporal distribution of the five most frequently reported behaviours is illustrated in Figure 1.

Table 1. Behavioural indicators in various moments of the veterinary visit

Indicator	Right Before Entering the Veterinary Practice (%)	Right After Entering the Veterinary Practice (%)	10 Minutes After Entering the Veterinary Practice (%)
Attempting Escape	20.00	11.84	4.84
Fearful	0	19.75	6.45
Trembling	14.67	6.58	8.06
Vocalizing	12.00	9.21	8.06
Agitation	8.00	7.89	9.68
Anxious	0	2.63	6.45
Hyperexcitable	4.00	3.95	0
Insecurity	5.33	2.63	0
Tail Tucking	1.33	0	0
Refusal to Enter	1.33	0	0
Aggressive	0	0	0
Shy	0	5.26	0
Other Behaviours	2.67	0	0

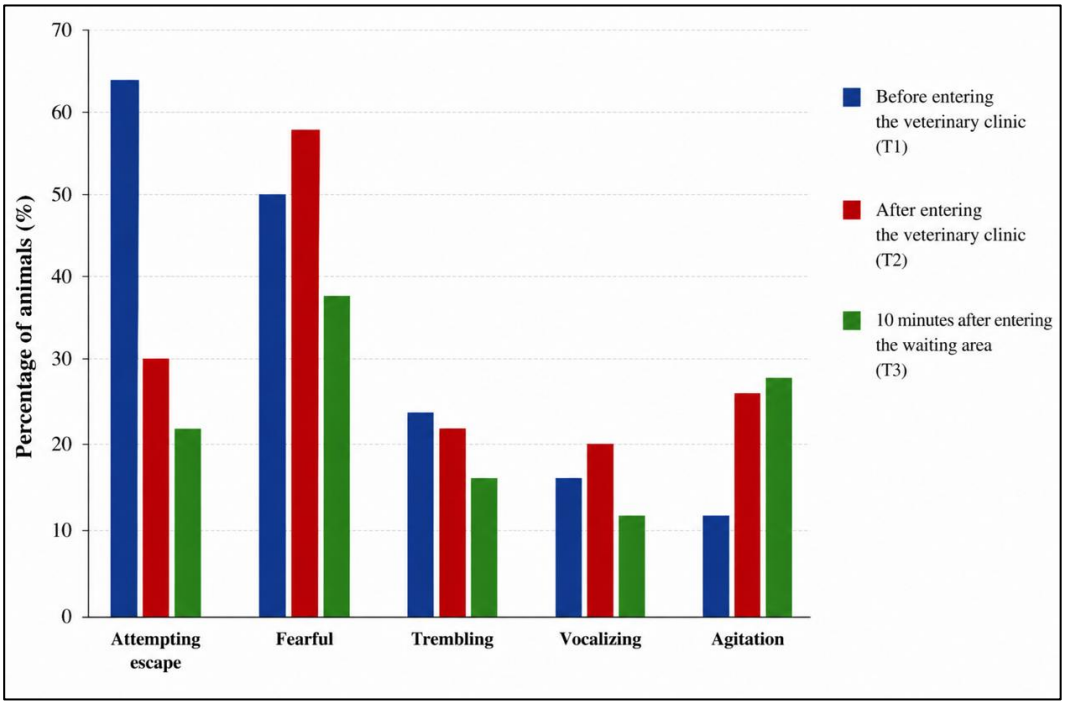


Figure 1. The five most frequently reported behaviours

3.3. Behavioural Profiles and Preliminary Clinical Interpretation

Based on the observed behavioural combinations and their apparent intensity, a preliminary clinical interpretation framework was developed to facilitate rapid recognition of different levels of acute stress during routine veterinary consultations (Table 2).

Table 2. Proposed preliminary clinical interpretation framework on stress-related behavioural indicators observed during veterinary consultations

Stress Level	Behavioural profile	Clinical interpretation	Suggested clinical approach
Low	No stress-related behavioural indicators or only one mild behavioural response	Animal appears to cope well with the veterinary environment	Routine consultation while maintaining calm handling and positive reinforcement
Moderate	Two or three concurrent stress-related behavioural indicators (e.g., fear, trembling, vocalizing or agitation)	Moderate acute stress that may influence behaviour during the consultation	Apply low-stress handling techniques, minimise restraint whenever possible, and allow acclimation before examination
High	Multiple concurrent stress-related behavioural indicators, particularly escape attempts associated with fear, agitation or vocalization	High likelihood of acute stress that may compromise the examination and negatively affect welfare	Consider additional stress-reduction strategies, behavioural support, or postponement of non-urgent procedures when appropriate

4. Discussion

4.1. Behavioural Responses During Veterinary Consultations

Veterinary consultations expose companion animals to a sequence of potentially stressful events, including transportation, unfamiliar environments, restraint, handling procedures, and interactions with unfamiliar people [2,6,10,15]. Consequently, behavioural responses observed during veterinary visits are dynamic and may vary throughout the consultation depending on the animal's previous experiences, coping ability, and the cumulative effect of multiple stressors [2,3,6,16].

The present pilot study identified attempting escape, fear, trembling, vocalization, and agitation as the most frequently reported stress-related behavioural indicators during veterinary consultations. Behavioural responses varied considerably among individual animals, with many owners reporting more than one stress-related behavioural indicator during the veterinary consultation. Many animals displayed multiple stress-related behavioural indicators simultaneously rather than isolated behavioural responses. Combinations of attempting escape, fear, trembling, vocalization, and agitation were characteristic of animals showing more pronounced behavioural responses during the consultation, whereas animals displaying none or only one behavioural indicator generally appeared to cope better with the veterinary environment.

Rather than occurring independently, these behaviours were commonly observed in combination, suggesting that behavioural profiles may provide more meaningful clinical information than isolated behavioural responses. Similar behavioural manifestations have been reported in previous studies investigating fear, anxiety, and stress in companion animals during veterinary visits [6,10,16–19].

Attempting escape was the most frequently reported behavioural indicator before animals entered the veterinary practice and became progressively less common after entering the clinic and during the waiting period. In contrast, fear-related behaviours reached their highest frequency immediately after entering the veterinary practice. Trembling and vocalization were consistently observed throughout the consultation but showed a tendency to decrease during the later stages of the visit. Agitation was reported at all observation stages and showed a slight increase after animals had remained in the waiting area for approximately 10 minutes.

Overall, these findings suggest that behavioural responses changed throughout the veterinary visit (according to pet owners), suggesting that different stages of the consultation were associated with distinct manifestations of acute stress.

The temporal variation observed among behavioural indicators is also consistent with previous reports describing behavioural adaptation during veterinary consultations [6,18]. Attempting escape was most frequently reported before animals entered the veterinary practice, whereas fear-related behaviours became more common immediately after entering the clinic. This pattern may reflect the transition from anticipation of an unfamiliar event to direct exposure to environmental and handling-related stressors [2,3,6].

4.2. Clinical Relevance of the Proposed Screening Framework

Behavioural assessment represents one of the most practical approaches for recognising acute stress during routine veterinary consultations because it is non-invasive, inexpensive, and requires no specialised equipment [6,8,18]. Early identification of stress-related behaviours may facilitate the implementation of low-stress handling techniques, improve communication with owners, and contribute to safer clinical examinations and improved patient management [6,8,18,20].

Unlike comprehensive behavioural assessments, which frequently require prolonged observation or specialised expertise, the framework proposed in the present study was designed as a rapid clinical screening approach suitable for routine veterinary practice. Its primary purpose is to organise behavioural observations in a structured manner and assist veterinary professionals in recognising animals that may benefit from stress-reduction strategies. The proposed framework should be regarded as an exploratory clinical aid intended to support behavioural observation rather than as a validated diagnostic or welfare assessment instrument.

The preliminary clinical interpretation framework proposed in Table 2 should not be regarded as a diagnostic or welfare assessment instrument but rather as a practical aid that supports systematic behavioural observation during routine consultations. Such an approach may improve consistency in recognising stress-related behavioural responses while providing a basis for future refinement and validation.

The proposed screening framework required minimal additional time during routine veterinary consultations and relied exclusively on owner-reported behavioural observations obtained without specialised equipment or additional clinical procedures.

Consequently, the proposed framework appears feasible for incorporation into routine veterinary practice as a preliminary behavioural screening approach. However, further validation using standardized behavioural assessment methods and larger study populations is required before broader clinical implementation.

4.3. Behavioural Observations within the Context of Animal Welfare

Behavioural indicators provide valuable information regarding the emotional experiences of companion animals and therefore contribute to animal welfare assessment [10,11]. Within the Five Domains Model, behavioural responses primarily reflect the Mental State domain, which integrates the affective experiences generated by nutrition, physical environment, health, and behavioural interactions [11].

Nevertheless, behavioural observations alone cannot determine the overall welfare status of an animal. Animal welfare is a multidimensional concept requiring integration of behavioural, physiological, environmental, and health-related information [11]. Consequently, the framework proposed in the present study should be interpreted as a behaviour-based stress screening approach rather than a comprehensive welfare assessment method.

This distinction is particularly important because the present study focused exclusively on behavioural manifestations of acute stress during veterinary consultations and did not include physiological indicators or validated behavioural assessment protocols.

4.4. Study Strengths, Limitations and Future Perspectives

The principal strength of the present study lies in its practical orientation. The proposed framework was developed using behavioural indicators that can be readily recognised by veterinary professionals during routine consultations without additional equipment or extensive behavioural training. Consequently, the framework has the potential to be easily incorporated into everyday clinical practice.

Several limitations should, however, be considered. The study was based on a relatively small sample of companion animals and relied exclusively on owner-reported behavioural observations, which may have been influenced by subjective interpretation and previous experience. In addition, behavioural classifications were not validated using physiological indicators, independent behavioural observers, or standardized ethograms. These limitations should be considered when interpreting the proposed behavioural profiles.

Future studies should evaluate the reproducibility, inter-observer agreement, construct validity, and clinical applicability of the proposed framework in larger and more diverse populations of companion animals. Integration of behavioural observations with physiological indicators of stress may further contribute to the development of standardized behaviour-based stress screening methods suitable for veterinary practice [10,11,20,21].

5. Conclusions

This pilot study identified a range of owner-reported stress-related behavioural indicators commonly observed in dogs and cats during routine veterinary consultations and organised these observations into a preliminary behaviour-based stress screening framework. The findings suggest that combinations of behavioural indicators may provide more meaningful information regarding acute stress than isolated behavioural responses.

The proposed framework offers a simple and practical approach for structuring behavioural observations during routine veterinary consultations. However, it should be regarded as a preliminary clinical aid rather than a validated diagnostic or welfare assessment instrument.

Further studies involving larger and more diverse populations, independent behavioural observers, standardized ethograms, and physiological indicators of stress are required to validate the proposed framework and evaluate its reliability, reproducibility, and clinical applicability.

The present study may serve as a starting point for the future development of standardized behaviour-based stress screening methods that may support early recognition of acute stress and contribute to improved welfare-oriented veterinary care.

Author Contributions: Conceptualisation, A.-S.C. and S.P.; methodology, A.-S.C.; software, A.-S.C.; validation, A.-S.C. and S.P.; formal analysis, A.-S.C. and S.P.; investigation, A.-S.C.; resources, A.-S.C.; data curation, A.-S.C.; writing—original draft preparation, A.-S.C.; writing—review and editing, A.-S.C. and S.P.; visualisation, A.-S.C.; supervision, S.P.; project administration, A.-S.C. and S.P. All authors have read and agreed to the published version of the manuscript.

Funding: This research received no external funding.

Institutional Review Board Statement: This study did not require ethical approval according to Romanian legislation (Law No. 206/2004) as it did not involve medical procedures, personal data processing beyond anonymized responses, or interventions affecting participants' rights or well-being.

Data Availability Statement: Data sharing is applicable to this article, and the data are available upon request from the authors.

Acknowledgements: The authors would like to express their gratitude to all the veterinary staff, including the practice managers, who assisted and participated in performing this study.

Conflicts of Interest: The authors declare no conflicts of interest.

References

1. Hargrave, C. Anxiety, Fear, Frustration and Stress in Cats and Dogs—Implications for the Welfare of Companion Animals and Practice Finances. *Companion Anim*. **2015**, *20*(3), 136–141. https://doi.org/10.12968/coan.2015.20.3.136.
2. Overall, K. L. Manual of Clinical Behavioral Medicine for Dogs and Cats; Elsevier Mosby: St. Louis, MO, **2014**. http://ebookcentral.proquest.com/lib/ed/detail.action?docID=1431145.
3. Mills, D.; Dube, M. B.; Zulch, H. How Animals Respond to Change. In Stress and Pheromonatherapy in Small Animal Clinical Behaviour; Mills, D., Dube, M. B., Zulch, H., Eds.; Wiley-Blackwell: Oxford, UK, **2012**. https://doi.org/10.1002/9781118702642.ch1.
4. Lefman, S. H.; Prittie, J. E. Psychogenic Stress in Hospitalized Veterinary Patients: Causation, Implications, and Therapies. *J. Vet. Emerg. Crit. Care* **2019**, *29*(2), 107–120. https://doi.org/10.1111/vec.12821.
5. Koolhaas, J. M.; Bartolomucci, A.; Buwalda, B.; De Boer, S. F.; Flügge, G.; Korte, S. M.; Meerlo, P.; Murison, R.; Olivier, B.; Palanza, P.; Richter-Levin, G.; Sgoifo, A.; Steimer, T.; Stiedl, O.; Van Dijk, G.; Wöhr, M.; Fuchs, E. Stress Revisited: A Critical Evaluation of the Stress Concept. *Neurosci. Biobehav. Rev.* **2011**, *35*(5), 1291–1301. https://doi.org/10.1016/j.neubiorev.2011.02.003.
6. Sinnott, L. Implementing Strategies to Reduce Stress in the Clinical Setting. *In Pract.* **2025**, *47*, 439–443. https://doi.org/10.1002/inpr.70010.
7. dvm360.com. Veterinarians' Attitudes About Fear Free Practice: Keep Calm and Fear Free On; **2013**. https://www.dvm360.com/view/keep-calm-and-fear-free.
8. Williams, T.; Carroll, A.; Montrose, V. T. Environmental Methods Used by Veterinary Centres to Reduce Stress of Cats and Dogs during Practice Visits. *Vet. Nurse* **2019**, *10*(1), 47–52. https://doi.org/10.12968/vetn.2019.10.1.47.
9. Mosedale, P. Clinical Audit in Veterinary Practice—The Role of the Veterinary Nurse. *Vet. Nurse* **2019**, *10*(1), 4–10. https://doi.org/10.12968/vetn.2019.10.1.4.

10. Polgár, Z.; Blackwell, E. J.; Rooney, N. J. Assessing the Welfare of Kennelled Dogs—A Review of Animal-Based Measures. *Appl. Anim. Behav. Sci.* **2019**, *213*, 1–13. https://doi.org/10.1016/j.applanim.2019.02.013.
11. Mellor, D. J.; Beausoleil, N. J.; Littlewood, K. E.; McLean, A. N.; McGreevy, P. D.; Jones, B.; Wilkins, C. The 2020 Five Domains Model: Including Human–Animal Interactions in Assessments of Animal Welfare. *Animals* **2020**, *10*(10), 1870. https://doi.org/10.3390/ani10101870.
12. Czycholl, I.; Skovlund, C. R.; Forkman, B. Literature Review of the Use of Qualitative Behaviour Assessment with a Fixed List of Terms. *Front. Vet. Sci.* **2026**, *12*, 1588346. https://doi.org/10.3389/fvets.2025.1588346.
13. European Parliament; European Council. Regulation (EU) 2016/679 of the European Parliament and of the Council; **2016**. https://eur-lex.europa.eu/legal-content/EN/TXT/PDF/?uri=CELEX:32016R0679 (accessed 2026-05-02).
14. Csiplo, A.-S.; Popescu, S. Pet Owners' Perceptions of Key Factors Affecting Animal Welfare During Veterinary Visits. *Animals* **2025**, *15*(6), 894. https://doi.org/10.3390/ani15060894.
15. Gazzano, V.; Curadi, M. C.; Baragli, P.; Mariti, C.; Cecchi, F.; Cavallo, S.; Sacchettino, L.; Gazzano, A. Physiological and Behavioral Evaluation of Shelter Dogs During Veterinary Routine Health Checks. *Vet. Sci.* **2025**, *12*(6), 583. https://doi.org/10.3390/vetsci12060583.
16. Jankord, R.; Herman, J. P. Limbic Regulation of Hypothalamo-Pituitary-Adrenocortical Function during Acute and Chronic Stress. *Ann. N. Y. Acad. Sci***. 2008**, *1148*, 64–73. https://doi.org/10.1196/annals.1410.012.
17. Hennessy, M. B. Using Hypothalamic–Pituitary–Adrenal Measures for Assessing and Reducing the Stress of Dogs in Shelters: A Review. *Appl. Anim. Behav. Sci.* **2013**, *149*(1–4), 1–12. https://doi.org/10.1016/j.applanim.2013.09.004.
18. Trevorrow, N. Helping Cats Cope with Stress in Veterinary Practice. *Vet. Nurs. J.* **2013**, *28*, 327–329. https://doi.org/10.1111/vnj.12074.
19. Abubakar, A. A.; Kaka, U.; Ngiow, E. W.; Goh, Y. M. Behavioural Indicators of Stress in Cats During Veterinary Visits: Effects of Transportation and Clinical Examinations. *Pertanika J. Trop. Agric. Sci.* **2025**, *48*(6), 1817–1829. https://doi.org/10.47836/pjtas.48.6.09.
20. Erickson, A.; Harbin, K.; MacPherson, J.; Rundle, K.; Overall, K. L. A Review of Pre-Appointment Medications To Reduce Fear and Anxiety in Dogs and Cats at Veterinary Visits. *Can. Vet. J.* **2021**, *62*(9), 952–960.
21. Steimer, T. The Biology of Fear- and Anxiety-Related Behaviors. *Dialogues Clin. Neurosci.* **2002**, *4*(3), 231–249. https://doi.org/10.31887/DCNS.2002.4.3/tsteimer.

CVJ CLUJ VETERINARY JOURNAL

Case Report

Occurrence of *Ozobranchus margoi* (Hirudinea), an Important Sea Turtle Ectoparasite, on a *Caretta caretta* Individual at Kızılot Beach, Antalya

Fatih Polat[1], Selma Köle[2], Hikmet Buru[2], Deniz İnnal[1]*

[1] Burdur Mehmet Akif Ersoy University, Department of Biology, Istiklal Campus, 15030, Burdur, Türkiye; innald@yahoo.com, fatihpolattt@gmail.com
[2] Ecological Research Society, EKAD, Ankara, Türkiye; selmakole7@gmail.com, hikmetburu@hotmail.com
* Correspondence: innald@yahoo.com

Abstract: Sea turtles function as keystone species within subtropical and Mediterranean marine ecosystems, playing a crucial role in maintaining ecosystem balance through nutrient cycling and the preservation of critical habitats. However, human activities including bycatch in fisheries, habitat degradation, and climate change pose significant threats to their survival. In addition to these anthropogenic pressures, parasitic infestations represent important biological factors affecting sea turtle health. This study reports the first record of *Ozobranchus margoi* infestation from Kızılot Beach (Antalya, Türkiye), documented on an adult female *Caretta caretta* during nesting on July 10, 2025. Morphometric measurements, including curved and straight carapace length and width, were recorded, and the general health condition of the individual was assessed. A total of 16 *O. margoi* individuals were detected on the ventral axillary surface. Macroscopic examination of the attachment site revealed mild erythema and superficial dermal erosion, although no histopathological analysis was performed. Species of the genus *Ozobranchus* are recognized as potential mechanical vectors of *Chelonid alphaherpesvirus 5* (ChHV5), the causative agent of fibropapillomatosis (FP) in sea turtles; however, no molecular screening for ChHV5 was conducted in this study, and no macroscopic signs of FP were observed. This report contributes baseline ectoparasite data for a newly monitored nesting site and highlights the importance of integrating parasitological assessments into routine sea turtle monitoring programs at Kızılot Beach.

Keywords: Sea turtle, Ectoparasite, Hirudinea, Mediterranean, Population health

1. Introduction

Sea turtles are keystone species of critical importance for the health and balance of marine ecosystems. The Mediterranean basin provides important nesting grounds, particularly for *Caretta caretta* (Loggerhead sea turtle) and *Chelonia mydas* (Green sea turtle). However, these populations are under intense anthropogenic pressure due to habitat loss, marine pollution, bycatch, and climate change [1, 2]. Apart from these physical threats, parasitic infestations are among the significant biological factors affecting the health status, immune system, and reproductive success of turtles [3]. While conservation efforts in the Mediterranean have gained momentum in recent years, parasitological studies have revealed that a wide range of parasitic organisms adversely affect sea turtle health. Specifically, parasitic prevalence and its associated physiological and pathological effects vary depending on the parasite species, seasonality, and host factors such as age and sex [4–7]. Among the ectoparasites of sea turtles, members of the family Ozobranchidae belonging to the class Hirudinea (leeches) occupy a specialized ecological niche [8]. Within this family, *Ozobranchus margoi* (Apáthy, 1890) and *Ozobranchus branchiatus* (Menzies, 1791) are known as obligate ectoparasites of sea turtles [3, 8]. While *O. margoi* shows host specificity mainly toward *Caretta caretta* and *O. branchiatus* mainly toward *Chelonia mydas*, cross-infestations have also been reported [9]. These hematophagous organisms survive by attaching to the soft tissues of turtles, especially under the flippers, in the neck region, and around the cloaca [8].

Received: 29.03.2026
Accepted: 04.05.2026
Published: 20.05.2026

*DOI:*10.52331/V31i2eg19

Copyright: © 2021 by the authors. Submitted for possible open access publication under the terms and conditions of the Creative Commons Attribution (CC BY) license (http://creativecommons.org/licenses/by/4.0/).

Heavy infestations of *Ozobranchus spp*., where a single host may carry more than one hundred leeches, cause debilitating conditions including anemia, ocular injuries, and ulcerative lesions in the dermis. This extensive tissue damage not only compromises the turtle's health but also creates entry points for secondary infections, potentially leading to host death [9, 10]. However, the primary importance of these leeches in terms of ecology and veterinary medicine lies in their relationship with fibropapillomatosis (FP), a disease that can be fatal in sea turtles. Molecular studies have revealed that *Ozobranchus* species have the potential to serve as mechanical vectors for *Chelonid alphaherpesvirus 5* (ChHV5), the causative agent of FP [11]. The hypothesis that leeches can carry the virus with a high viral load during blood feeding and transmit it to healthy individuals represents a major concern regarding the epidemiology of this disease [12].

On the Turkish Mediterranean coast, *O. margoi* was first reported by İşler et al. [13] from a severely infested *C. caretta* individual admitted to a sea turtle rescue center in Hatay province. More recently, Düşen et al. [14] conducted a comprehensive parasitological survey on 34 loggerhead and green sea turtles from the eastern Mediterranean coast of Türkiye, reporting *O. margoi* among the ectoparasite fauna and providing detailed data on prevalence. Despite these contributions, reports of *O. margoi* from the Turkish Mediterranean coast remain limited. Notably, no parasitological data have been reported from Kızılot Beach, a relatively newly monitored nesting site. The present study therefore constitutes the first record of *O. margoi* infestation from this locality and aims to provide baseline ectoparasite data for the local *C. caretta* population, while documenting the associated dermal pathology at the individual level.

2. Materials and Methods

2.1. Study Area

This study was carried out at Kızılot Beach (approximately 36S 0372662 E, UTM 4063138 N), located within the borders of Antalya province in southwestern Turkey. This beach is one of the most important *Caretta caretta* nesting areas in the Eastern Mediterranean and hosts the nesting activities of hundreds of females turtles every year. Fieldwork was conducted within the scope of the local sea turtle conservation and monitoring program permits.

2. 2. Examination of the Host Animal and Sampling

On the night of July 10, 2025, at approximately 02:00 local time, an adult female *Caretta caretta* individual coming ashore for nesting was detected. During the tagging and routine health check of the individual, clustered ectoparasites were observed in the ventral axillary surface. The general condition of the individual was evaluated as good; however, localized lesions were recorded in the region where the parasites were located. Morphometric measurements of the turtle were made using a tape measure and calipers in accordance with standard techniques. Measurements were recorded as Curved Carapace Length (CCL), Curved Carapace Width (CCW), Straight Carapace Length (SCL), and Straight Carapace Width (SCW).

2.3. Collection and Identification of Parasites

Parasites were carefully removed using soft-tipped forceps in order to avoid additional tissue damage to the host. A total of 16 leech specimens were collected and preserved in 70% ethanol for subsequent laboratory examination. In the laboratory, specimens were examined under a stereo microscope (Nikon SMZ745T). All individuals exhibited a clearly distinguishable body division into a trachelosome (anterior region) and urosome (posterior region), with a well-developed posterior sucker clearly visible. The urosome bore five pairs of lateral, digitiform branchiae (gills), which were symmetrically arranged along the midbody segments (Fig. 1). The anterior sucker was comparatively smaller than the posterior sucker, and the overall body morphology was consistent with members of the family Ozobranchidae. Based on the combination of these diagnostic morphological characteristics—particularly the presence of five pairs of lateral branchiae and the distinct trachelosome–urosome differentiation—the specimens were identified as *Ozobranchus margoi* (Apáthy, 1890), following the descriptions provided by the relevant taxonomic literature [15, 16].

3. Results

The morphometric measurements of the examined female *Caretta caretta* individual are presented in Table 1. All 16 parasite specimens collected from the host were identified as the marine leech *Ozobranchus margoi* based on morphological analysis (Fig. 1).

Table 1. Morphometric measurements of the *Caretta caretta* individual infected with *Ozobranchus margoi*.

Parameter	Abbreviation	Value (cm)
Curved Carapace Length	CCL	76.7
Curved Carapace Width	CCW	67.6
Straight Carapace Length	SCL	72.3
Straight Carapace Width	SCW	54.1

All parasites were found clustered in an area of approximately 2–3 cm in diameter in the ventral axillary surface. Macroscopic examination of the attachment site revealed mild erythema (redness) and superficial dermal erosion. It should be noted that these observations were based solely on visual inspection; no histopathological or microbiological analyses were performed to further characterize the tissue damage.

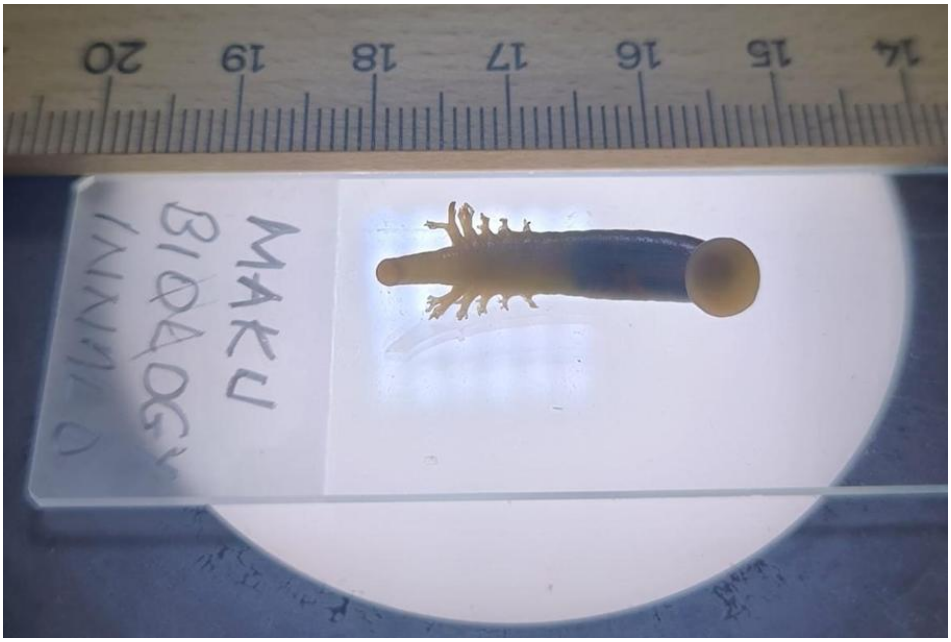


Figure 1. Stereo microscope image of an *Ozobranchus margoi* specimen collected from the infected *Caretta caretta* individual and fixed in 70% ethyl alcohol.

4. Discussion

This study presents the first record of *Ozobranchus margoi* infestation from Kızılot Beach, Antalya, documented on a nesting *Caretta caretta* female, along with the local pathological effects caused by the parasite on the host. The findings are consistent with the global literature confirming that this leech species is a common ectoparasite in *C. caretta* populations [9, 16].

The infestation intensity observed in this study (16 leeches on a single individual) is relatively low compared with the ranges reported in the Mediterranean literature. A severe infestation case was previously described in Hatay province, Türkiye, where hundreds of *O. margoi* individuals were detected on a single injured *C. caretta*; the parasites were densely clustered in the nasal cavity, neck, and cloacal regions, and were also found on the flippers, soft tissues, and even on the skull and jaw areas [13]. In contrast, Sterioti et al. [16] reported more than 1,000 individuals on two turtles from Greece. In a more comprehensive and recent study conducted on the eastern Mediterranean coast of Türkiye, Düşen et al. [14] reported the presence of *O. margoi* in 2 out of 34 turtles; however, the number of leeches per host was not quantified.

It is important to note that in those studies, turtles were examined as injured or dead individuals in laboratories or rehabilitation centers, whereas the *C. caretta* individual detected at Kızılot Beach in the present study had come ashore for nesting and was in good general health condition. Furthermore, only the leeches visible during the nighttime field survey were evaluated; additional parasites may have been present in other body regions (e.g., neck, cloaca, or under the rear flippers) that were not accessible during the brief

examination. Therefore, the recorded intensity of 16 leeches likely represents an underestimate of the actual parasite burden. Systematic and long-term surveys, ideally including thorough body examinations, are essential to establish reliable infestation trends and to evaluate the health status of the local sea turtle population.

The lesions detected in the axillary region of the examined turtle reflect the typical tissue damage caused by *Ozobranchus* species. Mild erythema and superficial dermal erosion were observed at the attachment site, likely resulting from the feeding activities of the leeches. Although these macroscopic findings are consistent with previously reported leech-associated tissue damage [9], the absence of histopathological examination in the present study precludes definitive conclusions regarding the depth and nature of tissue injury. Previous studies conducted on the Turkish coast also reported that *O. margoi* was found in similar attachment areas (neck and under flippers) and caused dermatitis [14]. These observations suggest that *O. margoi* attachment may compromise local skin integrity, although the broader physiological impact on the host cannot be determined from macroscopic assessment alone.

In the broader context of sea turtle health, *Ozobranchus* species have been identified as potential mechanical vectors for *Chelonid alphaherpesvirus 5* (ChHV5), the causative agent of fibropapillomatosis (FP), a debilitating neoplastic disease in sea turtles [11]. Previous studies have demonstrated that these leeches can harbor high viral loads acquired during blood feeding on infected hosts [12]. It is important to note, however, that in the present study, no molecular screening for ChHV5 was conducted on the collected leech specimens, and no macroscopic signs of FP (such as cutaneous or ocular tumors) were observed in the examined *C. caretta* individual. Therefore, while the presence of *O. margoi* at Kızılot Beach raises the theoretical concern of potential ChHV5 transmission within the local population, this remains speculative and requires dedicated molecular investigation in future studies.

Monitoring ectoparasites is important for understanding the general health status of sea turtles and detecting changes in the marine ecosystem. It has been predicted that shifts in the distribution of parasite populations and infestation rates may occur in response to climate change. Therefore, focusing on parasite load and associated health parameters, in addition to turtle population numbers, in monitoring studies conducted at important nesting areas such as Kızılot Beach is essential for the success of conservation strategies.

A further limitation of the present study is that species identification was based exclusively on morphological characters without molecular confirmation (e.g., COI barcoding). Although the morphological features observed were consistent and diagnostic for *O. margoi*, future studies should incorporate molecular tools to provide definitive species-level verification.

5. Conclusions

This case report documents the occurrence of *Ozobranchus margoi* on a nesting *Caretta caretta* female at Kızılot Beach, Antalya, representing the first ectoparasite record from this locality. The infestation of 16 leeches was associated with localized macroscopic tissue alterations at the attachment site. While the broader health implications cannot be determined from a single observation, this finding underscores the importance of incorporating parasitological assessments into routine monitoring protocols at Kızılot Beach, particularly given the potential role of *Ozobranchus* species as mechanical vectors of ChHV5. Future studies at this site should aim to: (I) determine the prevalence and intensity of *O. margoi* infestation across multiple nesting seasons; (II) perform molecular screening of collected leeches for ChHV5; and (III) conduct histopathological analyses of leech-associated lesions to better characterize tissue-level impacts.

Author Contributions: Conceptualization, D.İ.; methodology, F.P., S.K. and H.B.; validation, F.P., S.K., H.B. and D.İ.; formal analysis, D.İ. and F.P.; investigation, F.P., S.K. and H.B.; resources, D.İ.; data curation, D.İ.; writing—original draft preparation, F.P., S.K. and H.B.; writing—review and editing, D.İ.; visualization, D.İ.; supervision, D.İ. All authors have read and agreed to the published version of the manuscript.

Funding: This research was funded by Tüprag Metal Madencilik Sanayi ve Ticaret A.Ş.

Institutional Review Board Statement: This study was conducted under the permit issued by the Republic of Türkiye, Ministry of Agriculture and Forestry, General Directorate of Nature Conservation and National Parks (dated 19.03.2024, numbered E-21264211-288.04-13655744), titled "Investigation, Monitoring, and Conservation of Sea Turtle (*Caretta caretta, Chelonia mydas*) Populations at Kızılot Beach, Manavgat District, Antalya Province". The study was carried out in accordance with ethical principles and does not involve any invasive procedures or experimental applications. Therefore, no additional approval/letter from a Local Animal Ethics Committee was required.

Data Availability Statement: The relevant data are included in the results file/documentation prepared within the scope of the permit/project issued by the Republic of Türkiye, Ministry of Agriculture and Forestry.

Acknowledgments: We would like to thank Dr. Ali Fuat Canbolat, the project coordinator, for his support and for facilitating the fieldwork. We also thank Tüprag Metal Madencilik Sanayi ve Ticaret A.Ş. for financial support, and the Ecological Research Association (EKAD) along with all EKAD volunteers for their valuable contributions to the fieldwork.

Conflicts of Interest: The authors declare no conflict of interest. The funders had no role in the design of the study; in the collection, analyses, or interpretation of data; in the writing of the manuscript, or in the decision to publish the results.

References

1. Casale P., Broderick A. C., Camiñas J. A., Cardona L., Carreras C., Demetropoulos A., et al. Mediterranean sea turtles: current knowledge and priorities for conservation and research. *Endanger Species Res* **2018**, 36, 229-67.
2. Davenport J. Sea turtles in the Anthropocene. *Biology and Environment (PRIA)* **2024**, 124B(2/3), 103-29.
3. Lockley E. C., Fouda L., Correia S. M. Long-term survey of sea turtles reveals correlations between parasite infection, feeding ecology, reproductive success and population dynamics. *Sci Rep* **2020**, 10, 18569.
4. Kučinić M., Lazar B., Mladineo I., Zavodnik D., Žuljević A., Tvrtković N., editors. Intestinal helminths of loggerhead sea turtle, *Caretta caretta*, from eastern Adriatic Sea. Proceedings of the Twenty-fourth International Symposium on Sea Turtle Biology and Conservation; Part 2: Poster presentation; 2008: Miami (FL): National Marine Fisheries Service (NMFS).
5. Karaa S., Jrıbı I., Marouanı S., Jrıjer J., Bradaı M. N. Preliminary study on parasites in loggerhead turtles. *Am J Biomed Sci Res* **2019**, 5(5), 373-6.
6. Pace A., Rinaldi L., Ianniello D., Borrelli L., Cringoli G., Fioretti A., et al. Gastrointestinal investigation of parasites and Enterobacteriaceae in loggerhead sea turtles. *BMC Vet Res* **2019**, 15.
7. Marangi M., Carlino P., Profico C., Olivieri V., Totaro G., Furii G., et al. Coprological survey on helminth parasite communities of free-living loggerhead sea turtles. *Int J Parasitol Parasites Wildl* **2020**, 11, 207-12.
8. Rittenburg L. T., Kelley J. R., Mansfield K. L., Savage A. E. Marine leech parasitism of sea turtles varies across host species, seasons, and the tumor disease fibropapillomatosis. *Dis Aquat Org* **2021**, 143, 1-12.
9. Rodenbusch C. R., Marks F. S., Canal C. W., Reck J. Marine leech *Ozobranchus margoi* parasitizing loggerhead turtle (*Caretta caretta*) in Rio Grande do Sul, Brazil. *Rev Bras Parasitol Vet* **2012**, 21(3), 301-303.
10. Schwartz F. The marine leech *Ozobranchus margoi* (Hirudinea). *J Parasitol* **1974**, 60, 889-90.
11. Greenblatt R. J., Work T. M., Balazs G. H., Sutton C. A., Casey R. N., Casey J. W. The Ozobranchus leech is a candidate mechanical vector for the fibropapilloma-associated turtle herpesvirus. *Virology* **2004**, 321(1), 101-110.
12. Farrell J. A., Yetsko K., Whitmore L., Whilde J., Eastman C. B., Ramia D. R., et al. Environmental DNA monitoring of oncogenic viral shedding and genomic profiling of sea turtle fibropapillomatosis reveals unusual viral dynamics. *Commun Biol*, **2021**, 4:565.
13. İşler C. T., Orunç Kılınç Ö., Altuğ M. E., Yılmaz A. B., editors. Mustafa Kemal Üniversitesi Deniz Kaplumbağaları İlk Yardım Tedavi ve Kurtarma Araştırma ve Uygulama Merkezine getirilen bir *Caretta caretta* türü deniz kaplumbağasında şiddetli *Ozobranchus margoi* olgusu ve tedavisi. 19 Ulusal Parazitoloji Kongresi & Uluslararası Katılımlı Ekinokokkozis Sempozyumu; 2015; Erzurum, Turkey.
14. Düşen S., Kaska Y., Yılmaz M., Ulubeli S. A. Endoparasites and epibionts of loggerhead and green sea turtles from the eastern Mediterranean, Turkey: A detailed assessment. *Helminthologia* **2025**, 62(1), 40-49.
15. Sawyer R. T. Leech biology and behaviour. *Feeding, Biol, Ecol and Systematics* **1986**, 1:3.
16. Sterioti A., Doxa C. C., Grigoriou P., Vardanis G., Cascarano M. C., Katharios P. *Ozobranchus margoi* infections in loggerhead turtles (*Caretta caretta*) in Greece and potential treatment options. *J Exot Pet Med* **2017**, 26(3), 196-199.

CVJ CLUJ VETERINARY JOURNAL

Case report

Splenic Abscessation Due to a Migrating Grass Awn in a Cat

Alexandr Morozov [1,*], Caren Dolgopolov [2] and Ivan Manchev [2]

[1] Moldova State University, Institute of Zoology, Center of Research of Biological Invasions, Laboratory of Systematics and Molecular Phylogeny, MD-2028 Chişinău, Republic of Moldova; alexandr.morozov@sti.usm.md
[2] Ciavdar Private Clinic, Chişinău, Republic of Moldova; carendolgopolov@gmail.com (C.D.); ivan-manchev89@gmail.com (I.M.)
* Correspondence: alexandr.morozov@sti.usm.md;

Abstract: Migrating grass awns are a recognized cause of foreign-body inflammation and abscessation in dogs and cats; however, splenic involvement in feline patients is exceptionally rare. To the best of our knowledge, this is the second documented feline case of splenic abscessation associated with a migrating plant foreign body. This report describes a 6-year-old domestic shorthair cat that presented with pyrexia, anorexia and a mass in the left cranial abdomen. Ultrasonography revealed focal splenic lesions, and exploratory laparoscopy identified a splenic abscess with localized peritonitis. The procedure was converted to exploratory coeliotomy and total splenectomy. Histopathological examination showed multiple abscesses, microinfarctions and a plant awn embedded in the spleen. This case highlights the importance of considering migrating foreign bodies in the differential diagnosis of atypical splenic lesions and demonstrates that surgical intervention can result in a favorable short-term outcome.

Keywords: grass awn; splenic abscess; migrating foreign body; plant foreign body; splenectomy; cat

Received: 23.06.2026
Accepted: 24.07.2026
Published: 03.08.2026

DOI:10.52331/v31i36j09

Copyright: © 2021 by the authors. Submitted for possible open access publication under the terms and conditions of the Creative Commons Attribution (CC BY) license (http://creativecommons.org/licenses/by/4.0/).

1. Introduction

Grass awns (foxtails) are fusiform plant structures with sharp tips and backward-pointing barbs that favor unidirectional penetration and continued migration through tissue [1–3]. Entry may occur through the skin or a natural orifice, including the respiratory and gastrointestinal tracts; subsequent migration can cause chronic inflammatory tracts, granulomas and abscesses. Because the plant material is small and may be poorly conspicuous on routine imaging, the foreign body itself may not be identified even when secondary lesions are evident [3,4]. Splenic involvement is exceedingly rare in any species, and plant foreign bodies in the feline spleen have been reported only rarely [5]. A PubMed search performed on 10 March 2026, using combinations of the terms cat/feline, spleen/splenic and grass awn/foxtail/plant material/foreign body, identified only one previously published feline case in which plant material was embedded in the spleen and managed by splenectomy [5]. The present report describes an additional case of splenic abscessation associated with a migrating vegetal foreign body in a cat.

2. Materials and Methods

A six-year-old neutered male domestic shorthair cat with outdoor access presented with a five-day history of inappetence and intermittent pyrexia. On admission, the cat was quiet but responsive. Rectal temperature was 39.4 °C (adult reference 36.7–38.9 °C) [6]. Oral mucous membranes were pale and tacky, and skin tent was mildly prolonged. Heart rate was 180 beats/min. Respiratory rate was 58 breaths/min, which is within the range reported for cats examined in veterinary consultation rooms [7]. On abdominal palpation, a firm mass was detected in the left cranial abdomen.

As part of the diagnostic work-up, the following tests were conducted: haematology with manual blood-smear review (including platelet aggregation assessment), erythro-

cyte sedimentation rate, serum biochemistry, abdominal ultrasonography (Mindray Vetus 7, micro-convex transducer at 5–8 MHz), thoracic radiography in right lateral and ventrodorsal views (Mindray Vetix S300; 40–55 kVp, 2–4 mAs), and buccal mucosal bleeding time.

A diagnostic laparoscopy was undertaken initially to inspect the abdominal cavity; after purulent effusion and a splenic abscess were identified, the procedure was converted to a ventral midline coeliotomy for definitive source control. General anaesthesia was induced with propofol (4 mg/kg intravenously; PropoFlo, Zoetis, USA) after premedication with butorphanol (0.3 mg/kg intramuscularly (IM); Butomidor, Richter Pharma, Austria) and midazolam (0.2 mg/kg IM; B. Braun, Germany). Anaesthesia was maintained with isoflurane in oxygen. Broad-spectrum perioperative antimicrobial therapy was administered because infection was strongly suspected. The cat received amoxicillin–clavulanate (20 mg/kg intravenously every 12 h; Amoxigard 140 mg/mL, Nita-Farm, Russia) in accordance with local veterinary guidelines [8]. Analgesia comprised tramadol (2 mg/kg intravenously every 12 h; Tramadol 50 mg/mL, KRKA, Slovenia) and meloxicam (0.1 mg/kg subcutaneously; Meloxivet 5 mg/mL, Provet, Ukraine). Intravenous fluid therapy consisted of a balanced crystalloid solution (Ringer's lactate, Infomed, Moldova) delivered by infusion pump (Mindray BeneFusion, China) at 4 mL/kg/h during anaesthesia.

A total splenectomy was performed using a standard hilar approach. The splenic vascular pedicle and major hilar branches were isolated and ligated in a routine manner prior to transection, using 2 metric polydioxanone suture (PDS II; Ethicon, USA). Total operative time was approximately 95 min, and estimated intraoperative blood loss was approximately 25 mL. The abdominal cavity was thoroughly lavaged with copious volumes of warm 0.9% sterile saline (Iuria-Farm, Republic of Moldova).

The coeliotomy incision was closed routinely in layers: the abdominal wall (linea alba) with a simple continuous pattern using 2 metric polydioxanone (PDS II; Ethicon, USA), and the subcutaneous tissue and skin with simple interrupted sutures using 4-0 poliglecaprone 25 (Monocryl; Ethicon, USA). The excised spleen was submitted for histopathological analysis. Before closure, a homemade active closed-suction drain was placed in the abdominal cavity.

Histological sections of the excised spleen were stained with haematoxylin and eosin (H&E) and examined using a Motic Panthera DL light microscope (Motic, China) equipped with a UC-MF 10×/22 eyepiece (10× magnification; field number 22 mm) and 10× and 20× objectives. Representative fields were photographed using the 10× and 20× objectives; with the 10× eyepiece, these corresponded to nominal visual magnifications of 100× and 200×, respectively. Image scale was calibrated with a stage micrometer graduated in 0.01-mm divisions.

3. Results

Haematology demonstrated anaemia (haemoglobin 8.0 g/dL; reference interval: 10–16 g/dL), marked leucocytosis (16 × 10^9/L; reference interval: 5–14 × 10^9/L) characterized by neutrophilia with a left shift (65% segmented and 17% band neutrophils), and severe thrombocytopenia on the automated count (37 × 10^9/L; reference interval: 180–500 × 10^9/L). Manual review of a blood smear, including assessment for platelet aggregation, showed an adequate platelet estimate, raising suspicion that the automated platelet count was spuriously low. The erythrocyte sedimentation rate was markedly increased (70 mm/h; reference interval: <20 mm/h). Serum biochemistry demonstrated a mild increase in total protein (81 g/L; reference interval: 60–80 g/L). Other measured biochemical parameters were within reference intervals.

Ultrasonography (Figure 1a, b) showed an unevenly enlarged spleen with irregular but well-defined external margins and diffusely heterogeneous, moderately hypoechoic parenchyma. Two principal focal lesions, each approximately 1–2 cm in diameter, were hypoechoic to anechoic, with heterogeneous internal echogenicity, fine echogenic septations and irregular, poorly defined margins. Multiple hyperechoic foci casting distal acoustic shadowing were interpreted as possible mineralization. The splenic veins were mildly dilated. The adjacent omentum was moderately hyperechoic, consistent with focal omentitis, and a small volume of anechoic free fluid was present adjacent to the splenic tail. No discrete foreign body was visualized.

Thoracic radiography detected no pulmonary or mediastinal abnormalities. Buccal mucosal bleeding time (BMBT) was 3.5 min (reference interval: <4 min). Given the severely reduced automated platelet count, perioperative transfusion was considered; however, neither feline blood products nor a suitable donor were available.

Differential diagnoses included splenic abscess or granuloma, haematoma, lymphoma and haemangiosarcoma. The cavitary lesions and adjacent inflammatory change favored an inflammatory or infectious process, although neoplasia could not be excluded on ultrasonography alone. At laparoscopy, purulent effusion, fluctuant encapsulated splenic nodules and dense inflammatory adhesions made lymphoma and haemangiosarcoma less likely; histopathological examination subsequently excluded neoplasia.

On laparoscopic examination, the spleen appeared moderately enlarged and was adherent to the omentum and intestinal loops. A small amount of perisplenic fibrinous exudate and approximately 30 mL of purulent free fluid were observed; the volume was estimated visually during laparoscopy. Further exploration revealed several well-defined, encapsulated nodular lesions on the splenic surface, with firm adhesions to the adjacent mesentery, omentum, intestinal loops and abdominal wall. The lesions were fluctuant on palpation, suggesting fluid content; however, no rupture, penetrating wound or visible foreign material was observed at this stage. The procedure was converted to open coeliotomy.

Following surgery, the cat recovered steadily without complications. Within 48 h, appetite resumed, and body temperature stabilized at 38.3 °C (adult reference range: 36.7–38.9 °C) [6]. The patient received intravenous Ringer's solution (Iuria-Farm, Republic of Moldova) at 4 mL/kg/h for the first 24 h postoperatively. Antimicrobial therapy was continued with amoxicillin–clavulanate (Clavusan; KRKA, Slovenia) administered orally at 12.5 mg/kg every 12 h for 7 days. Analgesia was maintained with meloxicam (0.05 mg/kg per os once daily; Meloxivet 5 mg/mL, Provet, Ukraine) for 3 days postoperatively.

Postoperative haematology was performed to monitor recovery. Two days after surgery, haemoglobin was 10.0 g/dL (reference interval: 10–16 g/dL), platelets were 152 × 10^9/L (reference interval: 180–500 × 10^9/L), and white blood cells were 20.2 × 10^9/L (reference interval: 5–14 × 10^9/L).

The cat was discharged 48 h postoperatively with the drain in place and instructions for drain care, output monitoring and recognition of complications. Outpatient management was considered acceptable because the cat was clinically stable, a medically trained member of the household could provide the required care, and prompt re-evaluation was available.

Gross pathological examination of the excised spleen revealed multiple thick-walled cavities containing purulent material distributed throughout the parenchyma. Approximately 40–50% of the organ was estimated grossly to have been replaced by firm connective tissue. Several small, sharply demarcated infarcts were also evident on the capsular and cut surfaces. Within one of the abscess cavities, a linear fragment of plant material consistent with a grass awn, approximately 4 cm in length, was identified (Figure 1c–e).

Microscopically, in the affected regions, normal splenic architecture was completely effaced by severe pyogranulomatous inflammation, characterized by areas of coagulative necrosis surrounded by dense infiltrates of neutrophils, macrophages, lymphocytes and proliferating fibroblasts. Multifocal granulomas were present, and numerous small blood vessels showed thrombosis and disruption, correlating with the grossly observed microinfarcts. Multiple irregular refractile fragments of foreign material with preserved, regularly compartmentalized cellular architecture and discernible cell walls, consistent with plant tissue, were present within the affected splenic tissue (Figure 2). Clear spaces surrounded some fragments, which were closely associated with inflammatory and fibrous tissue. No evidence of neoplasia was detected in any examined section.

The abdominal drain produced a total of 10–15 mL of serosanguineous fluid and was removed without sedation four days postoperatively. The cat remained normothermic (38.3 °C; adult reference 36.7–38.9 °C). The incision was clean, with no swelling or discharge. At the two-week follow-up, the cat was bright, alert and eating well, and the surgical site had healed.

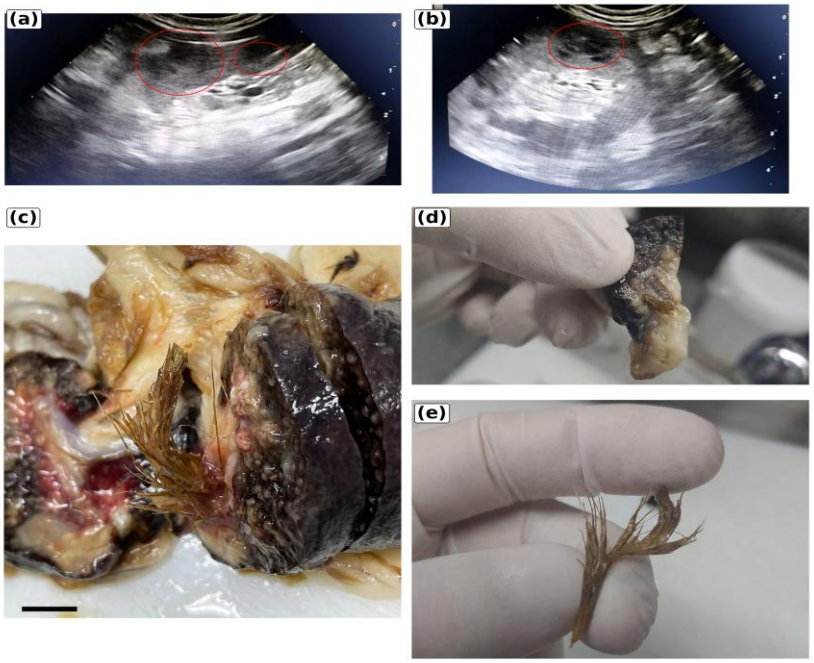


Figure 1. Composite imaging and gross pathological findings: (**a**,**b**) ultrasonographic appearance of heterogeneous cavitary splenic lesions with irregular internal architecture; (**c**) cross-section of the spleen demonstrating intraparenchymal abscessation and necrosis, with the plant awn visible in situ (scale bar = 1 cm); (**d**) gross appearance of the excised spleen with the foreign body in situ; (**e**) the approximately 4-cm barbed plant awn removed from the splenic abscess after splenectomy. Red circles indicate the focal splenic lesions.

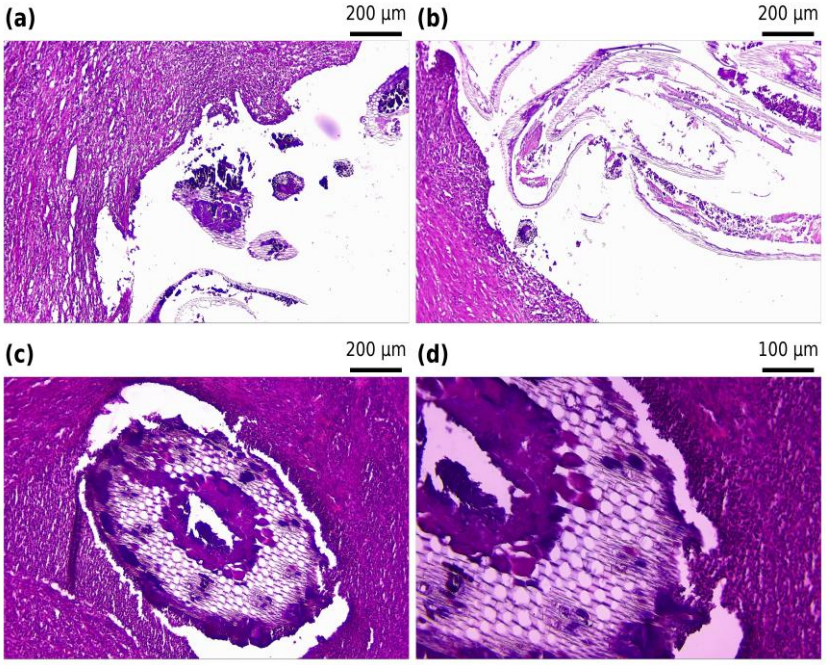


Figure 2. Histological appearance of plant material within the splenic lesion (H&E). (**a**, **b**) Photomicrographs obtained using a 10× objective, showing multiple irregular fragments with preserved, compartmentalized plant cellular architecture; clear spaces surround some fragments, with adjacent inflammatory and fibrous tissue. (**c**) obtained using a 10× objective, showing a larger plant fragment within the lesion. (**d**) Photomicrograph of the same fragment obtained using a 20× objective, demonstrating its organized cellular architecture and preserved cell walls.

4. Discussion

The initial haematological abnormalities (marked leucocytosis with a left shift, an apparently severe thrombocytopenia on the automated count and elevated erythrocyte sedimentation rate (ESR)) were consistent with an acute inflammatory or septic process. The discrepancy between the automated platelet count and the adequate platelet estimate on blood smear suggested pseudothrombocytopenia or analyzer underestimation; platelet clumping is common in feline samples. Inflammatory consumption and splenic sequestration could not be excluded. The rapid postoperative increase in platelet count was compatible with a transient process but did not distinguish among these possibilities. Although the BMBT was within the reference interval, this did not exclude a consumptive or evolving coagulopathy in the context of systemic inflammation.

ESR is a non-specific inflammatory marker that can increase during infection [9,10]. It was used in this case because the assay was locally available, whereas serum amyloid A, C-reactive protein and alpha-1 acid glycoprotein assays were unavailable. The absence of these more commonly used inflammatory biomarkers is a limitation. A complete blood count was repeated 48 h postoperatively to monitor the response to source control. Haemoglobin and platelet count increased, whereas the leucocyte count remained elevated; leucocyte counts are non-specific and may not decline within the first 48 h despite effective treatment [11].

Ultrasonography is a practical first-line imaging modality when a migrating plant foreign body is suspected. The foreign body is not always visualized directly, whereas secondary lesions along its migration path are often detectable [3]. Computed tomography (CT) can assist localization and surgical planning, but direct visualization is inconsistent: in a series of 44 dogs and 10 cats with confirmed grass seed foreign bodies, the seed was visible on CT in 19% of cases, while secondary lesions were visible in 96% [4]. CT might have provided additional information in the present case but was not available, which is a limitation.

The migration route could not be established. Ingestion followed by transmural migration from the stomach or adjacent gastrointestinal tract is anatomically plausible because of the spleen's position in the left cranial abdomen. Inhalation with caudal migration through the thorax and transdiaphragmatic extension is an alternative route [1–4]. The absence of thoracic radiographic abnormalities and of a visible diaphragmatic tract made the respiratory route less strongly supported, although a healed migration tract cannot be excluded; no gastrointestinal perforation was identified at surgery either.

Ultrasonographic splenic lesions in cats are non-specific, and imaging alone cannot reliably distinguish inflammatory from neoplastic disease [12]. Non-neoplastic lesions such as haematoma or hyperplasia accounted for only 4% (19/455) of submissions in a pathology-based survey [13], and neoplasia was diagnosed in 81% (50/62) of cats in a recent referral cohort undergoing splenectomy [14]. Lymphoma and haemangiosarcoma therefore remained initial considerations. At surgery, however, purulent rather than haemorrhagic effusion, fluctuant encapsulated lesions and dense inflammatory adhesions favored abscessation; histopathological examination excluded neoplasia. Once an infectious splenic focus was identified in this case, open exploration and splenectomy provided definitive source control.

Diagnostic laparoscopy was used to assess the spleen and extent of peritoneal involvement, not to establish a definitive diagnosis by visual inspection alone. Once purulent effusion was identified, conversion to open coeliotomy allowed comprehensive exploration, lavage, tissue sampling and definitive source control [15].

Preoperative abdominocentesis was not performed, which is a limitation. Cytological evaluation and comparison of peripheral blood and peritoneal fluid glucose concentrations might have supported an earlier diagnosis of septic peritonitis [16] and prompted earlier surgical exploration.

Neither peritoneal nor abscess fluid was submitted for bacterial culture; consequently, the organisms involved remain unknown and antimicrobial therapy could not be tailored to culture and susceptibility results. This is a notable limitation.

Migrating vegetal foreign bodies can introduce mixed environmental and host flora, including *Staphylococcus*, *Streptococcus*, *Pasteurella*, *Escherichia coli*, *Actinomyces* and *Nocardia* species [17]. *Actinomyces* species are anaerobic or facultatively anaerobic, whereas *Nocardia* species are aerobic, and both may require specific culture conditions [17,18]. *Staphylococcus* species and *E. coli* have also been commonly isolated from inhaled plant foreign bodies [19]. Empirical antimicrobial therapy should ideally provide coverage against likely aerobic and anaerobic pathogens and should be adjusted when culture and susceptibility results become available. Amoxicillin–clavulanate was selected empirically in this case; intraoperative culture would nevertheless have been preferable.

The homemade closed-suction drain was used because a commercial system was unavailable. Evidence has not established a single optimal approach to abdominal closure or drainage in septic peritonitis, and no consistent survival benefit has been demonstrated for one method [20–24]. Closed-suction drainage can evacuate inflammatory exudate but carries risks including obstruction, loss of suction, loss of protein-rich fluid and ascending infection [20,23]. Discharge with the drain in place was an individualized decision based on the cat's clinical stability, the presence of a medically trained caregiver able to monitor the system, and access to prompt re-evaluation; it should not be considered routine practice.

Deep abdominal migration of vegetal foreign bodies is uncommon in cats. In the previously reported feline splenic case, plant material was identified only during splenectomy and had not been detected ultrasonographically [5]. A separate report described a retroperitoneal abscess in which the migrating awn was discovered only at a second surgery several months later [25]. These cases illustrate the diagnostic difficulty posed by small, non-radiopaque plant material and the importance of investigating persistent focal inflammatory lesions.

Fragmented plant material may histologically resemble exogenous fiber or suture material, particularly when viewed without gross context or when different planes of section produce repeated angular or elongated profiles. As an informal check, selected photomicrographs were shown without case information to two experienced pathologists, both of whom initially considered the structures to represent thread or suture material. This illustrates a potential interpretive pitfall. In this case, the repeated demonstration of organized, cell-walled architecture in multiple microscopic fields, together with gross recovery of a grass awn from the splenic lesion, supported a plant origin. Histological interpretation of foreign material should therefore be correlated with the surgical and gross pathological findings.

5. Conclusions

This case describes a migrating plant awn within the spleen of a cat, associated with abscessation and localized peritonitis. Total splenectomy and peritoneal lavage resulted in complete clinical recovery during the two-week follow-up period.

Author Contributions: Conceptualization, A.M. and C.D.; investigation, C.D. and I.M.; writing—original draft preparation, A.M.; writing—review and editing, A.M. and C.D.; visualization, A.M. and C.D.; supervision, C.D. All authors have read and agreed to the published version of the manuscript.

Funding: This research received no external funding.

Institutional Review Board Statement: This is a case report on a patient from a veterinary practice. It is not an animal study and accordingly no ethics application was submitted to the competent authority in advance.

Acknowledgments: The authors thank Dr. Alexandru Neguleanu for his assistance with the histopathological analysis of the splenic specimen. We are also grateful to Dr. Irina Kudrenko, the referring veterinarian, who initially examined the cat and facilitated the referral for diagnostics and treatment.

Conflicts of Interest: The authors declare no conflict of interest.

References

1. Brennan, K.E.; Ihrke, P.J. Grass awn migration in dogs and cats: A retrospective study of 182 cases. *J. Am. Vet. Med. Assoc.* **1983**, *182*, 1201–1204. https://doi.org/10.2460/javma.1983.182.11.1201.
2. Marx, M.B. Grass awn migration in dogs and cats. *J. Am. Vet. Med. Assoc.* **1983**, *183*, 390–410. https://doi.org/10.2460/javma.1983.183.04.390.
3. Caivano, D.; Corda, F.; Corda, A.; Moretti, G.; Bufalari, A. Application of ultrasound in detecting and removing migrating grass awns in dogs and cats: A systematic review. *Animals* **2023**, *13*, 2071. https://doi.org/10.3390/ani13132071.
4. Vansteenkiste, D.P.; Lee, K.C.L.; Lamb, C.R. Computed tomographic findings in 44 dogs and 10 cats with grass seed foreign bodies. *J. Small Anim. Pract.* **2014**, *55*, 579–584. https://doi.org/10.1111/jsap.12278.
5. Culp, W.T.N.; Aronson, L.R. Splenic foreign body in a cat. *J. Feline Med. Surg.* **2008**, *10*, 380–383. https://doi.org/10.1016/j.jfms.2007.12.005.
6. Levy, J.K.; Nutt, K.R.; Tucker, S.J. Reference interval for rectal temperature in healthy confined adult cats. *J. Feline Med. Surg.* **2015**, *17*, 950–952. https://doi.org/10.1177/1098612X15582081.
7. Dijkstra, E.; Teske, E.; Szatmári, V. Respiratory rate of clinically healthy cats measured in veterinary consultation rooms. *Vet. J.* **2018**, *234*, 96–101. https://doi.org/10.1016/j.tvjl.2018.02.014.
8. Perianu, T. *Tratat de Boli Infecțioase ale Animalelor: Bacterioze, Volume I*; Universitas XXI: Iași, Romania, 2011; pp. 48–57. ISBN 978-606-538-062-2.

9. Diamanti, D.; Pieroni, C.; Pennisi, M.G.; Marchetti, V.; Gori, E.; Paltrinieri, S.; Lubas, G. The erythrocyte sedimentation rate (ESR) in veterinary medicine: A focused review in dogs and cats. *Animals* **2025**, *15*, 246. https://doi.org/10.3390/ani15020246.
10. Gori, E.; Pasquini, A.; Paltrinieri, S.; Lubas, G.; Militello, C.; Diamanti, D.; Carletti, C.; Pantoli, M.; Marchetti, V. Prospective application of the erythrocyte sedimentation rate (ESR) as a possible inflammatory marker in feline patients. *Vet. Med. Int.* **2024**, *2024*, 2313447. https://doi.org/10.1155/2024/2313447.
11. Kaneko, J.J.; Harvey, J.W.; Bruss, M.L., Eds. *Clinical Biochemistry of Domestic Animals*; 6th ed.; Academic Press: San Diego, CA, USA, 2008; pp. 117–118. https://doi.org/10.1016/B978-0-12-370491-7.X0001-3.
12. Bertal, M.; Norman Carmel, E.; Diana, A.; Desquilbet, L.; Specchi, S.; Pey, P. Association between ultrasonographic appearance of splenic parenchyma and cytology in cats. *J. Feline Med. Surg.* **2018**, *20*, 23–29. https://doi.org/10.1177/1098612X17697483.
13. Spangler, W.L.; Culbertson, M.R. Prevalence and type of splenic diseases in cats: 455 cases (1985–1991). *J. Am. Vet. Med. Assoc.* **1992**, *201*, 773–776. https://doi.org/10.2460/javma.1992.201.05.773.
14. Rossanese, M.; Williams, H.; De La Puerta, B.; Scott, P.; Chanoit, G.; Guillén, A. Prevalence of malignancy and factors affecting outcome of cats undergoing splenectomy. *J. Am. Vet. Med. Assoc.* **2023**, *261*, 1646–1652. https://doi.org/10.2460/javma.23.05.0258.
15. Campbell, B.G.; O'Marra, S.K. Diagnosis and surgical management of septic peritonitis in small animals: A review. *Vet. Surg.* **2026**, *55*, 13–31. https://doi.org/10.1111/vsu.70024.
16. Bonczynski, J.J.; Ludwig, L.L.; Barton, L.J.; Loar, A.; Peterson, M.E. Comparison of peritoneal fluid and peripheral blood pH, bicarbonate, glucose, and lactate concentration as a diagnostic tool for septic peritonitis in dogs and cats. *Vet. Surg.* **2003**, *32*, 161–166. https://doi.org/10.1053/jvet.2003.50005.
17. Whitney, J.; Barrs, V.R. Actinomycosis, nocardiosis, and mycobacterial infections. In *Clinical Small Animal Internal Medicine*; Bruyette, D.S., Ed.; Wiley-Blackwell: Hoboken, NJ, USA, 2020; pp. 977–984. https://doi.org/10.1002/9781119501237.ch108.
18. Clauss, H.E.; Lorber, B. Nocardiosis and actinomycosis. In *Principles and Practice of Transplant Infectious Diseases*; Safdar, A., Ed.; Springer: New York, NY, USA, 2019; pp. 473–480. https://doi.org/10.1007/978-1-4939-9034-4_27.
19. Flisi, S.; Dall'Aglio, M.; Spadini, C.; Cabassi, C.S.; Quintavalla, F. Microbial isolates from vegetable foreign bodies inhaled by dogs. *Vet. Med. Int.* **2018**, *2018*, 3089282. https://doi.org/10.1155/2018/3089282.
20. Mueller, M.G.; Ludwig, L.L.; Barton, L.J. Use of closed-suction drains to treat generalized peritonitis in dogs and cats: 40 cases (1997–1999). *J. Am. Vet. Med. Assoc.* **2001**, *219*, 789–794. https://doi.org/10.2460/javma.2001.219.789.
21. Staatz, A.J.; Monnet, E.; Seim, H.B. Open peritoneal drainage versus primary closure for the treatment of septic peritonitis in dogs and cats: 42 cases (1993–1999). *Vet. Surg.* **2002**, *31*, 174–180. https://doi.org/10.1053/jvet.2002.31043.
22. Greenfield, C.L.; Walshaw, R. Open peritoneal drainage for treatment of contaminated peritoneal cavity and septic peritonitis in dogs and cats: 24 cases (1980–1986). *J. Am. Vet. Med. Assoc.* **1987**, *191*, 100–105. https://doi.org/10.2460/javma.1987.191.01.100.
23. Culp, W.T.N.; Holt, D.E. Septic peritonitis. *Compend. Contin. Educ. Vet.* **2010**, *32*, E1–E14. Available online: https://vetfolio.s3.amazonaws.com/ae/f4/70668f0243289be84ffda261cd40/septic-peritonitis.pdf (accessed on 29 July 2026).
24. Zorn, C.M.; Walton, R.A.L.; McKeen, L.; Mochel, J.P.; Ward, M.; Blong, A.E. Retrospective comparison of outcomes in septic peritonitis with or without closed-suction abdominal drainage in 115 dogs (2009–2019). *Vet. Anim. Sci.* **2023**, *21*, 100304. https://doi.org/10.1016/j.vas.2023.100304.
25. Mastora, H.; Papazoglou, L.G.; Patsikas, M.; Kirmanidou, G.; Donas, A. Retroperitoneal abscess associated with a migrating grass awn in a cat: Treatment with omentalization and grass awn removal. *Top. Companion Anim. Med.* **2018**, *33*, 97–99. https://doi.org/10.1053/j.tcam.2018.08.007.

CVJ CLUJ VETERINARY JOURNAL

Review Article

Early Cancer Screening in Companion Animals: Combining Traditional Diagnostics with Emerging Methods

Zhang Zhen[1], Guo Meiliang[1], Ma Baihe[1], Chen Xin[1], Liu Shuhua[1], Li Lianrui[1]*

[1] College of Animal Science and Technology, Tarim University, Alar, Xinjiang 843300, China;
* Correspondence: lilianrui51@163.com

Abstract: Early tumor screening in companion animals (dogs and cats) integrates traditional and emerging diagnostic techniques to identify malignant lesions at the preclinical stage, enabling timely intervention and improved prognosis. Early-stage tumors in dogs and cats often lack specific clinical signs, frequently presenting only as palpable subcutaneous masses or nonspecific weight loss, which commonly leads to diagnostic delay. While histopathological examination remains the gold standard for tumor diagnosis, its invasive nature limits application in large-scale screening. Emerging non-invasive or minimally invasive methods including liquid biopsy (detection of circulating tumor DNA, circulating tumor cells, and exosomes), serum tumor marker analysis, and exhaled volatile organic compound testing complement traditional strategies and enable earlier, more precise tumor detection. For localized tumors detected at an early stage, radical surgical resection remains the cornerstone of treatment; emerging interventions such as tyrosine kinase inhibitors and immune checkpoint blockade further improve clinical outcomes, and their success is highly dependent on early diagnosis via screening. This review summarizes current advances in early tumor screening for companion animals, focusing on combined strategies of traditional diagnostics and emerging technologies, and highlights their translational potential to enhance diagnostic efficacy and optimize clinical management pathways.

Keywords: Early cancer screening; Dogs; Cats; Liquid biopsy; Circulating tumor DNA; Serum tumor markers; Histopathology; Immunotherapy; Metabolomics

Received: 08.06.2026
Accepted: 14.07.2026
Published: 28.07.2026

DOI:10.52331/v31i3q253

Copyright: © 2021 by the authors. Submitted for possible open access publication under the terms and conditions of the Creative Commons Attribution (CC BY) license (http://creativecommons.org/licenses/by/4.0/).

1. Introduction

Early tumor screening employs physical examinations, laboratory tests, imaging, and molecular biology techniques to detect malignant lesions in companion animals (dogs and cats) before overt clinical symptoms appear, with the goal of enabling timely intervention and improving prognosis [1,2]. In veterinary practice, the boundary between "screening" and "diagnosis" remains debated: some frameworks categorize early detection as a component of preventive health care, while others restrict screening to the detection of preclinical tumors in entirely asymptomatic animals [3]. For the purposes of this review, "early tumor screening" refers to all testing strategies employed before the onset of overt tumor-specific clinical signs, or when only nonspecific clinical manifestations are present.

Cancer is a leading cause of death in senior dogs and cats. Approximately 47% of deaths in dogs over 10 years of age are attributed to malignant tumors, and the corresponding proportion in cats exceeds 30% [4,5]. Cancer incidence increases with age, and can occur across all ages, sexes, and breeds [6]. However, breed-specific predispositions are well documented: Boxers, Golden Retrievers, Bernese Mountain Dogs, and Labrador Retrievers consistently show higher rates of lymphoma, mast cell tumors, osteosarcoma, and histiocytic sarcoma across epidemiological studies [7,8]. In cats, Siamese cats have been associated with elevated risk of lymphoma and mammary tumors, though most supporting data come from older, small-scale studies that require validation in larger cohorts [9,10].

Traditional early screening methods include systematic physical examination (including palpation of superficial lymph nodes and assessment of cutaneous/subcutaneous masses), basic hematology and serum biochemistry, thoracic and abdominal radiography and ultrasonography, and fine-needle aspiration cytology [11]. Molecular biomarkers are increasingly entering clinical practice: in dogs, serum thymidine kinase 1 (TK1) activity

and C-reactive protein (CRP) levels serve as adjunctive screening markers for lymphoma and select solid tumors [12]; in cats, serum thymidine kinase and specific microRNA profiles have shown preliminary utility as early tumor markers [13,14]. Liquid biopsy technologies, which detect tumor-derived nucleic acids, proteins, and circulating cells in peripheral blood, may identify tumor signals before masses are visible on conventional imaging [15].

The biological feasibility of early screening stems from nucleic acids, proteins, and metabolites released into peripheral blood by developing tumor cells, as well as associated epigenetic and immune microenvironment changes [16]. Genetic susceptibility, chronic inflammation, immunosenescence, and epigenetic reprogramming all contribute to companion animal tumorigenesis, and these molecular events provide detectable targets for early detection [17]. Advances in multi-omics research have further established that effective screening requires integration of multi-dimensional data including genomic, transcriptomic, proteomic, and metabolomic abnormalities rather than reliance on a single biomarker [18].

Early diagnosis remains challenging. While histopathology is the diagnostic gold standard, its invasiveness and sampling requirements limit its use as a first-line screening tool [2,19]. However, tumors detected at an early, localized stage are typically amenable to curative surgical resection, with significantly improved prognosis [20,21].

This review synthesizes literature retrieved from PubMed and Scopus (including reference list mining), covering publications through 2026. It summarizes established diagnostic techniques and emerging detection methods for early tumor screening in dogs and cats, and explores their translational potential to optimize clinical management and long-term prognosis.

2. Clinical Signs and Physical Examination Findings

Preclinical tumors in dogs and cats may produce only nonspecific findings, or no detectable abnormalities at all [1,22]. Cancer anorexia (reduced food intake secondary to neoplasia) and cancer cachexia (weight loss and metabolic dysfunction despite adequate nutrition) are the most prevalent and impactful paraneoplastic syndromes in companion animal oncology [23]. In dogs, approximately 14% lose 5–10% of body weight in the 12 months before diagnosis, and 23% lose more than 10%. In cats, 45–55% of patients with lymphoma or solid tumors present with a body condition score (BCS) ≤5/9 at diagnosis; 93% exhibit muscle wasting, including 72% with BCS in the adequate range (≥5) [24,25]. Pre-diagnostic weight loss is a negative prognostic indicator in both species, with more pronounced effects in cats.

Palpable superficial masses or subcutaneous nodules are among the most notable early physical findings. According to the 2026 AAHA Oncology Guidelines, mast cell tumors are the most common canine skin tumor (16–21% of all skin neoplasms), while lymphoma is one of the most prevalent malignant tumors in cats [26,27]. Canine multicentric lymphoma typically presents with painless, elastic generalized lymphadenopathy affecting submandibular, prescapular, and popliteal nodes, with or without hepatosplenomegaly [28]. Feline lymphoma most commonly presents as the gastrointestinal form, which does not cause generalized lymphadenopathy and produces nonspecific signs (anorexia, weight loss) that are easily confused with pancreatitis, renal failure, or other chronic conditions [29]. Osteosarcoma, the most common primary canine bone tumor (85% of canine bone neoplasms), presents as persistent lameness and localized swelling, with strong predisposition in large breeds [30].

Non-healing wounds or ulcers are key warning signs for cutaneous and oral tumors. Feline cutaneous squamous cell carcinoma occurs most frequently on sparsely haired, lightly pigmented sites (ear tips, nasal planum, eyelids), presenting as red, ulcerated, crusted lesions with alopecia or pink discoloration [31]. Feline oral squamous cell carcinoma is highly aggressive, with early signs including oral ulcers, ptyalism, weight loss, halitosis, and loose teeth that are often misattributed to dental disease [32].

Lymph node evaluation is a core component of tumor screening. Using histopathology as the reference standard, Langenbac et al. (2001) assessed the diagnostic performance of palpation, fine-needle aspiration, and core needle biopsy for regional lymph node metastasis in dogs and cats with solid tumors [33]. The 2026 AAHA guidelines emphasize systematic regional lymph node assessment, with follow-up imaging, cytology, or histopathology as indicated. Importantly, lymphadenopathy may stem from metastatic disease or non-neoplastic causes (infection, inflammation), and size assessment via palpation alone is unreliable [34]. Monthly at-home full-body palpation is recommended as an adjunctive measure to detect hidden masses and facilitate early referral.

Recognition of paraneoplastic syndromes can provide early clues to occult tumors. Hypercalcemia is the most common paraneoplastic syndrome in companion animals. In dogs, the most common associated malignancies are T-cell lymphoma (35–55% of cases), anal sac adenocarcinoma, multiple myeloma, and thymoma; in cats, it is most frequently linked to oral squamous cell carcinoma [35,36]. Clinical signs include polyuria/polydipsia, vomiting, anorexia, bradycardia, and muscle weakness; in cats, anorexia and lethargy predominate, with less frequent gastrointestinal and urinary signs [37]. Paraneoplastic hypoglycemia occurs primarily in canine insulinomas, caused by aberrant insulin secretion from pancreatic β-cells, and presents as muscle weakness, collapse, ataxia, and seizures; it is rare in cats [38,39]. Additional notable paraneoplastic manifestations include cancer cachexia, fever of unknown origin, non-regenerative anemia, thrombocytopenia, and cutaneous paraneoplastic syndromes (e.g., feline paraneoplastic alopecia, canine superficial necrolytic dermatitis) [40,41,42].

Common clinical and physical examination findings are summarized in Table 1.

3. Diagnosis

3.1. Integrated Strategies Combining Traditional and Emerging Screening Methods

No single gold-standard method exists for universal early cancer screening in dogs and cats; the combination of physical examination, basic imaging (radiography, ultrasonography), and cytology forms the core of traditional screening protocols [2,43]. In recent years, liquid biopsy, circulating tumor DNA (ctDNA) testing, metabolomics, and AI-assisted image interpretation have expanded screening capabilities, though these remain supplementary to traditional methods rather than replacements, pending broader clinical validation.

All screening protocols begin with a thorough history and physical examination, with prioritization of senior animals (generally dogs ≥7 years, cats ≥10 years), high-risk breeds (e.g., Golden Retrievers, Boxers, Siamese cats), and individuals with known genetic predispositions [45,46]. Baseline hematology and serum biochemistry help rule out non-neoplastic causes of clinical signs and assess organ function [47].

Traditional imaging (thoracic and abdominal radiography, abdominal ultrasonography) is accessible and cost-effective, with good sensitivity for mass-forming solid tumors (e.g., splenic hemangiosarcoma, hepatic tumors, bladder transitional cell carcinoma). However, it has limited ability to detect micrometastases <3–5 mm in diameter or early carcinoma in situ [1,48]. Liquid biopsy, by contrast, detects tumor-derived nucleic acids, proteins, or circulating cells in peripheral blood, and shows preliminary potential to identify tumor signals before masses are radiologically visible [2]. A prospective study of canine lymphoma and hemangiosarcoma reported that ctDNA point mutation-based liquid biopsy achieved 62% and 71% sensitivity for early detection of these two tumor types, respectively, with >95% specificity [49]. Sensitivity is lower (30–50%) for non-hematologic solid tumors such as osteosarcoma and lung cancer [15].

Fine-needle aspiration cytology is low-cost and rapid, and can distinguish benign from malignant lesions. However, its accuracy is highly operator- and pathologist-dependent, and it cannot provide molecular subtype information [50,51]. Emerging tools including flow cytometry, immunocytochemistry, and machine learning-based image analysis can improve cytologic interpretation consistency, but require specialized equipment and sample processing that are not widely available in most veterinary diagnostic laboratories [52].

Screening strategies should be tiered based on individual risk factors, owner financial capacity, and clinical utility (i.e., whether early intervention improves prognosis) [45]. For high-risk animals (senior patients, high-incidence breeds), abdominal ultrasound and thoracic radiography may be added to annual wellness examinations; liquid biopsy may be added as a supplementary test when feasible [53]. The high specificity of liquid biopsy corresponds to low false-positive rates, but its limited sensitivity means a negative result does not rule out early-stage tumors [15]. Positive results from any emerging screening method require confirmation via conventional imaging or cytology, and negative results do not justify discontinuing clinical follow-up.

Combined modalities improve performance over single tests. For example, combining liquid biopsy with abdominal ultrasound increases sensitivity for canine splenic and hepatic solid tumors from ~50–70% (single modality) to >85% [54,55]. Similarly, AI-assisted imaging interpretation paired with cytology reduces inter-observer variability and improves detection of pulmonary nodules and small abdominal masses [56]

Table 1. Common clinical signs and physical examination findings in dogs and cats with tumors

Clinical sign / Finding	Associated tumor type/condition	Key features or incidence	References
Weight loss and muscle wasting (cancer cachexia)	Various tumors, especially lymphoma and solid tumors	Dogs: 14% lose 5–10% body weight pre-diagnosis, 23% lose >10%; Cats: 45–55% have BCS ≤5/9, 93% have muscle wasting (72% even with BCS ≥5)	[24,25]
Palpable superficial mass / subcutaneous nodule	Most common skin tumors: mast cell tumor (dog); lymphoma (cat)	Dogs: MCT accounts for 16-21% of all skin tumors; Cats: lymphoma is one of the most common malignant tumors	[26,27]
Generalized lymphadenopathy (painless, elastic)	Multicentric lymphoma (dog)	Submandibular, prescapular, popliteal nodes; with/without hepatosplenomegaly	[28]
Non-specific gastrointestinal signs (anorexia, weight loss)	Feline gastrointestinal lymphoma	No generalized lymphadenopathy; easily confused with pancreatitis, renal failure	[29]
Persistent lameness + localized limb swelling	Osteosarcoma (dog)	Most common primary bone tumor (85% of canine bone tumors); large breeds predisposed	[30]
Red, ulcerated, crusted lesions on sparsely haired/lightly pigmented areas (ear tips, nasal planum, eyelids)	Cutaneous squamous cell carcinoma (cat)	May present with alopecia or pink appearance	[31]
Oral ulceration, drooling, halitosis, loose teeth	Oral squamous cell carcinoma (cat)	Highly aggressive; early stage often mistaken for dental disease	[32]
Lymphadenopathy (unreliable by palpation alone)	Regional lymph node metastasis	Palpation alone has low sensitivity (60%) and specificity (72%); cytology/histopathology required	[33,34]
Hypercalcemia	Most common paraneoplastic syndrome; in dogs: T-cell lymphoma (35–55%), anal sac adenocarcinoma, multiple myeloma, thymoma; in cats: oral SCC	Clinical signs: polyuria/polydipsia, vomiting, anorexia, bradycardia, muscle weakness	[35,36,37]
Hypoglycemia (muscle weakness, collapse, ataxia, seizures)	Insulinoma (dog)	Caused by abnormal insulin secretion from pancreatic β-cells; rare in cats	[38,39]
Fever of unknown origin, non-regenerative anemia, thrombocytopenia	Various paraneoplastic syndromes	Important and noteworthy manifestations	[40,42]
Cutaneous paraneoplastic syndromes	Feline paraneoplastic alopecia; Canine superficial necrolytic dermatitis	May precede diagnosis of underlying neoplasia	[41]

Owner awareness and compliance are key determinants of screening effectiveness [57]. Veterinarians should communicate the benefits and limitations of each method clearly, and develop individualized screening plans. For animals undergoing liquid biopsy or other emerging tests, follow-up testing every 6–12 months is recommended to monitor biomarker trends.

If initial screening is negative but nonspecific tumor-associated signs persist (unexplained weight loss, anorexia, chronic gastrointestinal signs, persistent fever), re-evaluation after 2–3 months with additional modalities (e.g., PET/CT at referral centers, metabolomic serum testing) is advised [1,58,59]. Interpretation of screening markers is more complex in animals with concurrent chronic inflammatory disease (e.g., inflammatory bowel disease, chronic kidney disease), as these conditions can independently elevate inflammation-related cytokines and metabolites [60].

Asymptomatic high-risk animals may undergo routine screening (physical exam + baseline blood work + imaging) without pharmacologic intervention [1]. Short-acting sedation may be administered as needed before invasive procedures (e.g., ultrasound-guided biopsy) to reduce patient stress and procedural risk [61].

Histopathological examination remains the reference standard for definitive diagnosis of clinically actionable lesions; imaging and liquid biopsy results indicate high suspicion but cannot confirm malignancy independently [62]. Following mass detection on imaging, cytologic or histologic confirmation via fine-needle aspiration or core needle biopsy is mandatory to avoid overtreatment [51].

When liquid biopsy is positive but no lesion is identified on initial imaging, targeted imaging follow-up with biopsy attempt is indicated; if biopsy is negative but clinical suspicion remains high, combined imaging and liquid biopsy re-evaluation after 3–6 months is recommended to detect progressive lesions [15,16]. No evidence-based standard exists for optimal follow-up intervals after a positive liquid biopsy result, and decisions should be individualized based on patient risk level.

Analogous to cross-reactivity in food allergy diagnosis, some circulating biomarkers (e.g., TK1) may be elevated across multiple tumor types, and may also produce false positives in non-neoplastic proliferative conditions (e.g., splenic extramedullary hematopoiesis, reactive lymphoid hyperplasia) [63,64]. No single biomarker elevation is sufficient for definitive diagnosis; all abnormal results require correlation with imaging and cytologic findings.

A core challenge of screening programs is balancing early intervention against overdiagnosis [65]. Not all screen-detected tumors—particularly indolent neoplasms or low-grade mast cell tumors in geriatric patients—will become clinically relevant within the patient's lifespan. Decisions regarding immediate invasive treatment should integrate tumor type, grade, location, overall patient health, and owner preferences.

If initial screening is negative but clinical suspicion remains high, advanced imaging (whole-body CT or MRI) or repeat liquid biopsy on an alternative platform may be considered to reduce false-negative risk [66,67]. In patients with multiple comorbidities, alternative etiologies must be excluded before attributing abnormal screening results to neoplasia.

While no single standard confirms screening efficacy, the most reliable approach is histopathologic confirmation combined with ≥12 months of clinical follow-up to assess negative predictive value. For screen-positive patients, excisional biopsy with histopathology serves both therapeutic and diagnostic purposes.

3.2. Additional Diagnostic Methods

A range of additional in vivo and in vitro diagnostic approaches have been investigated for early tumor screening, but none are validated as standalone screening tools. Their utility ranges from diagnostic support to risk stratification, and none replace traditional screening protocols combined with histopathologic confirmation.

3.2.1. Serum Biomarkers and Conventional Auxiliary Assays

Multiple serum tumor markers are commercially available, including thymidine kinase 1 (TK1), vascular endothelial growth factor (VEGF), and carcinoembryonic antigens (e.g., CEA, CA15-4). However, current evidence indicates single-marker testing lacks sufficient sensitivity and specificity for early cancer screening in dogs and cats [68–71]. Flory et al. (2021) reported that combining serum TK1 with abdominal ultrasound improves detection of occult splenic and hepatic tumors compared to annual physical examination alone, but cannot reliably distinguish malignant tumors from benign proliferative lesions [15].

Detection of specific metabolites or DNA methylation markers in feces, urine, or oral swabs is not currently recommended for independent tumor screening. While non-invasive sampling is convenient for owners, most supporting studies involve small cohorts or specific tumor types (e.g., bladder transitional cell carcinoma), and performance across breeds, ages, and tumor stages remains unvalidated [72]. Overreliance

on these non-specific markers carries risks of false positives (leading to unnecessary invasive testing and owner anxiety) and false negatives (delaying diagnosis) [67].

Serum TK1 activity is markedly elevated in canine lymphoma and hemangiosarcoma, but shows minimal or no increase in other solid tumors such as osteosarcoma and thyroid cancer; this heterogeneity likely reflects differences in tumor proliferative activity [15,68,69]. TK1 reference ranges vary by assay platform (ELISA, chemiluminescence) and laboratory, with divergent diagnostic thresholds across studies, which contributes to inconsistent reported performance [73,74]. Additional confounders include age-related baseline changes and non-specific elevations associated with concurrent inflammation or infection, which complicate establishment of a universal clinical cutoff [63].

Similarly, ELISA-based detection of serum matrix metalloproteinases (MMPs), endostatin, and other cytokines is not validated for early tumor screening. In a small single-center cohort of 26 dogs with mammary tumors and 26 healthy controls, Khaki et al. (2023) measured serum MMP-2 and MMP-9 levels via gelatinase zymography. The study found that the presence of active MMP-9 was associated with elevated risk of tumor metastasis and recurrence, but the assay had limited capacity to distinguish benign from malignant mammary lesions. The previously included remark regarding a "diagnostic AUC of 0.68" was an erroneous leftover note from internal fact-checking that was incorrectly retained in the manuscript. Given the small sample size and limited discriminative performance, this method is not currently suitable for standalone early cancer screening [75].

3.2.2. Emerging Molecular and Liquid Biopsy Tools

Proteomic and metabolomic fingerprinting methods, while still in the research phase, have shown utility in specific scenarios such as differentiating benign from malignant pleural or peritoneal effusions. Ko et al. (2025) applied machine learning to analyze cell-free DNA fragment size and copy number variations, achieving an average AUC of 0.93 in 10-fold cross-validation for distinguishing canine hemangiosarcoma from healthy controls [76]. However, these methods require specialized mass spectrometry equipment and standardized sample processing, limiting current use to research settings.

Circulating tumor cell (CTC) enumeration has demonstrated higher specificity than traditional serum biomarkers in preliminary studies of canine mammary and lung adenocarcinoma. In a small pilot investigation, Marconato et al. used the automated CellSearch platform to test 27 dogs with metastatic mammary tumors, detecting CTCs in 44.4% (12/27) of malignant cases and no CTCs in 5 healthy control dogs. As these findings are limited by small sample size and the absence of a benign lesion control group, they should be interpreted as preliminary. A separate ctDNA analysis of 48 dogs demonstrated significantly higher ctDNA fractions in malignant splenic tumors (11.2%) compared to benign lesions (3.2%) and healthy dogs (1.4%), supporting the differential diagnostic value of circulating tumor markers [77].

Proliferative or metastatic tumors may shed CTCs early in disease progression, suggesting CTC testing could detect hematogenous dissemination before radiologically visible micrometastases [78]. A prospective analysis of 57 histologically confirmed canine soft tissue sarcomas detected CTCs in 28.1% (16/57) of peripheral blood samples, even in cases without imaging evidence of metastasis. CTC detection was significantly associated with higher tumor proliferative activity (high histologic grade) and predicted postoperative recurrence risk [79]. This dissociation between radiologic metastasis timing and CTC positivity suggests CTC testing can provide prognostic information independent of imaging.

Kanayama et al. (2024) developed a polymer-based microfluidic "CTC Chip" that can be conjugated with anti-EpCAM or anti-cell surface vimentin antibodies to capture epithelial or mesenchymal tumor cells, respectively. As a proof-of-concept using in vitro spiked tumor cell lines, the EpCAM chip achieved 99.4% capture efficiency for epithelial (PC9) cells and 88.8–90.8% for intermediate-type cells, but only 13.4% for mesenchymal (A549) cells. The CSV chip achieved 88.4% capture efficiency for mesenchymal cells at 100 μg/ml antibody concentration [80]. These performance data are derived from laboratory-based cell line experiments and have not yet been validated in clinical patient samples. A key conceptual advantage is that the platform does not rely on tumor-specific mutation profiles; in theory, switching antibody panels can adapt it to different tissue origins. While multicenter, large-scale prospective clinical validation is still required, CTC detection shows preliminary promise as a complement to traditional imaging, particularly for tumor types at high risk of micrometastatic spread.

Flory et al. (2024) reported a liquid biopsy assay integrating cfDNA quantification with NGS for canine cancer screening. In a clinical validation study across seven predefined cancer types, the assay achieved 71.3% overall sensitivity (95% CI: 62.9–78.5%) in 122 dogs with cancer and 98.7% specificity (95% CI: 97.0–

99.3%) in 473 healthy dogs, using multi-dimensional cfDNA features including copy number variations and fragmentomics [49]. Ko et al. (2025) further confirmed the utility of cfDNA fragmentomics for canine hemangiosarcoma detection via whole-genome sequencing and machine learning, with an AUC of 0.93 [76].

Quantitative PCR (qPCR) targeting specific ctDNA hotspot mutations, such as BRAF V595E for canine bladder transitional cell carcinoma, shows auxiliary diagnostic utility for specific tumor types. However, performance is dependent on the tumor's mutational status, making these assays unsuitable for tumors with low or no characteristic mutations, including most soft tissue sarcomas and lymphoma subtypes [81–85]. They are best applied as risk stratification tools for high-risk breeds (e.g., bladder cancer screening in Scottish Terriers and West Highland White Terriers) rather than universal screening modalities.

Despite promising preliminary results, most emerging diagnostic methods suffer from small sample sizes, lack of independent external validation, and methodological heterogeneity. Most studies are single-center or laboratory-based, limiting reproducibility and clinical applicability. Some commercial kits also lack multicenter prospective validation, carrying risk of result overinterpretation or false positives. These tools provide supplementary information and risk stratification value but cannot replace the traditional diagnostic workflow of physical examination, imaging screening, and histopathologic confirmation. Figure 1 summarizes a practical screening strategy prioritizing validated traditional tools, with adjunctive and emerging methods incorporated as clinically appropriate.

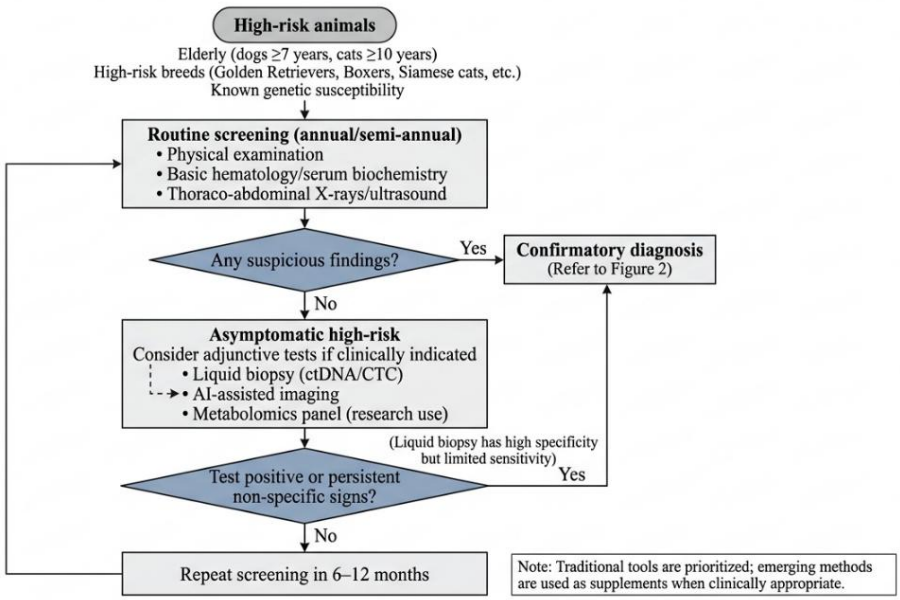


Figure 1. Practical screening strategy for early cancer detection in dogs and cats

4. Management Strategies Following a Positive Screening Result

The primary goal of post-screening management is to obtain a definitive diagnosis via confirmatory testing (e.g., histopathology) while minimizing overdiagnosis and overtreatment, and to develop an appropriate monitoring or intervention plan based on tumor type, stage, and patient characteristics. No screening result alone should be used to initiate treatment; all cases require confirmatory diagnostic follow-up.

4.1. Confirmatory Diagnosis and Staging Assessment

For animals with screen-positive findings on imaging or liquid biopsy, cytologic or histopathologic specimens should be obtained via fine-needle aspiration (FNA) or core needle biopsy to confirm tumor nature (benign/malignant) and histologic type [51]. If screening shows only elevated hematologic biomarkers (e.g., TK1, ctDNA fragmentomic abnormalities) with no definitive mass on imaging, recheck of biomarkers and repeat imaging after 2–3 months is recommended to avoid unnecessary invasive procedures.

Following malignant tumor diagnosis, clinical staging is performed based on anatomic location, local invasion extent, and regional lymph node or distant metastasis status. For suspected metastatic cases, thoracic CT, triphasic contrast-enhanced abdominal CT, or whole-body 18F-FDG PET-CT are recommended [86,87,88]. Staging accuracy directly impacts treatment decisions (surgery alone vs. surgery with adjuvant chemotherapy) and prognostic assessment.

Treatment and monitoring plans should integrate patient age, body condition score, vital organ function (particularly hepatic and renal), comorbidities (chronic kidney disease, heart disease, diabetes), and owner financial capacity and treatment willingness. For geriatric patients or those with severe comorbidities, palliative supportive care with regular follow-up may be appropriate even for confirmed malignant tumors, if life expectancy is limited or surgical risk is prohibitive.

4.2. Surgical and Medical Interventions

For confirmed malignant tumors where intervention provides clear survival benefit, complete surgical resection with adequate margins remains first-line treatment for most solid tumors (mast cell tumors, soft tissue sarcomas, mammary tumors, splenic hemangiosarcoma) [89]. Preoperative evaluation includes baseline hematology, coagulation testing, and cardiac function assessment; transfusion preparation is evaluated for large, deep-seated tumors.

When complete resection is not feasible (e.g., tumors adjacent to major vessels or nerves), multiple metastases are present, or owners decline surgery, alternative options are selected based on histologic type: chemotherapy (e.g., multi-agent protocols for lymphoma, NSAIDs combined with chemotherapy for transitional cell carcinoma), targeted therapy (e.g., toceranib for mast cell tumors with c-Kit mutations), or palliative radiation therapy [90–94]. All pharmacologic interventions should be guided by a veterinary oncologist, with close monitoring for adverse effects including myelosuppression, gastrointestinal toxicity, and cardiotoxicity.

While awaiting biopsy results or when definitive treatment cannot be initiated immediately, symptomatic and supportive medications may be used to alleviate clinical signs: NSAIDs (e.g., meloxicam, carprofen) for tumor-related inflammation and mild pain; opioids for moderate to severe pain; glucocorticoids to reduce peritumoral edema or for temporary control of select lymphoproliferative diseases [95,96]. Such symptomatic treatment does not replace or delay etiologic treatment.

All treatment decisions (including decision to forego treatment and monitor) should be made after histopathologic confirmation. Attending veterinarians should fully discuss expected benefits, risks, costs, and alternatives with owners, with written documentation of the discussion.

4.3. Adjuvant and Emerging Treatment Strategies

Adjuvant strategies include immunotherapy, molecular biomarker-guided personalized treatment, and nutritional and microbiome support. Most remain in clinical evaluation and should be administered at specialized referral centers or within clinical trial frameworks.

Immunotherapy: The xenogeneic DNA vaccine (Oncept®) for canine malignant melanoma has been shown to prolong disease-free survival, but is only indicated for surgically resected early-stage (II–III) cases and must be used with an adjuvant [97,98,99]. A heat shock protein-based vaccine for bladder transitional cell carcinoma has shown preliminary safety in small studies, but efficacy requires further validation [100].

Tyrosine kinase inhibitors: Toceranib and masitinib may be used for canine mast cell tumors carrying c-Kit mutations; c-Kit genotyping is recommended prior to use to predict treatment response [101]. Response rates are significantly lower for mast cell tumors without these mutations, and routine use is not recommended.

Minimal residual disease (MRD) monitoring: ctDNA- or CTC-based MRD monitoring has shown ability to detect recurrence 2–4 months earlier than imaging in preliminary studies of canine lymphoma and mammary carcinoma. However, use to guide treatment adjustments remains experimental and is not standard of care [102,103].

Nutritional and microbiome support: Dogs with cancer frequently experience reduced appetite, muscle wasting, and gut dysbiosis. Prospective studies indicate prebiotic (e.g., fructooligosaccharides) and omega-3 polyunsaturated fatty acid supplementation can improve body weight and inflammatory status, but randomized controlled trials confirming direct effects on tumor progression or survival are lacking [104]. These interventions are recommended as components of holistic supportive care, not as substitutes for anti-tumor therapy.

Table 2. Summary of management strategies following a positive screening result

Category	Specific strategy	Indication / notes	References
Staging assessment	Chest CT, triphasic contrast-enhanced abdominal CT, or whole-body 18F-FDG PET-CT	Suspected metastasis; influences treatment planning	[86,87,88]
Treatment decision factors	Age, body condition score, organ function (liver/kidney), comorbidities, owner's financial capacity and willingness	Comprehensive evaluation needed	[45,46]
First-line treatment (solid tumors)	Surgical resection with complete margins	Mast cell tumor, soft tissue sarcoma, mammary tumor, splenic hemangiosarcoma	[89]
Alternative therapies (when surgery not feasible or refused)	Chemotherapy (e.g., CHOP for lymphoma; NSAID + chemo for TCC); Targeted therapy (toceranib/masitinib for c-Kit+ MCT); Palliative radiotherapy	Based on tumor histology	[90–94]
Symptomatic/supportive care while awaiting definitive diagnosis	NSAIDs (meloxicam, carprofen) for mild pain/inflammation; Opioids for moderate-severe pain; Glucocorticoids for peritumoral edema or temporary control of lymphoproliferative diseases	Improves quality of life; does not replace etiological treatment	[95,96]
Immunotherapy (adjunctive)	Xenogeneic DNA vaccine (Oncept®) for canine oral malignant melanoma	Only for surgically resected stage II–III cases; use with adjuvant	[97,98,99]
	Heat-shock-protein-based vaccine for bladder TCC (investigational)	Small study; safe but efficacy needs validation	[100]
Tyrosine kinase inhibitors	Toceranib or masitinib for canine mast cell tumors with c-Kit mutations	c-Kit genotyping recommended prior to use to predict response	[101]
Minimal residual disease monitoring	ctDNA or CTC-based monitoring	In canine lymphoma/mammary carcinoma; may detect recurrence 2–4 months earlier than imaging; still experimental	[102,103]

For screen-positive patients with negative biopsy results (false-positive screening) or benign lesions, individualized follow-up plans are indicated: benign nodules (e.g., splenic nodules, hepatic cysts) may be monitored with imaging every 6–12 months; suspicious atypical hyperplastic lesions require shorter 3–6 month intervals with repeat biopsy as needed [105,106]. For rare cases with positive liquid biopsy and negative conventional workup, no evidence-based guidelines exist; repeat liquid biopsy with whole-body diffusion-weighted MRI after 3 months may be considered, but long-term repeated testing is discouraged to avoid owner anxiety and unnecessary costs.

Key management strategies are summarized in Table 2, and Figure 2 illustrates the recommended workflow from positive screening to final decision-making.

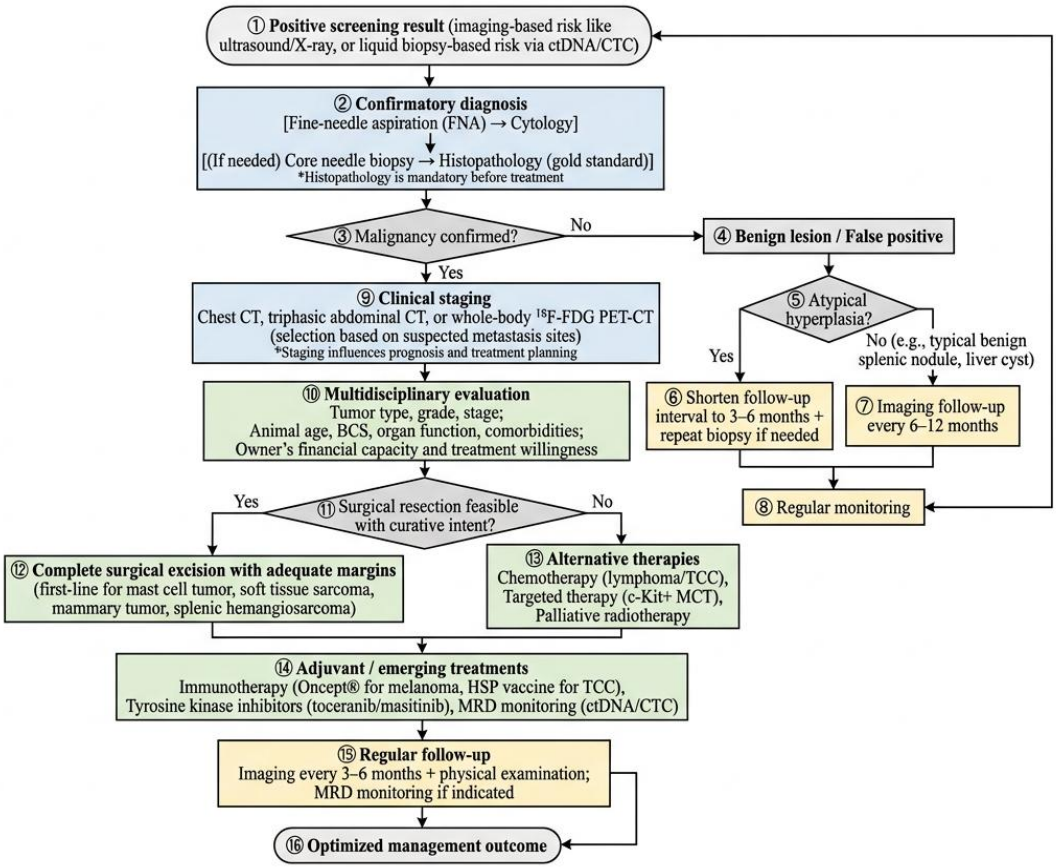


Figure 2. Recommended workflow following a positive cancer screening result

5. Conclusion

Early cancer screening in dogs and cats remains clinically challenging, primarily due to a lack of large-scale validated early biomarkers with robust sensitivity and specificity. Traditional screening methods (physical examination, imaging, cytology) have limited ability to detect micrometastases, early carcinoma in situ, and occult lesions, and are time- and operator-dependent. However, ongoing technological advances are progressively addressing these gaps.

Liquid biopsy technologies (ctDNA testing, metabolomic analysis, CTC enumeration) and AI-assisted image interpretation enable detection of peripheral blood molecular abnormalities before radiologically visible lesions appear, providing pathways for earlier, more precise screening and risk stratification. Quantitative ctDNA mutation detection (e.g., BRAF V595E for canine bladder cancer), multi-omics discriminative models, and machine learning-enhanced cytomorphologic analysis can complement traditional cytologic and histopathologic diagnoses, supporting clinical decision-making and reducing unnecessary invasive procedures.

The future of companion animal early cancer screening lies in the seamless integration of traditional clinical methods with emerging molecular diagnostics, AI-assisted image analysis, and multi-panel

biomarker testing. Realizing this potential requires large-scale, multicenter, prospective clinical validation studies to define diagnostic accuracy, clinical utility, and cost-effectiveness, and to establish standardized operating procedures and result interpretation criteria. The ultimate goal is to deliver efficient, precise, quality-of-life-aligned early screening tailored to individual patient risk profiles, ensuring timely diagnosis for cases that benefit from early intervention while avoiding excessive medical intervention.

Author Contributions: Conceptualization, Z.Z. and G.M.L.; methodology, Z.Z.; software, Z.Z.; validation, Z.Z., L.S.H. and M.B.H.; formal analysis, Z.Z.; investigation, Z.Z.; resources, G.M.L.; data curation, L.S.H., M.B.H. and C.X.; writing—original draft preparation, Z.Z.; writing—review and editing, Z.Z., L.S.H., M.B.H., C.X. and G.M.L.; visualization, Z.Z.; supervision, G.M.L.; project administration, G.M.L.; funding acquisition, L.L.R. All authors have read and agreed to the published version of the manuscript.

Funding: This work was supported by the Xinjiang Production and Construction Corps Funding Project (Grant No. 2018CB037)

Institutional Review Board Statement: Not applicable. This review article does not involve any animal or human studies performed by any of the authors.

Data Availability Statement: No datasets were generated or analysed during the current study.

Acknowledgments: In this section, you can acknowledge any support given which is not covered by the author contribution or funding sections. This may include administrative and technical support, or donations in kind (e.g., materials used for experiments).

Conflicts of Interest: The authors declare no competing interests.

References

1. Flory, A.; Wilson-Robles, H. Noninvasive blood-based cancer detection in veterinary medicine. *Vet. Clin. North Am. Small Anim. Pract.* **2024**, 54, 541–558. https://doi.org/10.1016/j.cvsm.2023.12.008
2. Alshammari, A.H.; Oshiro, T.; Ungkulpasvich, U.; Yamaguchi, J.; Morishita, M.; Khdair, S.A.; Hatakeyama, H.; Hirotsu, T.; di Luccio, E. Advancing veterinary oncology: Next-generation diagnostics for early cancer detection and clinical implementation. *Animals* **2025**, 15, 389. https://doi.org/10.3390/ani15030389
3. Henry, C.J. Biomarkers in veterinary cancer screening: Applications, limitations and expectations. *Vet. J.* **2010**, 185, 10–14. https://doi.org/10.1016/j.tvjl.2010.04.005
4. Dias-Pereira, P. Morbidity and mortality in elderly dogs—A model for human aging. *BMC Vet. Res.* **2022**, 18, 457. https://doi.org/10.1186/s12917-022-03518-8
5. Withrow, S.J.; Vail, D.M.; Page, R.L. Introduction: Why worry about cancer in companion animals? In *Withrow and MacEwen's Small Animal Clinical Oncology*, 5th ed.; Withrow, S.J., Vail, D.M., Page, R.L., Eds.; Saunders/Elsevier: Philadelphia, PA, USA, 2013; pp. 1–8. https://doi.org/10.1016/B978-1-4377-2362-5.00040-2
6. Pinello, K.; Amorim, I.; Pires, I.; Canadas-Sousa, A.; Catarino, J.; Faísca, P.; Branco, S.; Peleteiro, M.C.; Silva, D.; Severo, M.; Niza-Ribeiro, J. Vet-OncoNet: Malignancy analysis of neoplasms in dogs and cats. *Vet. Sci.* **2022**, 9, 535. https://doi.org/10.3390/vetsci9100535
7. Dobson, J.M. Breed-predispositions to cancer in pedigree dogs. *ISRN Vet. Sci.* 2013, **2013**, 941275. https://doi.org/10.1155/2013/941275
8. Hédan, B.; Cadieu, É.; Rimbault, M.; Vaysse, A.; Dufaure de Citres, C.; Devauchelle, P.; Botherel, N.; Abadie, J.; Quignon, P.; Derrien, T.; André, C. Identification of common predisposing loci to hematopoietic cancers in four dog breeds. *PLoS Genet.* **2021**, 17, e1009395. https://doi.org/10.1371/journal.pgen.1009395
9. Court, E.A.; Watson, A.D.; Peaston, A.E. Retrospective study of 60 cases of feline lymphosarcoma. *Aust. Vet. J.* **1997**, 75, 424–427. https://doi.org/10.1111/j.1751-0813.1997.tb14347.x
10. Hayes, H.M., Jr.; Milne, K.L.; Mandell, C.P. Epidemiological features of feline mammary carcinoma. *Vet. Rec.* **1981**, 108, 476–479. https://doi.org/10.1136/vr.108.22.476
11. American Animal Hospital Association (AAHA). *2026 AAHA Oncology Guidelines for Dogs and Cats: Section 3—Tumor Diagnostics & Staging*. Available online: https://www.aaha.org/resources/2026-aaha-oncology-guidelines-for-dogs-and-cats/ (accessed on 15 June 2026)
12. Selting, K.A.; Sharp, C.R.; Ringold, R.; Knouse, J. Serum thymidine kinase 1 and C-reactive protein as biomarkers for screening clinically healthy dogs for occult disease. *Vet. Comp. Oncol.* **2015**, 13, 373–384. https://doi.org/10.1111/vco.12052
13. Wang, L.; Sharif, H.; Saellström, S.; Rönnberg, H.; Eriksson, S. Feline thymidine kinase 1: Molecular characterization and evaluation of its serum form as a diagnostic biomarker. *BMC Vet. Res.* **2021**, 17, 316. https://doi.org/10.1186/s12917-021-03030-5
14. Howard, J.; Browne, J.; Bollard, S.; Peters, S.; Sweeney, C.; Wynne, K.; Potter, S.; McCann, A.; Kelly, P. The protein and miRNA profile of plasma extracellular vesicles (EVs) can distinguish feline mammary adenocarcinoma patients from healthy feline controls. *Sci. Rep.* **2023**, 13, 9178. https://doi.org/10.1038/s41598-023-36110-7

15. Flory, A.; Kruglyak, K.M.; Tynan, J.A.; McLennan, L.M.; Rafalko, J.M.; Fiaux, P.C.; Hernandez, G.E.; Marass, F.; Nakashe, P.; Ruiz-Perez, C.A.; et al. Clinical validation of a next-generation sequencing-based multi-cancer early detection "liquid biopsy" blood test in over 1,000 dogs using an independent testing set: The CANcer Detection in Dogs (CANDiD) study. *PLoS ONE* **2022**, 17, e0266623. https://doi.org/10.1371/journal.pone.0266623
16. Chibuk, J.; Flory, A.; Kruglyak, K.M.; Leibman, N.; Nahama, A.; Dharajiya, N.; van den Boom, D.; Jensen, T.J.; Friedman, J.S.; Shen, M.R.; et al. Horizons in veterinary precision oncology: Fundamentals of cancer genomics and applications of liquid biopsy for the detection, characterization, and management of cancer in dogs. *Front. Vet. Sci.* **2021**, 8, 664718. https://doi.org/10.3389/fvets.2021.664718
17. Bray, J.; Eward, W.; Breen, M. Defining the relevance of surgical margins. Part two: Strategies to improve prediction of recurrence risk. *Vet. Comp. Oncol.* **2023**, 21, 145–158. https://doi.org/10.1111/vco.12881
18. Kehl, A.; Aupperle-Lellbach, H.; de Brot, S.; van der Weyden, L. Review of molecular technologies for investigating canine cancer. *Animals* **2024**, 14, 769. https://doi.org/10.3390/ani14050769
19. *Veterinary Practice News*. Non-Invasive Tumor Detection for Dogs Improves Patient Outcome. Available online: https://www.veterinarypracticenews.com/non-invasive-tumor-detection-for-dogs-improves-patient-outcome/ (accessed on 20 June 2026)
20. Vieira, T.C.; Prado, M.E.; Ruiz Sueiro, F.A.; Cassali, G.D.; Jark, P.C. Small canine mammary tumours have different prognostic factors: A study of 3,470 tumours. *J. Comp. Pathol.* **2025**, 219, 6–10. https://doi.org/10.1016/j.jcpa.2025.02.004
21. Erickson, A.K.; Tremolada, G.; Sztukowski, K.E.; Thamm, D.H.; Husbands, B.D. Clinical, pathological and prognostic features of surgically excised cutaneous and subcutaneous digital and distal limb mast cell tumours in dogs. *J. Small Anim. Pract.* **2026**, 67, 67–76. https://doi.org/10.1111/jsap.70020
22. Burton, J.H.; Vail, D.M.; Willcox, J.L.; Al-Nadaf, S.; Adrianowycz, S.; Biggs, D.; Hayim, R.; Magee, K.; McMahon, R.; Mok, I.; et al. Low prevalence of occult cancer diagnosis when screening healthy, higher-risk, middle-aged to older dogs. *J. Am. Vet. Med. Assoc.* **2024**, 263, 492–498. https://doi.org/10.2460/javma.24.07.0463
23. Amaral, A.R.; Finardi, G.L.F.; Marchi, P.H.; de Oliveira, N.M.C.; Príncipe, L.A.; Teixeira, N.; Pappalardo, M.C.F.; Lima, L.O.C.; Cirillo, J.V.; Balieiro, J.C.C.; et al. Connection between nutrition and oncology in dogs and cats: Perspectives, evidence, and implications—A comprehensive review. *Front. Vet. Sci.* **2025**, 11, 1490290. https://doi.org/10.3389/fvets.2024.1490290
24. Michel, K.E.; Sorenmo, K.; Shofer, F.S. Evaluation of body condition and weight loss in dogs presented to a veterinary oncology service. *J. Vet. Intern. Med.* **2004**, 18, 692–695. https://doi.org/10.1892/0891-6640(2004)18<692:eobcaw>2.0.co;2
25. Baez, J.L.; Michel, K.E.; Sorenmo, K.; Shofer, F.S. A prospective investigation of the prevalence and prognostic significance of weight loss and changes in body condition in feline cancer patients. *J. Feline Med. Surg.* **2007**, 9, 411–417. https://doi.org/10.1016/j.jfms.2007.02.005
26. de Nardi, A.B.; Dos Santos Horta, R.; Fonseca-Alves, C.E.; de Paiva, F.N.; Linhares, L.C.M.; Firmo, B.F.; Ruiz Sueiro, F.A.; de Oliveira, K.D.; Lourenço, S.V.; De Francisco Strefezzi, R.; et al. Diagnosis, prognosis and treatment of canine cutaneous and subcutaneous mast cell tumors. *Cells* **2022**, 11, 618. https://doi.org/10.3390/cells11040618
27. Louwerens, M.; London, C.A.; Pedersen, N.C.; Lyons, L.A. Feline lymphoma in the post-feline leukemia virus era. *J. Vet. Intern. Med.* **2005**, 19, 329–335. https://doi.org/10.1892/0891-6640(2005)19[329:flitpl]2.0.co;2
28. Zandvliet, M. Canine lymphoma: A review. *Vet. Q.* **2016**, 36, 76–104. https://doi.org/10.1080/01652176.2016.1152633
29. Chan, J.Y.; Fujimoto, A.; Chang, E.W.Y.; Gan, G.G.; Tan, S.M.; Ng, S.C.; Chang, K.M.; Caguioa, P.; Datukan, J.; Hong, H.; et al. Peripheral T-cell lymphoma management in East and Southeast Asia: Real-world challenges and aspirations of the Asian Lymphoma Study Group. *JCO Glob. Oncol.* **2025**, 11, e2500353. https://doi.org/10.1200/GO-25-00353
30. Morello, E.; Martano, M.; Buracco, P. Biology, diagnosis and treatment of canine appendicular osteosarcoma: Similarities and differences with human osteosarcoma. *Vet. J.* **2011**, 189, 268–277. https://doi.org/10.1016/j.tvjl.2010.08.014
31. Murphy, S. Cutaneous squamous cell carcinoma in the cat: Current understanding and treatment approaches. *J. Feline Med. Surg.* **2013**, 15, 401–407. https://doi.org/10.1177/1098612X13483238
32. Tutu, P.; Daraban Bocaneti, F.; Altamura, G.; Dascalu, M.A.; Horodincu, L.; Soreanu, O.D.; Tanase, O.I.; Borzacchiello, G.; Mares, M. Feline oral squamous cell carcinoma: Recent advances and future perspectives. *Front. Vet. Sci.* **2025**, 12, 1663990. https://doi.org/10.3389/fvets.2025.1663990
33. Langenbach, A.; McManus, P.M.; Hendrick, M.J.; Shofer, F.S.; Sorenmo, K.U. Sensitivity and specificity of methods of assessing the regional lymph nodes for evidence of metastasis in dogs and cats with solid tumors. *J. Am. Vet. Med. Assoc.* **2001**, 218, 1424–1428. https://doi.org/10.2460/javma.2001.218.1424
34. American Animal Hospital Association (AAHA). *2026 AAHA Oncology Guidelines for Dogs and Cats: Section 3—Tumor Diagnostics & Staging*. Available online: https://www.aaha.org/resources/2026-aaha-oncology-guidelines-for-dogs-and-cats/section-3-tumor-diagnostics-staging/#content (accessed on 15 June 2026)
35. Bergman, P.J. Paraneoplastic hypercalcemia. *Top. Companion Anim. Med.* **2012**, 27, 156–158. https://doi.org/10.1053/j.tcam.2012.09.003
36. Evans, M.; Smithson, C.W.; Peak, R.M.; Coyle, V. Canine oral lymphoma: A review and 3 case studies. *J. Vet. Dent.* **2023**, 40, 358–367. https://doi.org/10.1177/08987564231158511
37. Klausner, J.S.; Bell, F.W.; Hayden, D.W.; Hegstad, R.L.; Johnston, S.D. Hypercalcemia in two cats with squamous cell carcinomas. *J. Am. Vet. Med. Assoc.* **1990**, 196, 103–105.
38. Buishand, F.O. Current trends in diagnosis, treatment and prognosis of canine insulinoma. *Vet. Sci.* **2022**, 9, 540. https://doi.org/10.3390/vetsci9100540

39. Shorten, E.; Swallow, A.; McCallum, K.E.; Holzhausen, C.; Hughes, K.; Genain, M.A. Computed tomographic findings in a case of feline insulinoma. *Vet. Rec. Case Rep.* 2020, 8, e001054. https://doi.org/10.1136/vetreccr-2019-001054
40. Vilmis, D.A. Hematological manifestations of paraneoplastic syndromes in dogs. *Int. J. Vet. Med.* **2024**, 1, 381–391. https://doi.org/10.52419/issn2072-2419.2024.1.381
41. Turek, M.M. Cutaneous paraneoplastic syndromes in dogs and cats: A review of the literature. *Vet. Dermatol.* **2003**, 14, 279–296. https://doi.org/10.1111/j.1365-3164.2003.00346.x
42. Childress, M.O. Hematologic abnormalities in the small animal cancer patient. *Vet. Clin. North Am. Small Anim. Pract.* **2012**, 42, 123–155. https://doi.org/10.1016/j.cvsm.2011.09.009
43. Ménard, M.; Fontaine, M.; Morin, M. Fine needle aspiration biopsy of malignant tumors in dogs and cats: A report of 102 cases. *Can. Vet. J.* **1986**, 27, 504–510.
44. Aupperle-Lellbach, H.; Kehl, A.; de Brot, S.; van der Weyden, L. Clinical use of molecular biomarkers in canine and feline oncology: Current and future. *Vet. Sci.* **2024**, 11, 199. https://doi.org/10.3390/vetsci11050199
45. Rafalko, J.M.; Kruglyak, K.M.; McCleary-Wheeler, A.L.; Goyal, V.; Phelps-Dunn, A.; Wong, L.K.; Warren, C.D.; Brandstetter, G.; Rosentel, M.C.; DiMarzio, L.; et al. Age at cancer diagnosis by breed, weight, sex, and cancer type in a cohort of more than 3,000 dogs: Determining the optimal age to initiate cancer screening in canine patients. *PLoS ONE* **2023**, 18, e0280795. https://doi.org/10.1371/journal.pone.0280795
46. American Animal Hospital Association. *2026 AAHA Oncology Guidelines for Dogs and Cats*. Available online: https://www.aaha.org/resources/2026-aaha-oncology-guidelines-for-dogs-and-cats/ (accessed on 15 June 2026)
47. Steenkamp, G. Neoplasia of the canine and feline tongue: A review and treatment options. In *Proceedings of the World Small Animal Veterinary Association World Congress*, 2014. Available online: https://www.vin.com/apputil/project/defaultadv1.aspx?pId=12886&catId=57092&id=7054676 (accessed on 20 June 2026)
48. Klaengkaew, A.; Sutthigran, S.; Thammasiri, N.; Yuwatanakorn, K.; Thanaboonnipat, C.; Ponglowhapan, S.; Choisunirachon, N. The evaluation of non-anesthetic computed tomography for detection of pulmonary parenchyma in feline mammary gland carcinoma: A preliminary study. *BMC Vet. Res.* **2021**, 17, 237. https://doi.org/10.1186/s12917-021-02950-6
49. Flory, A.; Ruiz-Perez, C.A.; Clavere-Graciette, A.G.; Rafalko, J.M.; O'Kell, A.L.; Flesner, B.K.; McLennan, L.M.; Hicks, S.C.; Nakashe, P.; Phelps-Dunn, A.; et al. Clinical validation of a blood-based liquid biopsy test integrating cell-free DNA quantification and next-generation sequencing for cancer screening in dogs. *J. Am. Vet. Med. Assoc.* **2024**, 262, 665–673. https://doi.org/10.2460/javma.23.10.0564
50. De Vos, S.; Broeckx, B.J.G.; Cian, F.; Ploeg, M.; De Cock, H.; De Spiegelaere, W.; de Rooster, H. When assessing representative images of fine-needle aspirate cytological smears of canine mast cell tumours, interobserver agreement is influenced by educational attainment. *J. Small Anim. Pract.* **2025**, 66, 739–746. https://doi.org/10.1111/jsap.13883
51. Ghisleni, G.; Roccabianca, P.; Ceruti, R.; Stefanello, D.; Bertazzolo, W.; Bonfanti, U.; Caniatti, M. Correlation between fine-needle aspiration cytology and histopathology in the evaluation of cutaneous and subcutaneous masses from dogs and cats. *Vet. Clin. Pathol.* **2006**, 35, 24–30. https://doi.org/10.1111/j.1939-165x.2006.tb00084.x
52. Chu, C.P. Computer vision and deep learning in small animal cytology and slide review. *Vet. Clin. North Am. Small Anim. Pract.* **2026**, in press. https://doi.org/10.1016/j.cvsm.2026.03.019
53. Goldschmidt, S.; Soltero-Rivera, M.; Quiroz, A.; Wong, K.; Rebhun, R.; Zwingenberger, A.; Ren, Y.; Taylor, S.; Arzi, B. The diagnostic yield of preoperative screening for oral cancer in dogs over 15 years, part 2: Distant screening. *J. Am. Vet. Med. Assoc.* **2023**, 261, S24–S33. https://doi.org/10.2460/javma.23.05.0300
54. Flory, A.; Gray, S.; McLennan, L.M.; Rafalko, J.M.; Marshall, M.A.; Wotrang, K.; Kroll, M.; Flesner, B.K.; O'Kell, A.L.; Cohen, T.A.; et al. Study design and interim analysis of the Cancer Lifetime Assessment Screening Study in Canines (CLASSiC): The first prospective cancer screening study in dogs using next-generation sequencing-based liquid biopsy. *bioRxiv* **2024**, preprint. https://doi.org/10.1101/2024.04.01.587600
55. Pecceu, E.; Serra Varela, J.C.; Handel, I.; Piccinelli, C.; Milne, E.; Lawrence, J. Ultrasound is a poor predictor of early or overt liver or spleen metastasis in dogs with high-risk mast cell tumours. *Vet. Comp. Oncol.* **2020**, 18, 389–401. https://doi.org/10.1111/vco.12563
56. Pomerantz, L.K.; Solano, M.; Kalosa-Kenyon, E. Performance of a commercially available artificial intelligence software for the detection of confirmed pulmonary nodules and masses in canine thoracic radiography. *Vet. Radiol. Ultrasound* **2023**, 64, 881–889. https://doi.org/10.1111/vru.13287
57. Silva, V.B.D.; Brito, P.L.; Brito, R.L.; Costa-Neto, J.M.D.; Ribeiro, L.G.R.; Solcà, M.D.S.; Rodrigues, G.M.; Silva, L.P.; Rocha, M.A.N.; Barrouin-Melo, S.M.; Estrela-Lima, A. Impact of owners' perception and socioeconomic status on the treatment and clinical outcome of mammary neoplasms in female dogs. *Prev. Vet. Med.* **2025**, 245, 106690. https://doi.org/10.1016/j.prevetmed.2025.106690
58. Kulkarni, V.; Tsigelny, I.F.; Kouznetsova, V.L. Implementation of machine learning-based system for early diagnosis of feline mammary carcinomas through blood metabolite profiling. *Metabolites* 2024, 14, 501. https://doi.org/10.3390/metabo14090501
59. Sabattini, S.; Bottero, E.; Turba, M.E.; Vicchi, F.; Bo, S.; Bettini, G. Differentiating feline inflammatory bowel disease from alimentary lymphoma in duodenal endoscopic biopsies. *J. Small Anim. Pract.* **2016**, 57, 396–401. https://doi.org/10.1111/jsap.12494
60. Marsilio, S.; Freiche, V.; Johnson, E.; Leo, C.; Langerak, A.W.; Peters, I.; Ackermann, M.R. ACVIM consensus statement guidelines on diagnosing and distinguishing low-grade neoplastic from inflammatory lymphocytic chronic enteropathies in cats. *J. Vet. Intern. Med.* **2023**, 37, 794–816. https://doi.org/10.1111/jvim.16690

61. Gaschen, L. How I do ultrasound-guided tissue sampling. In *Proceedings of the World Small Animal Veterinary Association Congress*, 2016. Available online: https://veterinarypartner.vin.com/apputil/project/defaultadv1.aspx?pId=19840&catId=105878&id=8249664 (accessed on 20 June 2026)
62. O'Kell, A.L.; Lytle, K.M.; Cohen, T.A.; Wong, L.K.; Sandford, E.; Rafalko, J.M.; Brandstetter, G.; DiMarzio, L.R.; Phelps-Dunn, A.; Rosentel, M.C.; et al. Clinical experience with next-generation sequencing-based liquid biopsy testing for cancer detection in dogs: A review of 1,500 consecutive clinical cases. *J. Am. Vet. Med. Assoc.* **2023**, 261, 827–836. https://doi.org/10.2460/javma.22.11.0526
63. Taylor, S.S.; Dodkin, S.; Papasouliotis, K.; Evans, H.; Graham, P.A.; Belshaw, Z.; Westberg, S.; von Euler, H.P. Serum thymidine kinase activity in clinically healthy and diseased cats: A potential biomarker for lymphoma. *J. Feline Med. Surg.* **2013**, 15, 142–147. https://doi.org/10.1177/1098612X12463928
64. Sharif, H.; Saellström, S.; Kolli, B.; Jagarlamudi, K.K.; Wang, L.; Rönnberg, H.; Eriksson, S. A monoclonal antibody-based sandwich ELISA for measuring canine thymidine kinase 1 protein and its role as biomarker in canine lymphoma. *Front. Vet. Sci.* **2023**, 10, 1243853. https://doi.org/10.3389/fvets.2023.1243853
65. Brodersen, J. Overdiagnosis: An unrecognised and growing worldwide problem in healthcare. *Zdravstveno Varstvo* **2017**, 56, 147–149. https://doi.org/10.1515/sjph-2017-0019
66. Finora, K. Common paraneoplastic syndromes. *Clin. Tech. Small Anim. Pract.* **2003**, 18, 123–126. https://doi.org/10.1053/svms.2003.36629
67. Ruiz-Perez, C.A.; Nakashe, P.; Marshall, M.A.; Marass, F.; Tang, T.; McLennan, L.M.; Kroll, M.; Flesner, B.K.; Gray, S.; Rafalko, J.M.; et al. Proof-of-concept evaluation of next-generation sequencing-based liquid biopsy for non-invasive cancer detection in cats. *Front. Vet. Sci.* **2024**, 11, 1394686. https://doi.org/10.3389/fvets.2024.1394686
68. Kim, Y.; Park, J.; Kim, B.; Yu, K.R.; Kim, H.S.; Oh, Y.; Seo, K.; Ryu, M.; Park, C.; Bhang, D.; et al. Serum thymidine kinase 1 protein concentrations and presence of its autoantibody as biomarkers for screening dogs with malignant tumors. *J. Vet. Intern. Med.* **2024**, 38, 300–307. https://doi.org/10.1111/jvim.16946
69. Sharif, H.; Arabi Belaghi, R.; Jagarlamudi, K.K.; Saellström, S.; Wang, L.; Rönnberg, H.; Eriksson, S. A novel cross-validated machine learning based Alertix-Cancer Risk Index for early detection of canine malignancies. *Front. Vet. Sci.* **2025**, 12, 1570106. https://doi.org/10.3389/fvets.2025.1570106
70. Kim, Y.; Lee, W.; Kim, B.; Jang, B.; Yu, K.R.; Kim, H.S.; Ryu, M.; Oh, Y.; Seo, K.; Park, C.; et al. Use of thymidine kinase 1 autoantibody, thymidine kinase antigen, extracellular protein kinase A autoantibody, and C-reactive protein for early detection of malignant tumors in dogs. *J. Vet. Intern. Med.* **2025**, 39, e17266. https://doi.org/10.1111/jvim.17266
71. Çolakoğlu, H.E.; Fidan, Ç.; Alçığır, M.E.; Göbekçi, A.E.; Devrim, E.; Anteplioğlu, T.; Yazlık, M.O.; Özmen, Ö.; Reçber, T.; Nemutlu, E.; Kaya, U. Evaluation of serum CA15-3, CEA, Ki-67, PDL-1 and VEGF as potential diagnostic and prognostic biomarkers in canine mammary tumors. *Theriogenology* 2025, 247, 117579. https://doi.org/10.1016/j.theriogenology.2025.117579
72. Renzi, A.; Morandi, L.; Bellei, E.; Marconato, L.; Rigillo, A.; Aralla, M.; Lenzi, J.; Bettini, G.; Tinto, D.; Sabattini, S. Validation of oral brushing as a non-invasive technique for the identification of feline oral squamous cell carcinoma by DNA methylation and TP53 mutation analysis. *Vet. Comp. Oncol.* **2021**, 19, 501–509. https://doi.org/10.1111/vco.12688
73. Von Euler, H.P.; Rivera, P.; Aronsson, A.C.; Bengtsson, C.; Hansson, L.O.; Eriksson, S.K. Monitoring therapy in canine malignant lymphoma and leukemia with serum thymidine kinase 1 activity—Evaluation of a new, fully automated non-radiometric assay. *Int. J. Oncol.* **2009**, 34, 505–510. https://doi.org/10.3892/ijo_00000123
74. Jagarlamudi, K.K.; Moreau, L.; Westberg, S.; Rönnberg, H.; Eriksson, S. A new sandwich ELISA for quantification of thymidine kinase 1 protein levels in sera from dogs with different malignancies can aid in disease management. *PLoS ONE* **2015**, 10, e0137871. https://doi.org/10.1371/journal.pone.0137871
75. Khaki, Z.; Fathipour, V. Prognostic value of different forms of serum MMP-2 and MMP-9 in dogs with mammary tumors; a longitudinal study. *Res. Vet. Sci.* **2023**, 163, 104995. https://doi.org/10.1016/j.rvsc.2023.104995
76. Ko, S.; Jang, J.; Yi, S.S.; Kwon, C. Early detection of canine hemangiosarcoma via cfDNA fragmentation and copy number alterations in liquid biopsies using machine learning. *Front. Vet. Sci.* **2025**, 11, 1489402. https://doi.org/10.3389/fvets.2024.1489402
77. Marconato, L.; Facchinetti, A.; Zanardello, C.; Rossi, E.; Vidotto, R.; Capello, K.; Melchiotti, E.; Laganga, P.; Zamarchi, R.; Vascellari, M. Detection and prognostic relevance of circulating and disseminated tumour cell in dogs with metastatic mammary carcinoma: A pilot study. *Cancers* **2019**, 11, 163. https://doi.org/10.3390/cancers11020163
78. Wright, T.F.; Brisson, B.A.; Belanger, C.R.; Tiessen, A.; Sabine, V.; Skowronski, K.; Wood, G.A.; Oblak, M.L.; Mutsaers, A.J.; Sears, W.; Bienzle, D. Quantification of circulating tumour cells over time in dogs with appendicular osteosarcoma. *Vet. Comp. Oncol.* **2023**, 21, 541–550. https://doi.org/10.1111/vco.12918
79. Lei, S.; Zhang, J.; Blum, N.T.; Li, M.; Zhang, D.Y.; Yin, W.; Zhao, F.; Lin, J.; Huang, P. In vivo three-dimensional multispectral photoacoustic imaging of dual enzyme-driven cyclic cascade reaction for tumor catalytic therapy. *Nat. Commun.* **2022**, 13, 1298. https://doi.org/10.1038/s41467-022-29082-1
80. Kanayama, M.; Yoneda, K.; Kuwata, T.; Mori, M.; Manabe, T.; Oyama, R.; Matsumiya, H.; Takenaka, M.; Kuroda, K.; Ohnaga, T.; Tanaka, F. Enhanced capture system for mesenchymal-type circulating tumor cells using a polymeric microfluidic device "CTC-Chip" incorporating cell-surface vimentin. *Oncol. Rep.* **2024**, 52, 156. https://doi.org/10.3892/or.2024.8815
81. Mochizuki, H.; Shapiro, S.G.; Breen, M. Detection of BRAF mutation in urine DNA as a molecular diagnostic for canine urothelial and prostatic carcinoma. *PLoS ONE* **2015**, 10, e0144170. https://doi.org/10.1371/journal.pone.0144170

82. Maeda, S.; Yoshitake, R.; Chambers, J.K.; Uchida, K.; Eto, S.; Ikeda, N.; Nakagawa, T.; Nishimura, R.; Goto-Koshino, Y.; Yonezawa, T.; Momoi, Y. BRAFV595E mutation associates CCL17 expression and regulatory T cell recruitment in urothelial carcinoma of dogs. *Vet. Pathol.* **2021**, 58, 971–980. https://doi.org/10.1177/0300985820967449
83. Tagawa, M.; Tambo, N.; Maezawa, M.; Tomihari, M.; Watanabe, K.I.; Inokuma, H.; Miyahara, K. Quantitative analysis of the BRAF V595E mutation in plasma cell-free DNA from dogs with urothelial carcinoma. *PLoS ONE* **2020**, 15, e0232365. https://doi.org/10.1371/journal.pone.0232365
84. Kuo, C.C.; Yang, S.Y.; Liu, R.M.; Lin, Y.H.; Liu, C.C.; Huang, W.H.; Lee, J.J.; Liao, A.T. Diagnostic value of conventional polymerase chain reaction for detecting BRAF V595E mutation in liquid and tissue specimens of canine urothelial and prostate carcinomas. *Animals* **2024**, 14, 2535. https://doi.org/10.3390/ani14172535
85. Smith, P.A.D.; Waugh, E.M.; Crichton, C.; Jarrett, R.F.; Morris, J.S. The prevalence and characterisation of TRAF3 and POT1 mutations in canine B-cell lymphoma. *Vet. J.* **2020**, 266, 105575. https://doi.org/10.1016/j.tvjl.2020.105575
86. Griebie, E.R.; David, F.H.; Ober, C.P.; Feeney, D.A.; Anderson, K.L.; Wuenschmann, A.; Jessen, C.R. Evaluation of canine hepatic masses by use of triphasic computed tomography and B-mode, color flow, power, and pulsed-wave Doppler ultrasonography and correlation with histopathologic classification. *Am. J. Vet. Res.* **20**17, 78, 1273–1283. https://doi.org/10.2460/ajvr.78.11.1273
87. Brody, A.; Crooks, J.C.; French, J.M.; Lang, L.G.; Randall, E.K.; Griffin, L.R. Staging canine patients with appendicular osteosarcoma utilizing fluorine-18 fluorodeoxyglucose positron emission tomography/computed tomography compared to whole body computed tomography. *Vet. Comp. Oncol.* **2022**, 20, 541–550. https://doi.org/10.1111/vco.12805
88. Mattoon, J.S.; Bryan, J.N. The future of imaging in veterinary oncology: Learning from human medicine. *Vet. J.* **2013**, 197, 541–552. https://doi.org/10.1016/j.tvjl.2013.05.022
89. Selmic, L.E.; Ruple, A. A systematic review of surgical margins utilized for removal of cutaneous mast cell tumors in dogs. *BMC Vet. Res.* **2020**, 16, 5. https://doi.org/10.1186/s12917-019-2227-8
90. Hawkes, C.; Morris, J.; Bavcar, S.; Wilkie, C.; Ray, S.; Auquier, C.; Benjamin, S.; Massó, J.B.; Bottin, S.; Davies, O.; et al. Comparison of CHOP-19 and CHOP-25 for treatment of peripheral nodal B-cell lymphoma in dogs: A European multicenter retrospective cohort study. *J. Vet. Intern. Med.* **2024**, 38, 3193–3205. https://doi.org/10.1111/jvim.17222
91. Tanis, J.B.; Mason, S.L.; Maddox, T.W.; Blackwood, L.; Killick, D.R.; Amores-Fuster, I.; Harper, A.; Finotello, R. Evaluation of a multi-agent chemotherapy protocol combining lomustine, procarbazine and prednisolone (LPP) for the treatment of relapsed canine non-Hodgkin high-grade lymphomas. *Vet. Comp. Oncol.* **2018**, 16, 361–369. https://doi.org/10.1111/vco.12387
92. Kim, H.J.; Heo, R.; Choi, E.W. A retrospective investigation of 28 cats with intermediate- to large-cell lymphoma treated with lomustine and prednisolone as a first-line chemotherapy. *Animals* **2026**, 16, 989. https://doi.org/10.3390/ani16060989
93. Gil da Costa, R.M. C-kit as a prognostic and therapeutic marker in canine cutaneous mast cell tumours: From laboratory to clinic. *Vet. J.* **2015**, 205, 5–10. https://doi.org/10.1016/j.tvjl.2015.05.002
94. Siegel, S.; Cronin, K.L. Palliative radiotherapy. *Vet. Clin. North Am. Small Anim. Pract.* **1997**, 27, 149–155. https://doi.org/10.1016/s0195-5616(97)50013-1
95. Fan, T.M. Pain management in veterinary patients with cancer. *Vet. Clin. North Am. Small Anim. Pract.* **2014**, 44, 989–1001. https://doi.org/10.1016/j.cvsm.2014.05.005
96. Mathews, K.A. Nonsteroidal anti-inflammatory analgesics: Indications and contraindications for pain management in dogs and cats. *Vet. Clin. North Am. Small Anim. Pract.* **2000**, 30, 783–vii. https://doi.org/10.1016/s0195-5616(08)70007-x
97. Bergman, P.J.; McKnight, J.; Novosad, A.; Charney, S.; Farrelly, J.; Craft, D.; Wulderk, M.; Jeffers, Y.; Sadelain, M.; Hohenhaus, A.E.; et al. Long-term survival of dogs with advanced malignant melanoma after DNA vaccination with xenogeneic human tyrosinase: A phase I trial. *Clin. Cancer Res.* **2003**, 9, 1284–1290.
98. Grosenbaugh, D.A.; Leard, A.T.; Bergman, P.J.; Klein, M.K.; Meleo, K.; Susaneck, S.; Hess, P.R.; Jankowski, M.K.; Jones, P.D.; Leibman, N.F.; et al. Safety and efficacy of a xenogeneic DNA vaccine encoding for human tyrosinase as adjunctive treatment for oral malignant melanoma in dogs following surgical excision of the primary tumor. *Am. J. Vet. Res.* **2011**, 72, 1631–1638. https://doi.org/10.2460/ajvr.72.12.1631
99. Sarbu, L.; Kitchell, B.E.; Bergman, P.J. Safety of administering the canine melanoma DNA vaccine (Oncept) to cats with malignant melanoma—A retrospective study. *J. Feline Med. Surg.* **2017**, 19, 224–230. https://doi.org/10.1177/1098612X15623319
100. Engbersen, D.J.M.; van Beijnum, J.R.; Roos, A.; van Beelen, M.; de Haan, J.D.; Grinwis, G.C.M.; Schalken, J.A.; Witjes, J.A.; Griffioen, A.W.; Huijbers, E.J.M. Vaccination against extracellular vimentin for treatment of urothelial cancer of the bladder in client-owned dogs. *Cancers* **2023**, 15, 3958. https://doi.org/10.3390/cancers15153958
101. Weishaar, K.M.; Ehrhart, E.J.; Avery, A.C.; Charles, J.B.; Elmslie, R.E.; Vail, D.M.; London, C.A.; Clifford, C.A.; Eickhoff, J.C.; Thamm, D.H. c-Kit mutation and localization status as response predictors in mast cell tumors in dogs treated with prednisone and toceranib or vinblastine. *J. Vet. Intern. Med.* **2018**, 32, 394–405. https://doi.org/10.1111/jvim.14889
102. McCleary-Wheeler, A.L.; Fiaux, P.C.; Flesner, B.K.; Ruiz-Perez, C.A.; McLennan, L.M.; Tynan, J.A.; Hicks, S.C.; Rafalko, J.M.; Grosu, D.S.; Chibuk, J.; et al. Next-generation sequencing-based liquid biopsy may be used for detection of residual disease and cancer recurrence monitoring in dogs. *Am. J. Vet. Res.* **2023**, 1–8. https://doi.org/10.2460/ajvr.23.07.0163
103. Darrah, J.M.; Herrera, A.F. Updates on circulating tumor DNA assessment in lymphoma. *Curr. Hematol. Malign. Rep.* **2018**, 13, 348–355. https://doi.org/10.1007/s11899-018-0468-4
104. Magalhães, T.R.; Lourenço, A.L.; Gregório, H.; Queiroga, F.L. Therapeutic effect of EPA/DHA supplementation in neoplastic and non-neoplastic companion animal diseases: A systematic review. *In Vivo* **2021**, 35, 1419–1436. https://doi.org/10.21873/invivo.12394

105. Mangano, C.; Macrì, F.; Di Pietro, S.; Pugliese, M.; Santoro, S.; Iannelli, N.M.; Mazzullo, G.; Crupi, R.; De Majo, M. Use of contrast-enhanced ultrasound for assessment of nodular lymphoid hyperplasia (NLH) in canine spleen. *BMC Vet. Res.* **2019**, 15, 196. https://doi.org/10.1186/s12917-019-1942-5
106. Acolty, V.; Thut, D.; Morrow, M.; McCarthy, S.; Alsina, J.; Kreychman, A.; Rakita, D. Management of splenic incidentalomas, a new evidence-based algorithm. *Surg. Open Dig. Adv.* **2025**, 18, 100197. https://doi.org/10.1016/j.soda.2025.100197